

Aus dem Walter-Brendel-Zentrum für Experimentelle Medizin  
der Ludwig-Maximilians-Universität München  
Vorstand: Prof. Dr. med. U. Pohl

MECHANISMS OF LEUKOCYTE  
TRANSENDOTHELIAL AND INTERSTITIAL MIGRATION  
DURING ACUTE INFLAMMATION *IN VIVO*

Dissertation  
zum Erwerb des Doktorgrades der Medizin  
an der Medizinischen Fakultät der  
Ludwig-Maximilians-Universität München

vorgelegt von  
Alexander Georg Khandoga  
aus Mosty/Belarus

2009

Mit Genehmigung der Medizinischen Fakultät  
der Universität München

1. Berichterstatter: Prof. Dr. F. Krombach  
2. Berichterstatter: Prof. Dr. Dr. J. Heesemann  
Mitberichterstatter: Priv. Doz. Dr. T. Herzinger  
Prof. Dr. B. Walzog

Mitbetreuung durch den promovierten

Mitarbeiter: Priv. Doz. Dr. A. Khandoga

Dekan: Prof. Dr. med. Dr. h. c. M. Reiser, FACR, FRCR

Tag der mündlichen Prüfung: 29.10.2009

# CONTENTS

<b>1. INTRODUCTION .....</b>	<b>5</b>
<b>1.1 Cascade of leukocyte migration in the pathogenesis of inflammation .....</b>	<b>5</b>
1.1.1 Adhesion molecules involved in leukocyte transmigration .....	9
<b>1.2 Leukocyte interstitial migration .....</b>	<b>13</b>
<b>2. OBJECTIVES .....</b>	<b>16</b>
<b>3. MATERIAL AND METHODS .....</b>	<b>17</b>
<b>3.1 Animals .....</b>	<b>17</b>
<b>3.2 Reagents and inhibitors .....</b>	<b>17</b>
<b>3.3 Blocking antibodies .....</b>	<b>17</b>
<b>3.4 Model .....</b>	<b>18</b>
3.4.1 Anesthesia .....	18
3.4.2 Catheterization of a. femoralis .....	18
3.4.3 Catheterization of v. jugularis interna .....	19
3.4.4 Surgical preparation of cremaster muscle .....	19
3.4.5 Near-infrared reflected light oblique transillumination (RLOT) microscopy .....	20
3.4.6 Microinjection of inflammatory mediators .....	20
3.4.7 Microhemodynamic parameters .....	22
3.4.8 Parameters of leukocyte recruitment .....	22
3.4.9 Single cell tracking of emigrated leukocytes .....	23
3.4.10 Morphological changes and polarization in interstitially migrating leukocytes .....	24
3.4.11 Tissue distribution of applied fluorescent dye per time .....	25
3.4.12 Visualization of mitochondrial redistribution in interstitially migrating leukocytes ..	25
3.4.13 Imaging of the migratory behavior of leukocyte subsets .....	26
<b>3.5 Experimental protocols and experimental groups .....</b>	<b>27</b>
3.5.1 Role of ESAM for IL-1 $\beta$ -induced leukocyte migration <i>in vivo</i> .....	27
3.5.2 Role of CD99 and CD99L2 for IL-1 $\beta$ -induced leukocyte migration <i>in vivo</i> .....	28
3.5.3 Imaging and quantitative analysis of leukocyte directional migration <i>in vivo</i> .....	30
3.5.4 Statistical analysis .....	33
<b>4. RESULTS .....</b>	<b>34</b>
<b>4.1 The role of ESAM for IL-1<math>\beta</math>-induced leukocyte migration <i>in vivo</i> .....</b>	<b>34</b>
4.1.1 Microhemodynamic parameters .....	34
4.1.2 Leukocyte migration parameters .....	35
<b>4.2 The role of CD99 and CD99L2 for IL-1<math>\beta</math>-induced leukocyte migration <i>in vivo</i> .....</b>	<b>38</b>
4.2.1 Microhemodynamic parameters .....	38
4.2.2 Parameters of leukocyte migration .....	40
4.2.2.1 Leukocyte rolling flux fraction .....	40
4.2.2.2 Leukocyte adhesion .....	41
4.2.2.3 Leukocyte transmigration .....	43
<b>4.3 Imaging and quantitative analysis of leukocyte directional interstitial migration <i>in vivo</i> .....</b>	<b>46</b>
4.3.1 Microhemodynamic parameters and systemic leukocyte counts .....	46
4.3.2. Determination of the optimal distance for microinjection of chemoattractants .....	46
4.3.3 Tissue distribution of fluorescence dye rhodamine 6G applied via microinjection .....	48

4.3.4 Leukocyte adhesion.....	50
4.3.5 Leukocyte transmigration .....	52
4.3.6 Motility of interstitially migrating leukocytes .....	54
4.3.7 Effect of the Rho kinase inhibitor Y27632 on leukocyte motility.....	56
4.3.8 Morphological changes and polarization of interstitially migrating leukocytes .....	58
4.3.9 Colocalization of leukocyte migration to the site of microinjection of chemoattractant .....	61
4.3.10 Visualization of mitochondria redistribution in interstitially migrating leukocytes ...	63
4.3.11 Migration patterns of different leukocyte subsets.....	64
<b>5. DISCUSSION.....</b>	<b>66</b>
5.1 Discussion of material and methods.....	66
5.1.1 Animals.....	66
5.1.2 Experimental model and surgical preparation.....	66
5.1.3 Induction of an inflammatory response .....	67
5.1.4 Intravital microscopy.....	69
5.2 Discussion of the results.....	71
5.2.1 The role of ESAM for IL-1 $\beta$ -induced leukocyte migration in vivo .....	71
5.2.2 The role of CD99 and CD99L2 for IL-1 $\beta$ -induced leukocyte migration in vivo .....	73
5.2.3 Imaging and quantitative analysis of leukocyte directional interstitial migration in vivo .....	76
<b>6. SUMMARY .....</b>	<b>83</b>
<b>7. ZUSAMMENFASSUNG.....</b>	<b>85</b>
<b>8. REFERENCES .....</b>	<b>87</b>
<b>9. ACKNOWLEDGEMENTS .....</b>	<b>102</b>
<b>10. PUBLICATION LIST.....</b>	<b>103</b>
<b>11. CURRICULUM VITAE .....</b>	<b>106</b>

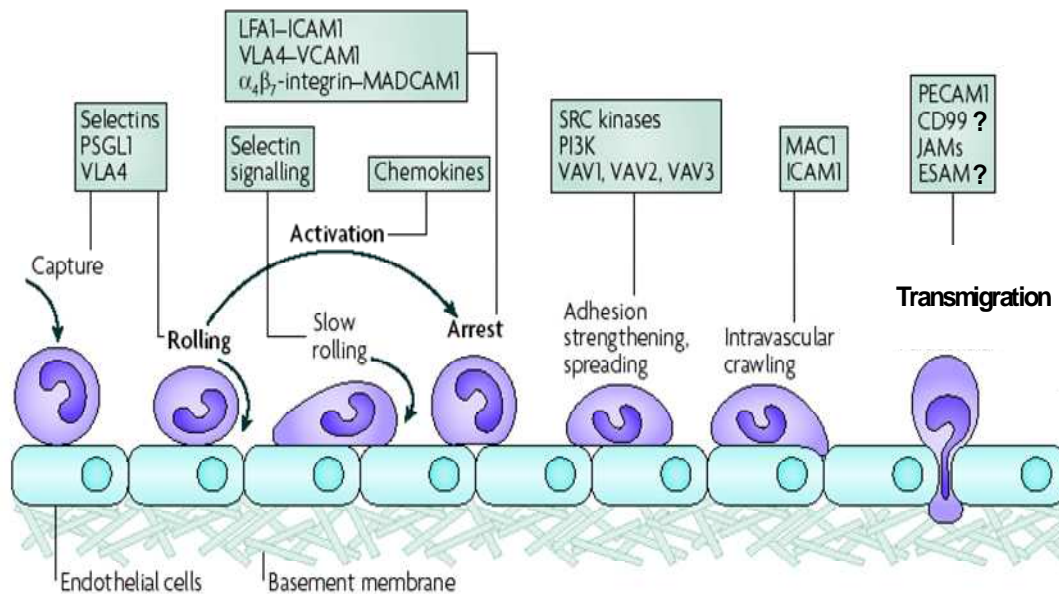
# 1. INTRODUCTION

## 1.1 Cascade of leukocyte migration in the pathogenesis of inflammation

Inflammation is the basic mechanism essential for tissue repair after an injury and consists of a cascade of cellular and microvascular reactions that serve to remove damaged and generate new tissue. Characterized by the classic clinical signs of inflammation - swelling, redness, pain, heat, and loss of function, the acute inflammation cascade includes increased permeability in microvessels, attachment of circulating cells to the vessels in the vicinity of the injury site, migration of several immune cell types, cell apoptosis, and growth of new tissue and blood vessels. Already at the end of XIXth century, *Metchnikov* laid the basic principles of inflammation by realizing that leukocytes escape from the blood vessels and then take up and digest bacteria that get into the body (1). In the next 100 years, his theory was extended and consolidated by discovering the molecular mechanisms underlying leukocyte activation, recruitment from the circulation, and trafficking toward the site of inflammation or injury. Recruitment and migration of leukocytes from the bloodstream to the site of injury or infection is a fundamental event in the inflammatory response, resulting in tissue dysfunction and damage (2), (3). Specific tissue infiltration by distinct leukocyte subpopulations indicates their critical function in the pathogenesis of inflammatory disease (4).

Leukocyte recruitment in the microvasculature involves a multistep cascade of interactions of adhesion receptors between leukocytes and endothelial cells (5). Leukocyte rolling, adhesion and transmigration were described already in the nineteenth century. In the past decade, new insights have been gained into the mechanisms underlying integrin activation (6), into the post-adhesion events strengthen leukocyte attachment to the endothelium, and into the molecules that are involved in leukocyte transendothelial migration (7), (8). Therefore, the original three-step version of the leukocyte adhesion cascade has been expanded and now includes slow rolling, adhesion strengthening, intraluminal crawling, transendothelial migration, migration through the basement membrane, and interstitial migration (8) (Fig. 1). Initial tethering and rolling are mediated by P-,

E- and L-selectins (9), which interact with P-selectin glycoprotein ligand 1 (PSGL1) and other ligands (10), (11). Recent works suggest that not only selectins but also integrins such as lymphocyte function-associated antigen-1 (LFA-1) and macrophage receptor-1 (MAC-1) support leukocyte rolling (12), (13). Rolling brings the leukocyte into proximity with endothelial cells, where it can be activated by luminal surface-bound chemokines or lipid chemoattractants (for example, platelet activating factor – PAF) (14). Ligation of specific G-protein coupled receptors (GPCRs) by chemokines leads to rapid integrin activation via “inside-out” signaling that causes leukocyte arrest under shear stress conditions (8). In contrast, an “outside-in” signaling, which is downstream of endothelial ligand (intercellular adhesion molecule-1 - ICAM-1, vascular cell adhesion molecule - VCAM-1) binding to activated integrins probably contributes to adhesion stabilization and cell motility. In addition to mediating adhesion, integrins generate intracellular signals that regulate various cellular functions (15), (16). In this context, ligand-induced integrin clustering and conformational changes contribute to “outside-in” signaling and the formation of “signalosomes” that activate recruitment of protein tyrosine kinases and the initiation of various signaling pathways, which facilitate strengthening of adherent leukocytes on the endothelium (17), (8). Subsequently, leukocytes crawl inside the blood vessels in a MAC-1- and ICAM-1-dependent manner, seeking the preferred sites of diapedesis (18) (Fig. 1). After crawling, leukocytes migrate to a nearby endothelial border and squeeze between the tightly opposed endothelial cells to the underlying basement membrane in a next process - transendothelial migration (also called diapedesis) (19), (20).

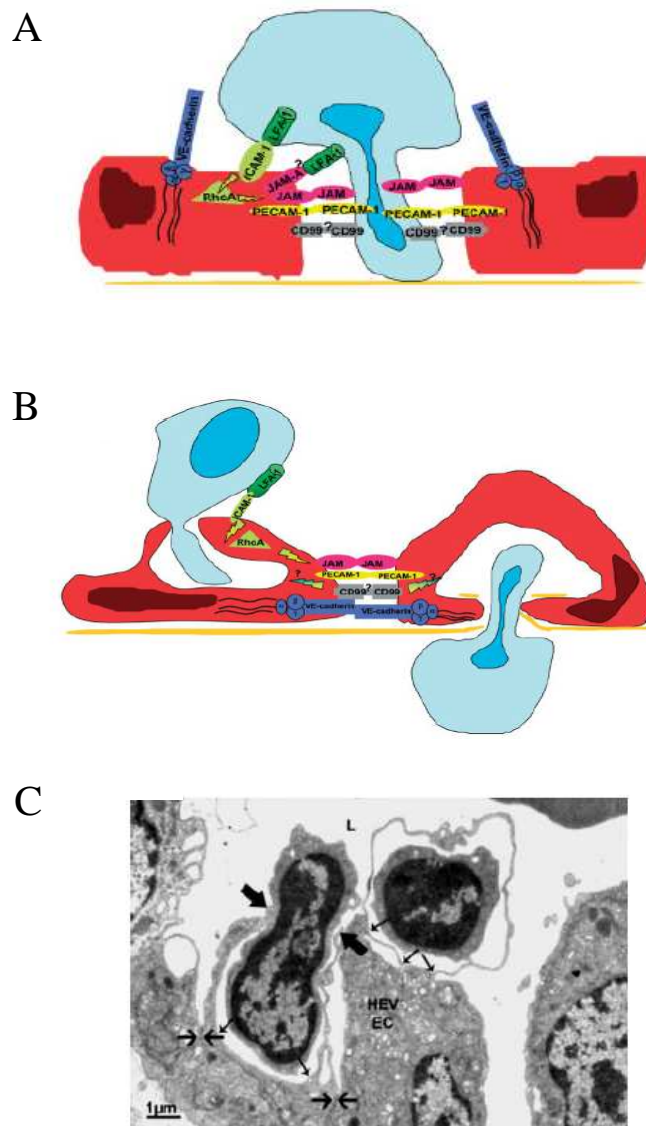


Ley K et al, *Nat Rev Immunol*, 2007 (modified)

**Fig. 1.** Cascade of leukocyte recruitment (description in text).

Two main routes of leukocyte transendothelial migration are described in the literature: i) the transcellular route, when leukocytes emigrate through the body of endothelial cells, and ii) the paracellular route, when leukocytes emigrate through junctions between adjacent endothelial cells (Fig. 2) (19), (8). The “transcellular pathway” is regulated by vesicles, which have specific receptors or enable the adhesiveness by unspecific absorption to the membrane (21), (22). A lot of studies suggest that an engagement of endothelial ICAM-1 in transcellular migration *via* binding to LFA-1 on leukocytes induces the formation of microvilli-like endothelial cell projections embracing the migrating leukocyte in a cup-like structure (23), (24). A similar docking structure enriched for ICAM-1 and VCAM-1 was described, when leukocytes were found to induce spike-like endothelial projections partially embracing those (24). Interestingly, cytoplasmic proteins and cytoskeletal components, such as alpha-actin, vinculin, and Wiskott–Aldrich syndrome protein (WASP) were also detected in the docking structures (25), (23). Most of the recently published studies identify, however, the paracellular migration route as the main mechanism by which leukocytes emigrate from the intravascular compartment into the interstitium (23). The current literature defines several endothelial cell contact proteins, such as platelet endothelial cell adhesion

molecule-1 (PECAM-1), members of the junctional adhesion molecule (JAM) family (JAM-A, JAM-B, and JAM-C), CD99, and ICAM-2, as important receptors during transendothelial leukocyte migration, although the detailed mechanisms by which they mediate this process are not yet fully understood (7), (8).

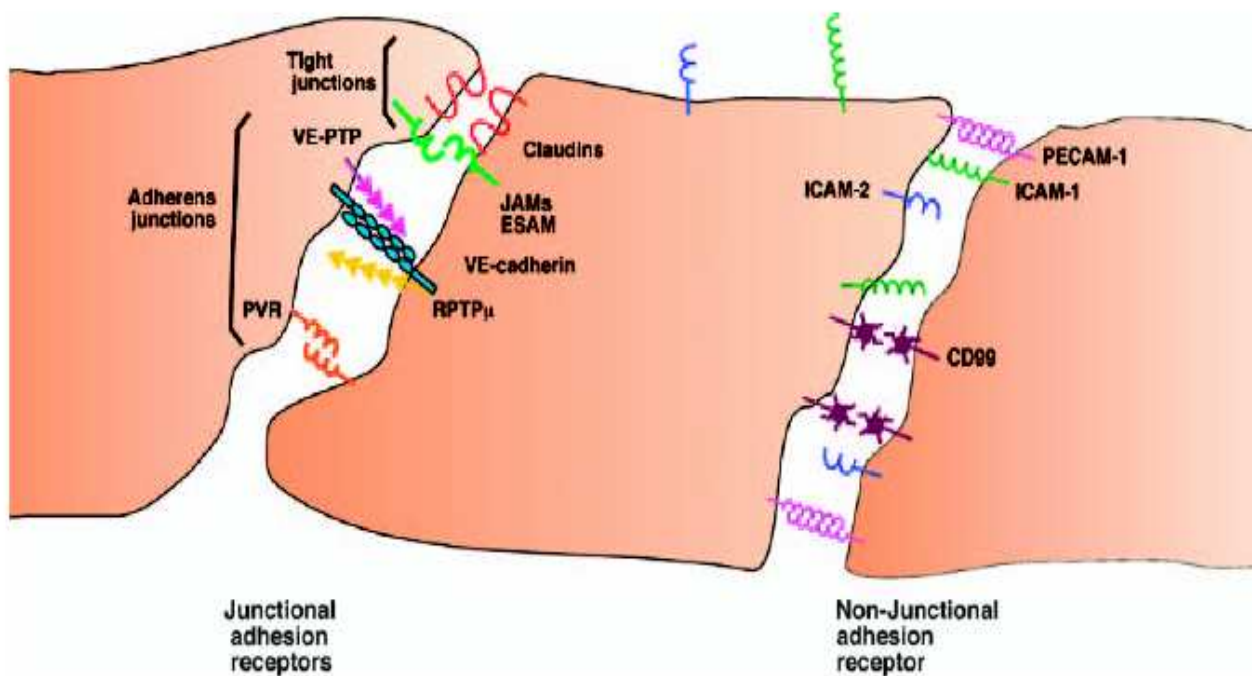


Engelhardt B et al, *Eur J Immun*, 2004

**Fig. 2.** Alternative passageways of leukocyte migration across endothelium. A - Leukocyte paracellular migration, which is mediated by homophilic interactions with endothelial adhesion molecules, such as PECAM-1, members of the JAM family, and probably ESAM and CD99, whereas VE-cadherin redistributes to the endothelial cell surface. B - Transcellular route of leukocyte transendothelial migration, which seems to be triggered by the ICAM-1. C - Electron microscopy image demonstrating both routes of transendothelial migration.

### 1.1.1 Adhesion molecules involved in leukocyte transmigration .

Endothelial cells are tightly connected through various proteins that regulate the organization of the junctional complex and govern transendothelial leukocyte migration (8). In the endothelium, junctional complexes comprise tight junctions, adherens junctions, and gap junctions (Fig. 3). Gap junctions are communication structures which allow the passage of small molecular weight solutes between neighboring cells. Tight junctions are situated at the apical, intravascular side and include claudins, occludins, JAM, and endothelial cell-selective adhesion molecule (ESAM). They provide a "barrier" and a "fence" within the membrane. Adherens junctions are presented by cadherins, such as vascular endothelial cadherin (VE-cadherin) and catenins ( $\beta$ -catenin, placoglobin, p120), and play an important role for endothelial cell growth, angiogenesis, and paracellular endothelial permeability. In addition, endothelial cells express other adhesive proteins which are concentrated at the intercellular clefts but not specifically confined to adherens or tight junctions, such as PECAM-1, ICAM-1 and -2, and CD99.



<http://www.mpi-muenster.mpg.de>

**Fig. 3.** Endothelial cell-cell contacts (description in text).

**PECAM-1** (CD31) is one of the widely studied adhesion molecules involved in leukocyte transmigration. It is a member of the immunoglobulin gene superfamily that is expressed on leukocytes, platelets, neutrophils, monocytes, and selected T cell subsets (26). On endothelial cells, PECAM-1 is concentrated at intercellular junctions. Studies with neutralizing antibodies have indicated a role of PECAM-1 in leukocyte transmigration without any effect on adherence (27). It is well known that this adhesion molecule organizes endothelial cell-cell contact *via* homophilic interactions and binds to ligands on migrating leukocytes *via* heterophilic interactions. Disruption of PECAM-1-PECAM-1 homophilic interactions allows leukocytes to emigrate through the endothelial barrier (28), (29). Moreover, the homophilic interactions of PECAM-1 upregulate  $\alpha 6$ -integrins as well as neutrophil elastase on transmigrating leukocytes that enables further neutrophil trafficking through the basement membrane (30), (31).

**JAMs** are a family of glycoproteins characterized by two immunoglobulin folds (Vh- and C2-type) in the extracellular domain (32), (33). JAM proteins are localized in the intercellular junctions of polarized endothelial and epithelial cells but can also be expressed on circulating leukocytes and platelets (34). Blocking antibodies against JAM or JAM-deficiency decrease neutrophil or monocyte extravasation during meningitis and peritonitis as well as in inflammation models in skin, cremaster muscle, heart, and liver (35), (36). The mechanism of action of JAM-A in promoting leukocyte extravasation is not completely clarified because endothelial JAM-A may direct the movement of leukocytes through cell-cell junctions by either homophilic interactions with JAM-A expressed on the leukocyte membrane or by heterophilic interactions with endothelial JAM-A *via* binding to LFA-1 on leukocytes. Recent works showed that JAM-A is also required for neutrophil directional motility to the site of inflammation *via* integrin dynamic activation/inactivation and cytoskeleton reorganization (37). In addition, also other members of the JAM family, such as JAM-B and JAM-C, are discussed to be involved in leukocyte adhesion, transmigration, and interactions between different cell subsets during inflammation (38).

**VE-cadherin** is an adhesion molecule that plays a role for the maintenance of interendothelial cell contacts (39). This protein is expressed at adherens junctions and associates with the cytoplasmic catenins. Plakoglobin ( $\gamma$ -catenin) and  $\beta$ -catenin connect VE-cadherin *via*  $\alpha$ -catenin to the actin cytoskeleton (40). It was found that antibodies against human VE-cadherin dissociate the contacts of endothelial cells in culture (41). As shown in cultured cells as well as in vascular tissues, VE-cadherin-containing adherent junctions during leukocyte diapedesis were relocated aside, not opened or disrupted and then moved back to their original positions when the leukocyte transmigration process was completed (42).

**ICAM-1 and ICAM-2** are members of the immunoglobulin superfamily of adhesion molecules composed of 2 N-terminal Ig domains with 35% homology, a transmembrane domain, and a short cytoplasmic tail of 27 amino acids (43). ICAM-1 is constitutively expressed on endothelial cells, platelets, and most leukocytes (43), (44). In contrast to ICAM-1, ICAM-2 appears to be concentrated at endothelial cell junctions (43). Both ICAMs represent endothelial ligands for the leukocyte  $\beta$ -2 integrin LFA-1 and have been shown to participate in the docking of leukocytes to the endothelium (24), (44). The role of ICAM-1 for leukocyte diapedesis was demonstrated in various *in vitro* studies with T cells (45) and monocytes *in vivo* (44), (46), (47). Several studies suggested a role of ICAM-2 for transmigration of all leukocyte subsets through stimulated and unstimulated HUVECs (45; 48).

**VCAM-1** is an adhesion molecule that is not constitutively expressed on endothelial cells but is upregulated by chemokines (49). It has been found that this molecule interacts with monocytes and lymphocytes and participates in leukocyte transmigration during the inflammatory response (7). A study in LFA-1-deficient mice revealed that VCAM-1 might play also a role in lymphocyte homing into primary lymphatic organs (50). Since VCAM-1 has not been identified at endothelial cell-cell contacts, it appears that this molecule exclusively mediates the attachment of leukocytes to the endothelium (7).

In addition to these relatively well investigated adhesion molecules, three recently discovered members of cell-contact proteins, ESAM, CD99, and CD99L2, are suggested to play an important role during leukocyte transendothelial migration. **ESAM** is an adhesion molecule that is specifically expressed at endothelial tight junctions and on platelets (51). ESAM is related to the JAM family, but differs considerably in structure, cytosolic binding partners (52), and tissue distribution (51). In contrast to the JAMs, expression of ESAM is strictly limited to endothelial cells and platelets and can not be found on leukocytes or epithelia (51). On platelets, ESAM is only expressed upon activation, whereas on endothelial cells it is strictly bound to tight junctions as demonstrated by immunogold labeling (53). Since ESAM is localized at endothelial tight junctions and has been shown to play a role in tumor angiogenesis (54), it might be also involved in leukocyte migration during the acute or chronic inflammatory response. However, the role of ESAM for leukocyte migration has not yet been analyzed.

**CD99** is a small (about 100 amino acids, 32 kD) membrane protein with a highly O-glycosylated extracellular part that is expressed on the surfaces of most leukocytes and is concentrated at the borders between confluent endothelial cells (55). It has been shown *in vitro* that CD99 plays a role in transmigration of human monocytes through the monolayer of human endothelial cells (55). In addition, antibodies against mouse CD99 inhibited the recruitment of lymphocytes in inflamed skin (56). Using HUVEC monolayers as a model of inflammation *in vitro*, Lou *et al.* found that antibodies against CD99 blocked over 80% of human neutrophil transmigration (57). It has been also shown that blocking of either the neutrophil or the endothelial CD99 led to quantitatively equivalent reduction of leukocyte extravasation (57). This fact suggests that an interaction between CD99 on the neutrophil and CD99 on the endothelial cell might occur to allow neutrophil diapedesis. In addition, blockade of both CD99 and PECAM-1 resulted in additive effects on monocyte migration *in vitro*, assuming that the two molecules work at distinct steps (57). However, the question of whether CD99 is involved in transendothelial migration *in vivo* has been not answered, so far.

**CD99L2** represents a protein of unknown function with moderate sequence homology to CD99 which is expressed on leukocytes and endothelial cells (58), (59). In tissues, this molecule is widely distributed with prominent expression on neuronal cells, choroid plexus, Sertoli cells, and granulosa and theca cells of the ovary (58). Although no studies have been performed that would attribute any function to CD99, it was tentatively named CD99 antigen like-2 (CD99L2) (59). Despite the structural homology to CD99, there are no data in the literature demonstrating a role of this receptor for leukocyte migration.

## 1.2 Leukocyte interstitial migration

After penetration of the endothelial barrier, leukocytes move in the interstitium to the site of injury. Leukocyte interstitial migration is suggested to be of a critical importance not only for tissue injury, but also for reparative events (60), (61), (62).

Emigrated immune cells moving within the interstitium are suggested to accomplish **leukocyte chemotaxis** – directed migration along gradients of chemotactic agents toward their destinations (63), (64), (65). Leukocyte chemotaxis is dependent on the ability of migrating cells to sense gradients of chemoattractants, serving as a “driving force” for immune cells (65), (66), (67). Several signaling pathways have been proposed to be involved in this gradient-amplification process, the most predominant being the phosphatidylinositol-3 kinase (PI3K) pathway (68). Thereby leukocytes use an „internal compass“ for sensing the direction of chemotactic gradients, and undergo polarization characterized by the formation of lamellipodia at the leading edge of the cell and an uropod at the trailing edge (69), (70). **Chemokines** are released by mast cells, smooth muscle cells, fibroblasts, myocytes, dendritic cells, and endothelial cells (67). The intercellular communication in the extracellular matrix (ECM) is mediated by **glycosaminoglycans** which interact with chemokines using low affinity interaction and, therefore, control the site and duration of soluble chemokine gradient (71), (72). In addition, glycosaminoglycans are suggested to be involved in transport, clearance, and degradation of chemokines (65). So called “interceptors” such

as DARC (Duffy antigen receptor for chemokines) and D6 are considered to transport chemokines and present them on the apical side of endothelium (13), (19). The effect of chemokines on leukocyte migration is accomplished by triggering GPCRs on the leukocyte surface. Recent studies have reported that leukocytes integrate signals from different combinations of cytokines that they encounter either simultaneously or sequentially within the ECM (71). The combinatorial effects of multiple chemokines and cytokines affect interstitially migrating leukocytes in a step-by-step manner, whereby cells react to chemotactic signals in their immediate vicinity by directional movement and remodeling of the ECM (67).

Leukocytes moving within the interstitial tissue receive signals from neighboring cells as well as from the ECM, activate intracellular processes, release inflammatory mediators, and upregulate adhesion molecules and enzymes (73), (74). Although neutrophils display enhanced expression of  $\beta$ 1-integrins upon transmigration, it remains a controversial discussion whether integrins are relevant for interstitial leukocyte migration (75), (76), (64), (77). In this context, leukocyte-released proteolytic enzymes (proteases) such as heparase, elastase, and matrix metalloproteinases (MMP-2 and MMP-9) seem to play a critical role for leukocyte interstitial migration. They are required for the degradation of the components of the basement membrane as well as of the ECM and therefore allow leukocyte moving within interstitial microenvironment (78), (79).

The next important issue is the cytoskeleton reorganization during leukocyte interstitial migration. In response to chemoattractants, leukocytes rapidly polarize in the direction of the signal, forming a pseudopod on the side of highest chemotactic concentration and an uropod or posterior domain on the opposite side of the cell; these structures become the leading and trailing edges of the chemotaxing cell, respectively (80). This process is mediated by leukocyte cytoskeletal dynamics. Cytoskeleton reorganization has been found to be regulated by JAM-A- and C (34), calcium-dependent protease calpain (81), (52), LFA-1, CD11b/CD18 (Mac-1) and alpha-integrins (82) as well as by PI3Ks or the non-receptor tyrosine kinases, such as Syk or Btk (83), (84). Rho guanosine triphosphate proteases (Rho/GTPases) are also involved in regulation of cytoskeleton

reorganization during leukocyte chemotaxis (68), (73), (85). Being molecular switches that control a variety of signal transduction pathways in all eukaryotic cells, they are suggested to play a pivotal role in the regulation of cell polarity (86), microtubule dynamics (87), membrane transport pathways, and transcription factor activity in response to extracellular stimuli

Although leukocyte interstitial migration is suggested to be of critical importance for the development of an inflammatory response and tissue repair, this process remains not fully understood. The vast majority of the studies on leukocyte directional migration were performed *in vitro*. However, there is a growing body of evidence suggesting that the mechanisms underlying leukocyte directional migration within the interstitium might differ between *in vitro* and *in vivo* settings (19), (65). Although two-dimensional (2D) substrates were preferentially used for *in vitro* studies on leukocyte chemotaxis, the mechanisms mediating this process seem to be rather different in 2D vs. 3D (three-dimensional) settings (77).

Therefore, it has to be investigated which mechanisms mediate motility of leukocytes “primed” during transmigration in the interstitium *in vivo* in 3D-microenvironment and to which extent these mechanisms vary in dependency on the type of inflammation. Whilst 2-photon laser scanning microscopy enabled investigations on the dynamics of lymphocyte and dendritic cell migration in the lymph node (88), directional migration of leukocytes in inflamed “non-lymphatic” tissue is poorly understood. The studying of leukocyte interstitial migration in “non-lymphatic tissues” *in vivo* remains limited because of induction of diffuse inflammation with “chemotactic chaos” in the interstitium after usage of conventional routes of stimulation such as superfusion or local administration of chemoattractants (89), (90), (91).

## 2. OBJECTIVES

The objectives of the present study were:

- 1) To analyze the role of ESAM for leukocyte migration during IL-1 $\beta$ -induced acute local inflammation in the mouse cremaster muscle using *in vivo* microscopy (IVM).
- 2) To characterize the role of CD99 and CD99L2 for leukocyte migration during IL-1 $\beta$ -induced acute local inflammation in the mouse cremaster muscle using IVM.
- 3) To establish an *in vivo* approach enabling investigations of leukocyte directional interstitial migration in the natural 3D microenvironment.

### 3. MATERIAL AND METHODS

All experiments were performed at the Institute for Surgical Research, Walter Brendel Centre of Experimental Medicine, Ludwig-Maximilians-Universität München, according to German legislation on the protection of animals and Government of Bavaria (reference number: 97-03).

#### 3.1 Animals

Male C57BL/6 wild-type (Charles-River, Sulzfeld, Germany), ESAM<sup>-/-</sup>, and PECAM-1<sup>-/-</sup> mice with background C57BL/6 (generated and provided by the group of Prof. Dr. D. Vestweber, Max-Planck-Institute of Molecular Biomedicine, Muenster, Germany) and weight from 20 to 25 g were used. The mice were held under control of day/night cycle in groups from 3 to 5 animals in Makrolon-cages and had free access to tap water and pellet food (ssniff Spezialdiäten, Soest, Germany).

#### 3.2 Reagents and inhibitors

Recombinant mouse interleukin-1-beta (IL-1 $\beta$ ), recombinant murine macrophage inflammatory protein-1  $\alpha$  (MIP-1 $\alpha$ /Ccl3), and monocyte chemotactic protein-1 (MCP-1/Ccl2) were purchased from R&D Systems<sup>®</sup> (Wiesbaden-Nordenstadt, Germany). Phospholipid platelet-activating factor (PAF) and Rho kinase inhibitor Y27632 were purchased from Sigma Aldrich (Deisenhofen, Germany).

#### 3.3 Blocking antibodies

The blocking antibodies used in our study were generated and provided by the group of Prof. Dr. D. Vestweber. Polyclonal rabbit antisera against mouse CD99L2 were generated against the CD99L2-Fc fusion protein. Antibodies against the IgG1-Fc part were removed from the serum by incubation with human IgG1-coupled to CNBr-activated Sepharose (Amersham Pharmacia

Biothec, Freiburg). Specific antibodies against CD99L2 were affinity-purified with CD99L2 immobilized on CNBr-Sepharose. Affinity-purified polyclonal antibodies against mouse CD99 were generated as described previously (92). F(ab')<sub>2</sub>-fragments were generated with immobilized pepsin on beads (Pierce, Rockford, IL) according to the manufacturer's protocol. Uncleaved IgG and Fc-fragments were removed using protein A Sepharose (GE Healthcare). Purity (< 0.3% intact IgG) and proper size of the F(ab')<sub>2</sub>-fragments were confirmed by sodium dodecyl sulfate (SDS)-polyacrylamide gel electrophoresis (PAGE). Relative binding efficiency was tested by enzyme-linked immunosorbent assay using CD99L2-Fc as antigen. No endotoxin was detectable.

### 3.4 Model

#### 3.4.1 Anesthesia

Animals were narcotized using intraperitoneal injection of Ketavet<sup>®</sup> (ketaminhydrochloride; 100mg/kg) and Rompun<sup>®</sup> (xylazinhydrochloride; 10 mg/kg). This dose was sufficient to keep the mouse under anesthesia during 35-45 min. After initiation of anesthesia, the animals were fixed on a heating plate. The body temperature was controlled using a temperature sensor and kept constantly at 37°C. Additive intraperitoneal injections of ketamine (100 mg/kg) were performed during experiments lasting more than 1 hour. Short inhalation anesthesia (5 min) with isoflurane (2 Vol. %, Forene<sup>®</sup>, Abbott GmbH, Wiesbaden, Germany) and N<sub>2</sub>O (FiO<sub>2</sub> 0.35) was used for the intrascrotal injection of inflammatory mediators.

#### 3.4.2 Catheterization of *a. femoralis*

To administer fluorescent beads for the measurement of centerline blood flow velocity, the left femoral artery was catheterized in narcotized mice. Catheterization was performed on the microsurgical workstation with heated stage (37°) using a surgical microscope (Leica M651, Wetzlar, Germany). After incision of the skin in the middle of the hip, the fascia was removed and the *arteria femoralis* was dissected from *vena femoralis* and *nervus femoralis* (microscopic

magnification 25x). Then, the *a. femoralis* was ligated in the distal segment using silk ligature and clamped in the proximal segment using a vessel microclip (microscopic magnification 40x). After incision of the vessel, a propylene-catheter (0.28 ID/0.61 OD, Portex, UK) was inserted into the artery and then fixed using a silk ligature.

### **3.4.3 Catheterization of *v. jugularis interna***

Systemic application of antibodies was performed via a catheter placed in *v. jugularis interna*. After surgical preparation of the jugular vein from the surrounding tissue, a fine incision of the vessel was made using microscissors; the catheter was inserted into the vessel and fixed by two silk ligatures.

### **3.4.4 Surgical preparation of cremaster muscle**

The surgical procedure was performed according to the technique described by Baez with slight modifications (93). The scrotum was moderately extended by means of an anchoring thread passed through the hind pole. After coagulation of blood vessels using careful electrocautery to stop any bleeding, an initial longitudinal incision of skin and fascia was made in the midline in a relatively avascular zone over the ventral aspect of scrotum. The incision was extended up to 5-8 mm above inguinal fold and to the distal end of the scrotum. Epididymis and testicle were detached from the cremaster muscle and placed into the abdominal cavity. Then, the cremasteric tissue was spread over the mirroring pedestal of a custom-made microscopic stage. Throughout the procedure as well as after surgical preparation during IVM, the muscle was superfused with warm (37°C) buffered saline. After surgical preparation, which usually required 10-20 minutes, the stage was transferred to the microscope. The temperature of the superfusion buffer was maintained at 37°C by a heating lamp and a measured by digital thermometer (TFN 1093, Ebro Electronic GmbH, Ingolstadt, Germany).

### ***3.4.5 Near-infrared reflected light oblique transillumination (RLOT) microscopy***

The setup for IVM was centered on an Olympus BX50 upright microscope (Olympus Microscopy, Hamburg, Germany) equipped for stroboscopic fluorescence epi-illumination microscopy. Light from a 75-watt xenon source was narrowed to a near-monochromatic beam of a wavelength of 700 nm by a galvanometric scanner (Polychrome II; TILL Photonics, Gräfelfing, Germany) and directed onto the specimen via an FITC filter equipped with dichroic and emission filters (DCLP 500, LP515, Olympus Microscopy). Microscopic images were obtained with Olympus water immersion lenses (20x numerical aperture (NA) 0.5 and 40xNA 0.8) and recorded with an analog black and white charged-coupled device video camera (Cohu 4920, Cohu, San Diego, CA) and an analog video recorder (AG-7350-E, Panasonic, Tokyo, Japan). Oblique illumination was obtained by positioning a mirroring surface (reflector) directly below the specimen and tilting its angle relative to the horizontal plane. The reflector consisted of a round coverglass (thickness 0.19-0.22 mm, diameter 11.8 mm), which was coated with aluminum vapor (Freichel, Kaufbeuren, Germany) and brought into direct contact with the overlying specimen.

### ***3.4.6 Microinjection of inflammatory mediators***

Microinjection was performed using a semiautomatic microinjector (FemtoJet<sup>®</sup>, Eppendorf, Hamburg, Germany) and a micromanipulator (InjectMan<sup>®</sup> NI 2, Eppendorf), consisting of a control board and a module unit with capillary holder (Fig. 4A). The injection parameters (tip pressure: 120 hPa; time of injection: 0.5 sec) were adjusted on the microinjector. The module unit comprises the motor unit for horizontal and vertical movement and serves for the installation of injection angle (Fig. 4A). As microcapillaries, borosilicate micropipettes with tip diameter <1 µm, connected to the capillary holder on the module unit were used. Through an exertion of joystick on the control board of the micromanipulator, the movements of the microcapillary were regulated under control of IVM (lens 4x, numeric aperture 0.12, Leitz, Wetzlar, Germany) (Fig.4A).

Single unbranched postcapillary venules with diameters between 20-35  $\mu\text{m}$  and lengths  $>150 \mu\text{m}$  were selected for this study. Under control of IVM (objective magnification 4x), microinjection of chemoattractants was performed into the cremasteric tissue in the perivascular region 25-50  $\mu\text{m}$  from the venule (Fig. 4B). A successful microinjection was verified by the observation of visible swelling of the interstitial tissue during injection. In control experiments with usage of rhodamine 6G, the fluorescent dye could be clearly visualized in the tissue using fluorescence microscopy. Postcapillary venule as well as surrounding tissue were visualized at baseline conditions before stimulation as well as 60 min after microinjection under objective magnification 20x. Leukocyte recruitment and interstitial migration were analyzed after microinjection of either the CC chemokine MIP-1 $\alpha$  (250 nM), the phospholipid PAF (100 nM), or saline (6 animals in each group).

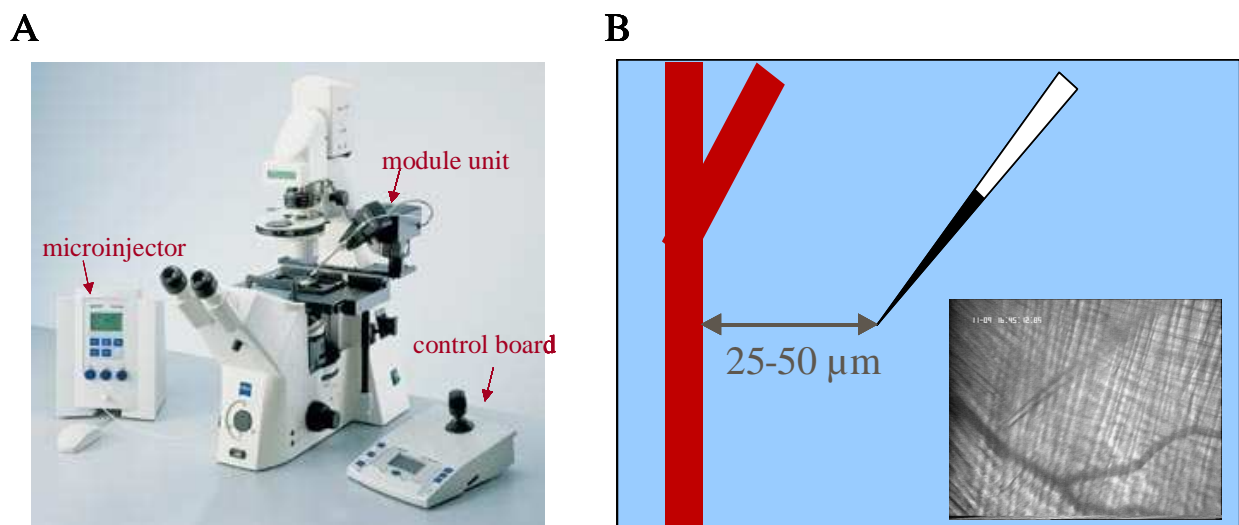


**Fig. 4.** A - Microinjection system comprising the microinjector FemtoJet<sup>®</sup> and the micromanipulator InjectMan<sup>®</sup> NI 2, which consists of control board and module unit (modified illustration from the catalogue of “Eppendorf”). B - Schematic representation and intravital microscopic image demonstrating the technique of microinjection (objective magnification 4x).

### **3.4.7 Microhemodynamic parameters**

Centerline blood flow velocity was measured using microspheres (2 $\mu$ m; FluoSpheres; Invitrogen, Karlsruhe, Germany) administered intraarterially. Quantitative analysis of velocity was performed off-line using CAPIImage<sup>®</sup> by measuring the distance between several images of one fluorescent bead under stroboscopic illumination. From measurement of the vessel diameters and centerline blood flow velocity, the Newtonian wall shear rate [ $s^{-1}$ ] was estimated as  $8 \times [V_b / d]$ , where  $V_b$  is the mean blood flow velocity,  $d$  is the diameter of the vessel. Mean blood velocity,  $V_b$ , was approximated by multiplying the centerline blood velocity by 0.625. The interfacial shear rate is the slope of the velocity profile at the interface of the endothelial surface layer and the vessel lumen, and it was calculated as  $4.9 \times 8 \times [V_b / d]$ , where 4.9 is a mean empirical correction factor (94).

### **3.4.8 Parameters of leukocyte recruitment**

Quantitative analysis of leukocyte-endothelial cell interactions was performed off-line using CAPIImage<sup>®</sup>. Rolling leukocytes were defined as those moving slower than the associated blood flow and quantified during 30 seconds. Leukocyte rolling flux fraction was determined from video recordings by counting all visible cells passing through a plane perpendicular to the vessel axis and dividing this number by the total leukocyte flux through the vessel, which can be estimated by the product of the systemic leukocyte count, mean blood flow velocity, and estimated vessel cross-sectional area. Firmly adherent cells were determined as those resting in the associated blood flow for more than 30 sec and related to the luminal surface per 100  $\mu$ m vessel length. Emigrated cells were counted in regions of interests (ROIs) reaching out 75  $\mu$ m to each side of a vessel over a distance of 100  $\mu$ m vessel length and are presented per  $10^4 \mu\text{m}^2$  tissue area.

### ***3.4.9 Single cell tracking of emigrated leukocytes***

Intravital microscopic video recordings were transferred into a computer system using a frame grabber. Digital video sequences were analyzed using the imaging software “Simple PCI” (Hamamatsu Corporation/Compix Inc., Cranberry Twp, PA). On each side of analyzed vessel, at least 15 emigrated leukocytes were identified (Fig. 5A) within ROIs and tracked in the perivascular space within a time period of 5 min. Parameters of leukocyte motility, such as migration velocity (curve-line and straight-line) and migration distance (curve-line and straight-line) were automatically calculated by the software. Curve-line migration distance is presented as a line connecting the position of migrating leukocyte at each time point (Fig. 5B, red line). Straight-line distance represents the shortest line connecting the start and end point of the leukocyte migration track (Fig. 5B, black line). Velocity is the speed along the curve-line distance or straight-line distance, respectively.

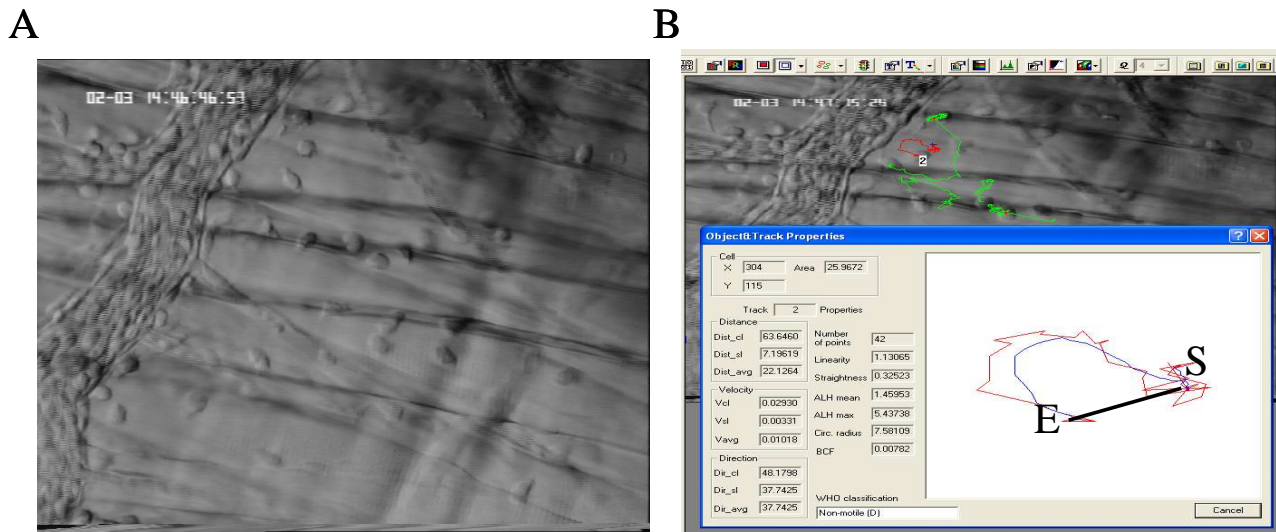


**Fig. 5.** Analysis of motility of interstitially migrating leukocytes. A – A representative RLOT image showing interstitially migrating leukocytes in a perivascular region of the inflamed cremasteric tissue. B - Semiautomatic tracking of single leukocytes using the imaging software; the red line represents the curve-line migration distance from start point “S” to the end point “E”, whereas the black line shows the straight-line migration distance from the start point “S” to the end point “E”; the average migration distance is demonstrated as a blue line.

#### 3.4.10 Morphological changes and polarization in interstitially migrating leukocytes

In separate experiments, morphological changes in interstitially migrating leukocytes were evaluated using RLOT microscopy under higher magnification (objective magnification 50x). Randomly chosen single leukocytes were visualized and recorded in ROIs for 5 min at 60 min after chemotactic stimulation performed either by microinjection or intrascrotal injection. Polarization of interstitially migrating leukocytes was analyzed in digitalized intravital microscopic images. The major axis and the minor axis of single interstitially migrating leukocytes were measured. Polarization was determined off-line by measuring the eccentricity of the cell which is equal to the ratio of the major axis of the cell (longest straight line that can be drawn across the cell) and minor axis (longest straight line that can be drawn across the cell at 90° to the major axis) (68). Leukocytes with eccentricity of  $\geq 1.2$  were considered as polarized (68).

### ***3.4.11 Tissue distribution of applied fluorescent dye per time***

In an attempt to get information about the character of tissue distribution of injected mediators, microinjection of the fluorescent dye rhodamine 6G (130  $\mu$ l, 0.05%, Sigma Aldrich) was performed in the cremaster muscle according to the above described technique in a separate set of experiments (n=7). The distribution of rhodamin 6G in the interstitium was analyzed in the areas of interests using *in vivo* fluorescence microscopy (excitation: 530 to 560 nm, emission: >580 nm, Olympus). Light from a 75-watt xenon source was narrowed to a near monochromatic beam by a digitally controlled galvanometric scanner (Polychrome II, TILL Photonics, Gräfelfing, Germany). Fluorescence emission was collected by a CCD camera (Sensicam, PCO, Kelheim, Germany) and subjected to digital image analysis (TILL Vision 4.0; TILL Photonics). Spatial dynamics of the fluorescence intensity were measured before and within 60 min after microinjection and expressed as mean gray value (95). Mean gray values of three regions of interests (ROIs) (100 x 75  $\mu$ m) were analyzed on the vessel side of the postcapillary venule ipsilateral to the microinjection, on the contralateral side as well as in the interstitial tissue 350  $\mu$ m from the site of microinjection (considered as background).

### ***3.4.12 Visualization of mitochondrial redistribution in interstitially migrating leukocytes***

Upon stimulation with chemoattractants, the redistribution of mitochondria was analyzed in single interstitially migrating leukocytes after intraarterial application of green-fluorescent mitochondrial stain MitoTracker® Green (200 nM, 150  $\mu$ l, Invitrogen, Germany) immediately before surgical preparation of the muscle. MitoTracker® Green-labeled interstitially migrating leukocytes were visualized in perivenular regions 60 min after intrascrotal injection of PAF using the following technical devices: epifluorescent microscope, AxioTech-Vario 100 Microscope (Carl Zeiss, Jena, Germany; objective magnification 63x, N.A 1.0 water dipping), LED (Light Emitting Diode Colibri, Zeiss) light source for fluorescent illumination (470 nm) and near-infrared RLOT illumination (625 nm, filter cube 62 HE, Zeiss). IVM images were obtained with a digital

Highspeed-camera AxioCam Hsm (Zeiss), time-lapse recordings (4.5 min) were analyzed using the AxioVision 4 software (Zeiss).

#### ***3.4.13 Imaging of the migratory behavior of leukocyte subsets***

Visualization and quantitative analysis of transendothelial and interstitial migration of neutrophils and Cx3CR1<sup>gfp/gfp</sup>-positive monocytes were made in Cx3CR1<sup>gfp/gfp</sup> mice 60-90 min after microinjection of MCP-1 (115 nM; n=1). The microinjection was performed at a distance of 25-50  $\mu$ m from the vessel. Cx3CR1<sup>gfp/gfp</sup> mice expressing green fluorescent protein (GFP) in blood monocytes were used. Interstitial migration of Cx3CR1<sup>gfp/gfp</sup>-positive cells (monocytes) and Cx3CR1<sup>gfp/gfp</sup>-negative cells (neutrophils) was visualized using the combination of RLOT and fluorescence microscopy (objective magnification 20x) and analyzed in perivenular ROI (100 x 75  $\mu$ m) on the vessel side ipsilateral to microinjection. Digital intravital microscopic video sequences were analyzed using Simple PCI software. Single cell tracking of extravasated Cx3CR1<sup>gfp/gfp</sup>-negative neutrophils or Cx3CR1<sup>gfp/gfp</sup>-positive monocytes (n=5 in each group) was performed at 60, 70, and 80 min after microinjection of MCP-1 for 5 min, respectively.

### 3.5 Experimental protocols and experimental groups

#### 3.5.1 Role of ESAM for IL-1 $\beta$ -induced leukocyte migration in vivo

The effect of ESAM deficiency on leukocyte migration was analyzed in wild-type and ESAM-deficient mice pretreated by intrascrotal injection of 50 ng of recombinant mouse IL-1 $\beta$  diluted in 0.3 mL PBS (30), (96). The intravital microscopic measurements were performed 4 h after stimulation (Tab. 1; Fig. 6). To evaluate a role of ESAM during an earlier phase of IL-1 $\beta$ -induced inflammation, leukocyte migration was analyzed 2 h after intrascrotal injection of IL-1 $\beta$  in wild-type and ESAM<sup>-/-</sup> mice (Tab. 1). Blood flow velocity and the systemic leukocyte count were measured at the end of each experiment (Fig. 6). The hemodynamic parameters as well as the parameters of leukocyte migration were analyzed as described above in 3.4.7 and 3.4.8.

**Tab. 1.** Experimental groups assessed in the study of the role of ESAM for leukocyte migration in vivo.

Stimulus	Application of IL-1 $\beta$	Animals	N
IL-1 $\beta$	4 h prior IVM	ESAM <sup>+/+</sup>	7
IL-1 $\beta$	4 h prior IVM	ESAM <sup>-/-</sup>	7
IL-1 $\beta$	2 h prior IVM	ESAM <sup>+/+</sup>	3
IL-1 $\beta$	2 h prior IVM	ESAM <sup>-/-</sup>	3

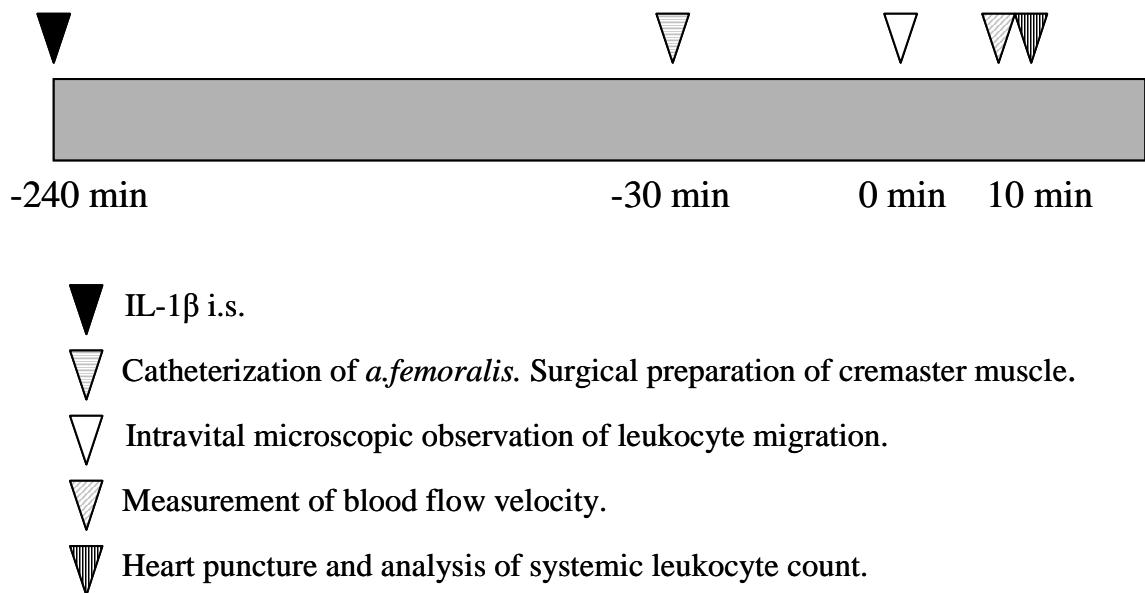


**Fig. 6.** Experimental protocol applied in the study of the role of ESAM for leukocyte migration in vivo.

### 3.5.2 Role of CD99 and CD99L2 for IL-1 $\beta$ -induced leukocyte migration in vivo

An acute inflammatory response in muscle tissue was achieved by intrascrotal injection of recombinant mouse IL-1 $\beta$  (50 ng). Mice were treated with either control IgG (50  $\mu$ g), anti-CD99 monoclonal antibody (50  $\mu$ g), or anti-CD99L2 monoclonal antibody (50  $\mu$ g) infused intravenously (Tab. 2; Fig. 8). The application of antibodies was performed immediately before intrascrotal injection of IL-1 $\beta$  (Fig. 8). To avoid unspecific activation of neutrophils via Fc-receptors, F(ab')<sub>2</sub>-fragments of anti-CD99 (75  $\mu$ g), anti-CD99L2 (75  $\mu$ g), and pre-immune control IgG (75  $\mu$ g) were infused after IL-1 $\beta$  stimulation (Tab. 2). In additional groups, potential synergistic effects between CD99 and CD99L2 with PECAM-1 during leukocyte migration were analyzed in PECAM-1<sup>-/-</sup> mice treated with either control-IgG, anti-CD99, or anti-CD99L2 antibody (Tab. 2). In all groups, the parameters of leukocyte migration were assessed at 4 h after stimulation, whereas the hemodynamic parameters and the systemic leukocyte count were measured at the end of each experiment (Fig. 7).

**Tab. 2.** Experimental groups assessed in the study of the role of CD99 and CD99L2 for leukocyte migration *in vivo*.

Stimulus	Animals	Treatment	N
IL-1 $\beta$	wild-type	IgG	6
IL-1 $\beta$	wild-type	anti-CD99	6
IL-1 $\beta$	wild-type	anti-CD99L2	6
IL-1 $\beta$	PECAM-1 $^{-/-}$	IgG	6
IL-1 $\beta$	PECAM-1 $^{-/-}$	anti-CD99	6
IL-1 $\beta$	PECAM-1 $^{-/-}$	anti-CD99L2	6
IL-1 $\beta$	wild-type	IgG-F(ab') <sub>2</sub>	6
IL-1 $\beta$	wild-type	anti-CD99-F(ab') <sub>2</sub>	6
IL-1 $\beta$	wild-type	anti-CD99L2-(Fab') <sub>2</sub>	6

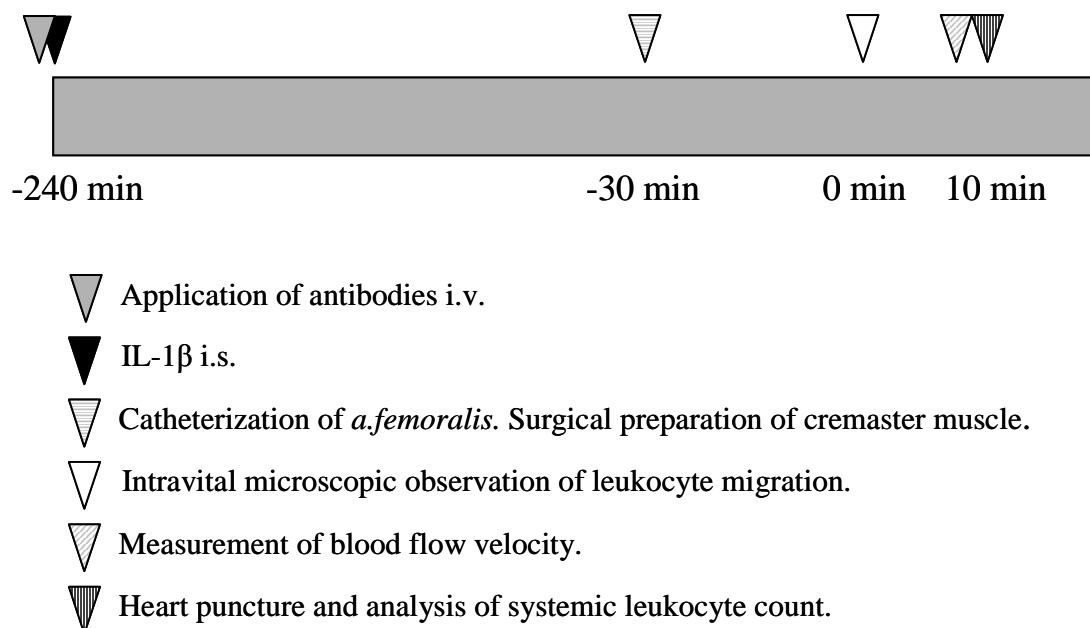


**Fig. 7.** Experimental protocol applied in the study of the role of CD99 and CD99L2 for leukocyte migration *in vivo*.

### ***3.5.3 Imaging and quantitative analysis of leukocyte directional migration in vivo***

In a first set of experiments, to find an optimal protocol for microinjection and to assess the extent of local inflammation in dependency on the distance between the site of microinjection and the adjacent vessel, microinjections of MIP-1 $\alpha$  were performed at three different distances from the venule: 25-50  $\mu\text{m}$ , 75-100  $\mu\text{m}$ , and 175-200  $\mu\text{m}$ . The numbers of adherent and transmigrated leukocytes were calculated 60 min after microinjections in ROIs (100 x 50  $\mu\text{m}$ ) along the venule.

Next, microinjection of rhodamine 6G (130 pl) was performed in the cremaster muscle according to the above described technique in order to investigate tissue distribution of injected mediators (n=7). The areas of interest (100x50  $\mu\text{m}$ ) were scanned using intravital fluorescence microscopy and fluorescence intensity was measured 1, 10, 30, 45, and 60 min after microinjection as described in 3.4.11.

In order to investigate the character of leukocyte migration upon stimulation with different mediators, either MIP-1 $\alpha$  (250 nM) or PAF (100 nM) were administered via microinjection in perivascular regions at the distance of 25-50  $\mu\text{m}$  from a postcapillary venule (6 animals in each group) (Tab. 4). The animals undergoing microinjection of saline served as controls (n=6). The vessel and the surrounding tissue were visualized by near-infrared RLOT IVM during a time period of 5 min 60 min after microinjection (Fig 8). In order to compare the character of leukocyte migration after microinjection of inflammatory mediators with that induced by the conventional route of stimulation, intrascrotal injection of PAF (100 nM in 0.3 ml PBS) was performed in an additional experimental group at 60 min prior to IVM (see Tab. 4).

**Tab. 4.** Experimental groups assessed in the study of leukocyte migration after microinjection of chemoattractants *in vivo*.

Stimulus	Animals	Application	N
saline	C57BL/6	microinjection	6
MIP-1 $\alpha$	C57BL/6	microinjection	6
PAF	C57BL/6	microinjection	6
PAF	C57BL/6	intrascrotal injection	3

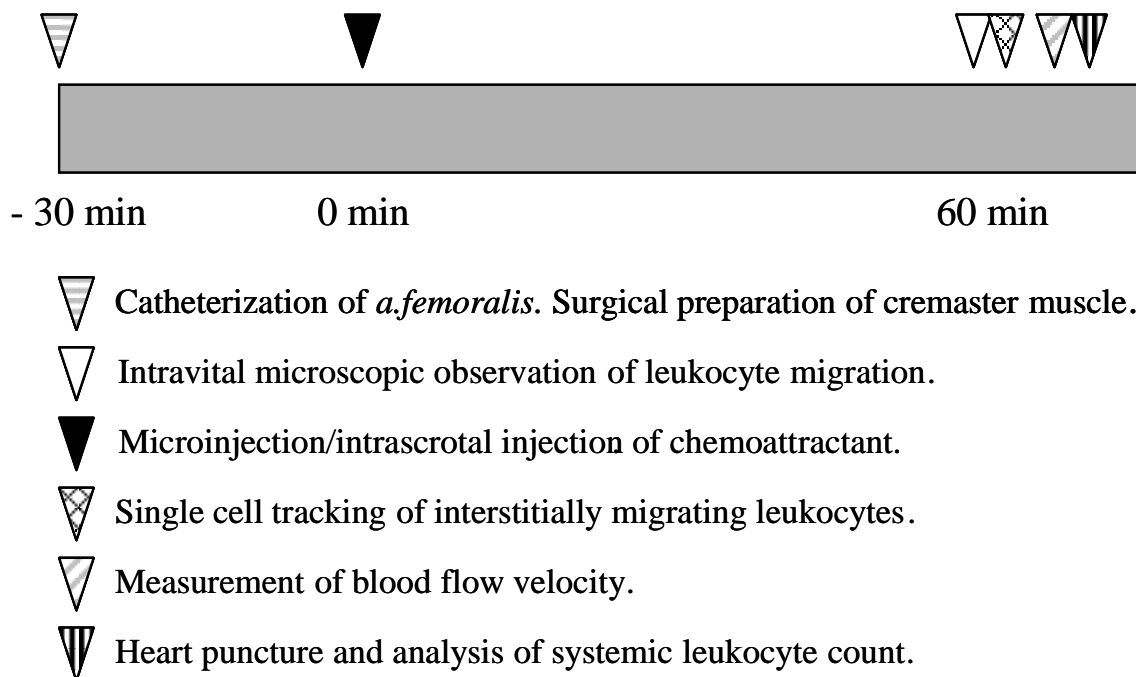


**Fig. 8.** Experimental protocol applied in the study of leukocyte migration after microinjection of chemoattractants *in vivo*.

In addition, we analyzed the role of Rho kinase for motility of interstitially migrating leukocytes *in vivo*. Parameters of leukocyte motility were analyzed after inhibition of Rho kinase with a selective

inhibitor Y-27632 (50  $\mu$ M) (87), (97)). Leukocyte migration was initiated by microinjection of MIP-1 $\alpha$ , as described above (Tab. 5). Sixty min after microinjection of MIP-1 $\alpha$ , the exteriorized cremaster muscle was superfused with Y-27632 for either 5 or 30 min (Tab. 5; Fig. 9). Intravital microscopic analysis was performed in two separate groups either 5 min or 30 min after superfusion of Y-27632. For both inhibitor-treated groups, corresponding time controls were performed with saline superfusion (Tab. 5; Fig. 9).

**Tab. 5.** Experimental groups assessed in the study of the role of Rho kinase for motility of interstitially migrating leukocytes *in vivo*.

Stimulus	Treatment	Observation time	Animals	Application	N
MIP-1 $\alpha$	-	60-65 min	C57BL/6	microinjection	3
MIP-1 $\alpha$	Y27632	60-65 min	C57BL/6	microinjection	3
MIP-1 $\alpha$	-	90-95 min	C57BL/6	microinjection	3
MIP-1 $\alpha$	Y27632	90-95 min	C57BL/6	microinjection	3

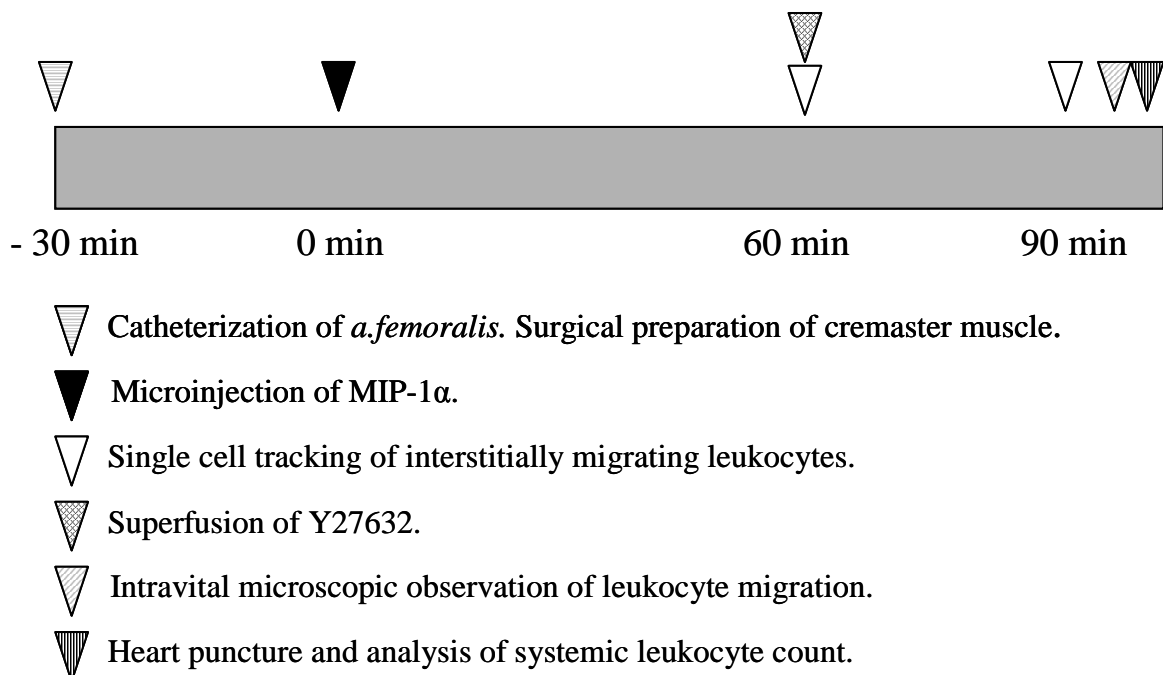


**Fig. 9.** Experimental protocol applied in the study of the role of Rho kinase for leukocyte interstitial migration *in vivo*.

Morphological changes and polarization of interstitially migrating leukocytes were evaluated using RLOT microscopy under a higher magnification (objective magnification 40x). Randomly chosen single leukocytes were visualized in ROIs i) 60 min after microinjection of PAF, ii) 60 min after intrascrotal injection of PAF, iii) and 60 min after microinjection of PAF followed by superfusion (30 min) with the Rho kinase inhibitor Y27632.

To visualize the redistribution of mitochondria in single interstitially migrating leukocytes upon stimulation with a chemoattractant, green-fluorescent mitochondrial stain MitoTracker<sup>®</sup> Green was applied via the *a. femoralis* catheter before surgical preparation of the cremaster muscle. MitoTracker<sup>®</sup> Green-positive interstitially migrating leukocytes were visualized in perivenular regions 60 min after intrascrotal injection of PAF.

In the last part of the study, we compared the migration patterns of neutrophils and monocytes upon microinjection of MCP-1. In these experiments, transgenic mice were used in which monocytes express green fluorescence protein (GFP). Intravital microscopic analysis was performed 60, 70, and 80 min after stimulation as described in *Material and Methods*.

#### **3.5.4 Statistical analysis**

Groups were compared with either ANOVA on ranks followed by Student-Newman-Keuls test (multigroup comparison) or t-test (two-group comparison) using SigmaStat statistic program (Jandel scientific, Erkrath, Germany). Mean values  $\pm$  standard error of the mean (SEM) are given. Differences between experimental groups reaching p value  $<0.05$  were considered significant.

## 4. RESULTS

### 4.1 The role of ESAM for IL-1 $\beta$ -induced leukocyte migration *in vivo*

#### 4.1.1 Microhemodynamic parameters

In the first part of our study, we investigated the role of ESAM for regulation of leukocyte migration *in vivo*. Microhemodynamic parameters, such as diameter of the vessel, centerline blood velocity, wall shear rate did not significantly differ among experimental groups (Tab. 6). Systemic white blood cell counts (WBC) were also comparable between all experimental groups (Tab. 6).

**Tab. 6.** Microhemodynamic parameters.

Parameter	IL-1 $\beta$ – 4h ESAM+/+ (n=7)	IL-1 $\beta$ – 4 h ESAM-/- (n=7)	IL-1 $\beta$ – 2h ESAM+/+ (n=2)	IL-1 $\beta$ – 2h ESAM-/- (n=2)
Vessel diameter ( $\mu\text{m}$ )	26.8 $\pm$ 0.9	26.4 $\pm$ 0.5	27.8 $\pm$ 3.9	28.1 $\pm$ 0.4
WBC ( $10^6$ cells x $\text{ml}^{-1}$ )	3.9 $\pm$ 0.5	3.1 $\pm$ 0.3	4.9 $\pm$ 0.2	4.6 $\pm$ 1.0
Centerline blood velocity ( $\mu\text{m}/\text{sec}$ )	1.8 $\pm$ 0.1	1.8 $\pm$ 0.1	1.6 $\pm$ 0.1	1.8 $\pm$ 0.1
Newtonian wall shear rate (8 x $V_{\text{mean}}$ / diameter)	339.1 $\pm$ 12.9	344.5 $\pm$ 9.4	475.0 $\pm$ 42.2	454.05 $\pm$ 28.9
Interfacial wall shear rate (4.9 x 8 x $V_{\text{mean}}$ / diameter)	1661.6 $\pm$ 63.1	1687.9 $\pm$ 45.9	2327.5 $\pm$ 206.8	2224.8 $\pm$ 141.6

mean  $\pm$  SEM, \*  $p < 0.05$ .

#### 4.1.2 Leukocyte migration parameters

Four hours after intrascrotal injection of IL-1 $\beta$ , leukocyte rolling flux fraction remained comparable between wild-type and ESAM $^{-/-}$  mice ( $16.9 \pm 4.5\%$  vs.  $15.9 \pm 1.3\%$ , respectively; Fig. 10A). Similarly, the number of adherent leukocytes in postcapillary venules did not differ between these two groups ( $13.1 \pm 0.6$  n/ $10^4\mu\text{m}^2$  vs.  $13.0 \pm 0.5$  n/ $10^4\mu\text{m}^2$ , respectively; Fig. 10B). In contrast, leukocyte transendothelial migration was reduced by about 50% in ESAM $^{-/-}$  mice ( $13.6 \pm 0.6$  n/ $10^4\mu\text{m}^2$ ) as compared to wild-type mice ( $24.9 \pm 1.1$  n/ $10^4\mu\text{m}^2$ ; Fig. 10C).

In an attempt to exclude that the effect observed at the level of leukocyte emigration was caused by differences in leukocyte rolling or adhesion at an earlier time point within the 4h period after stimulation, we assessed leukocyte migration 2h after the stimulation (Fig. 11). Leukocyte rolling flux fraction did not significantly differ between wild-type and ESAM $^{-/-}$  mice ( $16.2 \pm 1.7\%$  vs.  $16.2 \pm 1.6\%$ , respectively), and the results were comparable with the data obtained 4h after IL-1 $\beta$  application. The levels of leukocyte adhesion, however, were here clearly lower in both groups as compared to those 4 hours after IL-1 $\beta$  application (Fig. 10B and Fig. 11B) and remained similar between wild-type and ESAM $^{-/-}$  mice ( $7.6 \pm 0.3$  n/ $10^4\mu\text{m}^2$  vs.  $7.6 \pm 0.9$  n/ $10^4\mu\text{m}^2$ , respectively). The numbers of emigrated leukocyte were considerably lower as compared to those 4 hours after IL-1 $\beta$  application (Fig. 10C and Fig. 11C) and they were reduced in ESAM $^{-/-}$  mice ( $5.2 \pm 1.0$  n/ $10^4\mu\text{m}^2$ ) as compared to wild-type mice ( $7.1 \pm 1.3$  n/ $10^4\mu\text{m}^2$ ) (Fig. 11C).

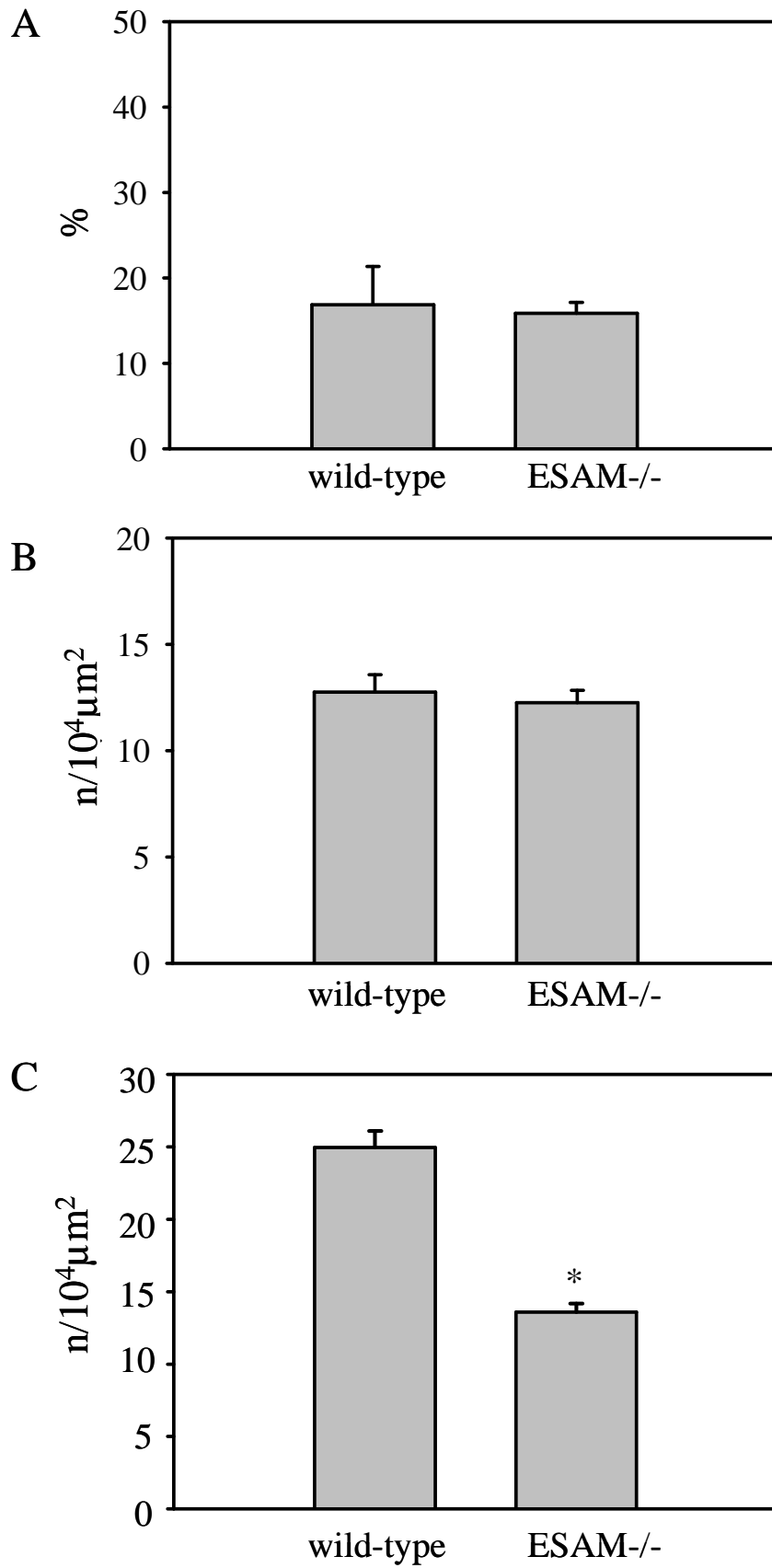


**Fig. 10.** Leukocyte rolling flux fraction (A), adhesion (B), and transmigration (C) in postcapillary venules of wild-type and ESAM<sup>-/-</sup> mice 4 h after intrascrotal injection of IL-1 $\beta$ ; mean  $\pm$  SEM, \*  $p < 0.05$ ;  $n = 7$ .

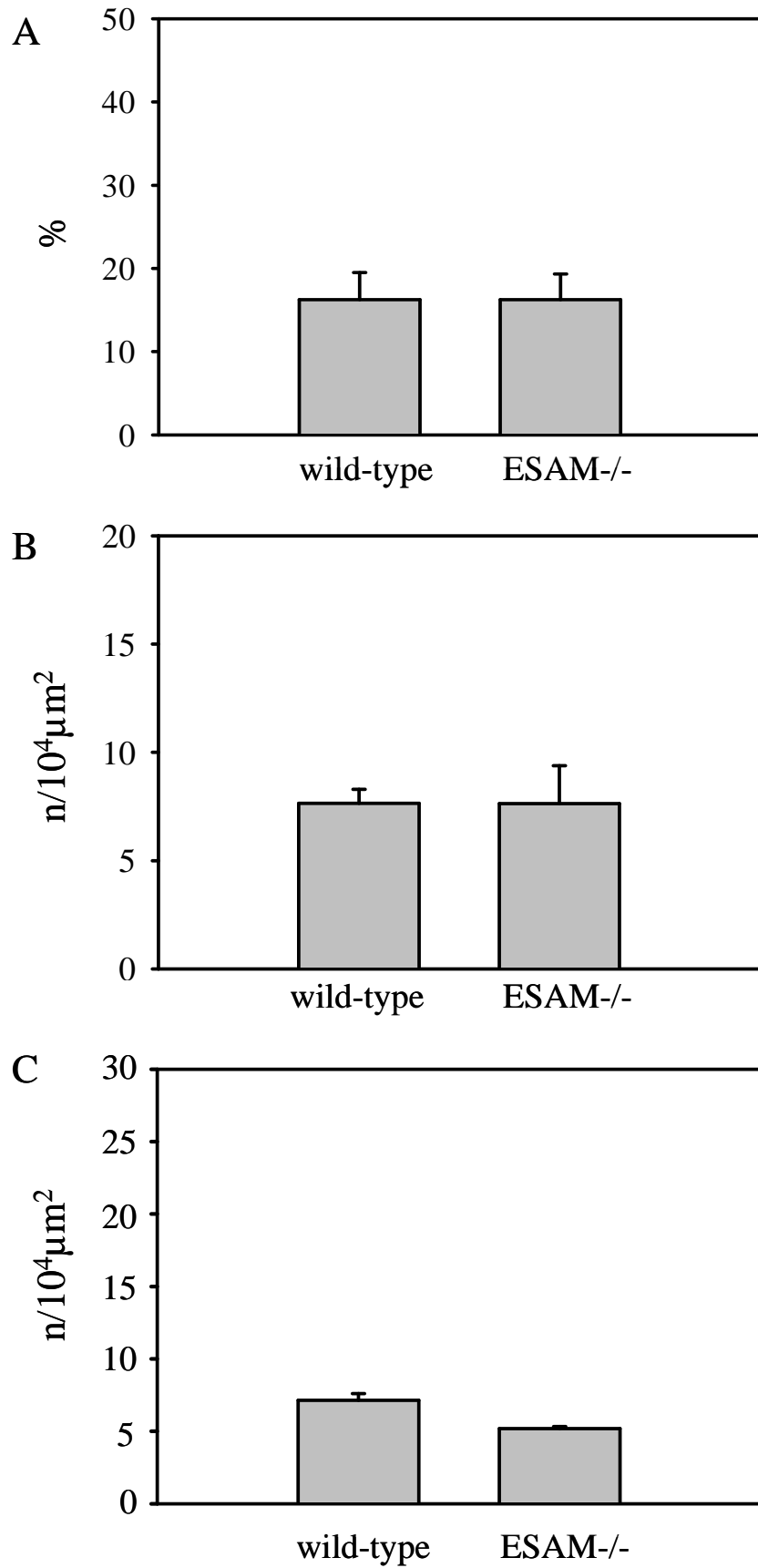


**Fig. 11.** Leukocyte rolling flux fraction (A), adhesion (B), and transmigration (C) in postcapillary venules of wild-type and ESAM<sup>-/-</sup> mice 2 h after intrascrotal injection of IL-1 $\beta$ ; mean  $\pm$  SEM; n=2.

## **4.2 The role of CD99 and CD99L2 for IL-1 $\beta$ -induced leukocyte migration *in vivo***

In this part of the study, we analyzed the role of CD99 and CD99L2 for leukocyte migration *in vivo*. In addition, we answered the question whether blockade of CD99 or CD99L2 in combination with PECAM-1-deficiency would have a synergistic inhibitory effect on leukocyte migration.

### **4.2.1 Microhemodynamic parameters**

Microhemodynamic parameters, such as diameter of the vessel, centerline blood flow velocity, wall shear rate, and systemic leukocyte counts did not significantly differ between all experimental groups (Tab. 7A). As shown in Tab. 7B, microhemodynamic parameters and systemic leukocyte counts were comparable among mice treated with anti-F(ab')<sub>2</sub> preimmune IgG, anti-F(ab')<sub>2</sub>-CD99L2, or anti-F(ab')<sub>2</sub>-CD99. The data were comparable with the findings obtained after application of intact antibodies (Tab. 7A-B).

**Tab. 7A.** Microhemodynamic parameters.

Parameter	wild-type IgG	wild-type anti- CD99L2	wild-type anti-CD99	PECAM-1/ IgG	PECAM-1/ anti- CD99L2	PECAM-1/ anti-CD99
Vessel diameter ( $\mu\text{m}$ )	$28.3 \pm 0.6$	$27.0 \pm 0.4$	$24.8 \pm 0.8$	$26.4 \pm 0.4$	$27.6 \pm 1.1$	$26.6 \pm 0.7$
Centerline blood flow velocity ( $\text{mm} \times \text{s}^{-1}$ )	$1.82 \pm 0.04$	$1.75 \pm 0.04$	$1.77 \pm 0.03$	$1.78 \pm 0.03$	$1.80 \pm 0.03$	$1.73 \pm 0.04$
Newtonian wall shear rate ( $\text{s}^{-1}$ )	$319.0 \pm 12.9$	$332.2 \pm 8.8$	$366.3 \pm 15.3$	$335.4 \pm 9.0$	$348.6 \pm 8.8$	$335.4 \pm 9.1$
Interfacial wall shear rate ( $\text{s}^{-1}$ )	$1563.1 \pm 63.2$	$1627.7 \pm 43.1$	$1794.8 \pm 74.9$	$1643.4 \pm 44.1$	$1708.1 \pm 43.1$	$1643.4 \pm 44.6$
WBC ( $\times 10^6$ cells $\times \text{ml}^{-1}$ )	$5.6 \pm 0.7$	$4.8 \pm 0.6$	$3.9 \pm 0.6$	$4.9 \pm 0.8$	$3.7 \pm 0.4$	$5.0 \pm 0.5$

mean  $\pm$  SEM, \*  $p < 0.05$ ;  $n = 6$ .

**Tab. 7B.** Microhemodynamic parameters.

Parameter	wild-type anti-IgG- F(ab') <sub>2</sub>	wild-type anti- CD99L2F(ab') <sub>2</sub>	wild-type antiCD99- F(ab') <sub>2</sub>
WBC ( $\times 10^6$ cells $\times \text{ml}^{-1}$ )	$4.9 \pm 0.6$	$4.8 \pm 0.8$	$5.0 \pm 0.85$
Vessel diameter ( $\mu\text{m}$ )	$26.9 \pm 0.8$	$26.6 \pm 1.0$	$28.6 \pm 0.6$
Centerline blood flow velocity ( $\text{mm} \times \text{s}^{-1}$ )	$1.75 \pm 0.04$	$1.73 \pm 0.04$	$1.76 \pm 0.01$
Newtonian wall shear rate ( $\text{s}^{-1}$ )	$335 \pm 16.2$	$336 \pm 13.7$	$318 \pm 8.1$
Interfacial shear rate ( $\text{s}^{-1}$ )	$1641.5 \pm 79.3$	$1646 \pm 67.1$	$1558 \pm 39.6$

mean  $\pm$  SEM, \*  $p < 0.05$ ;  $n = 6$ .

#### 4.2.2 Parameters of leukocyte migration

##### 4.2.2.1 Leukocyte rolling flux fraction

Leukocyte rolling flux fraction was determined in postcapillary venules upon application of IL-1 $\beta$  in either wild-type or PECAM-1 $^{-/-}$  mice pretreated with control antibody (IgG), anti-CD99, or anti-CD99L2 antibody. As shown in the Fig. 12, no significant differences were detected between the experimental groups irrespective applied interventions.

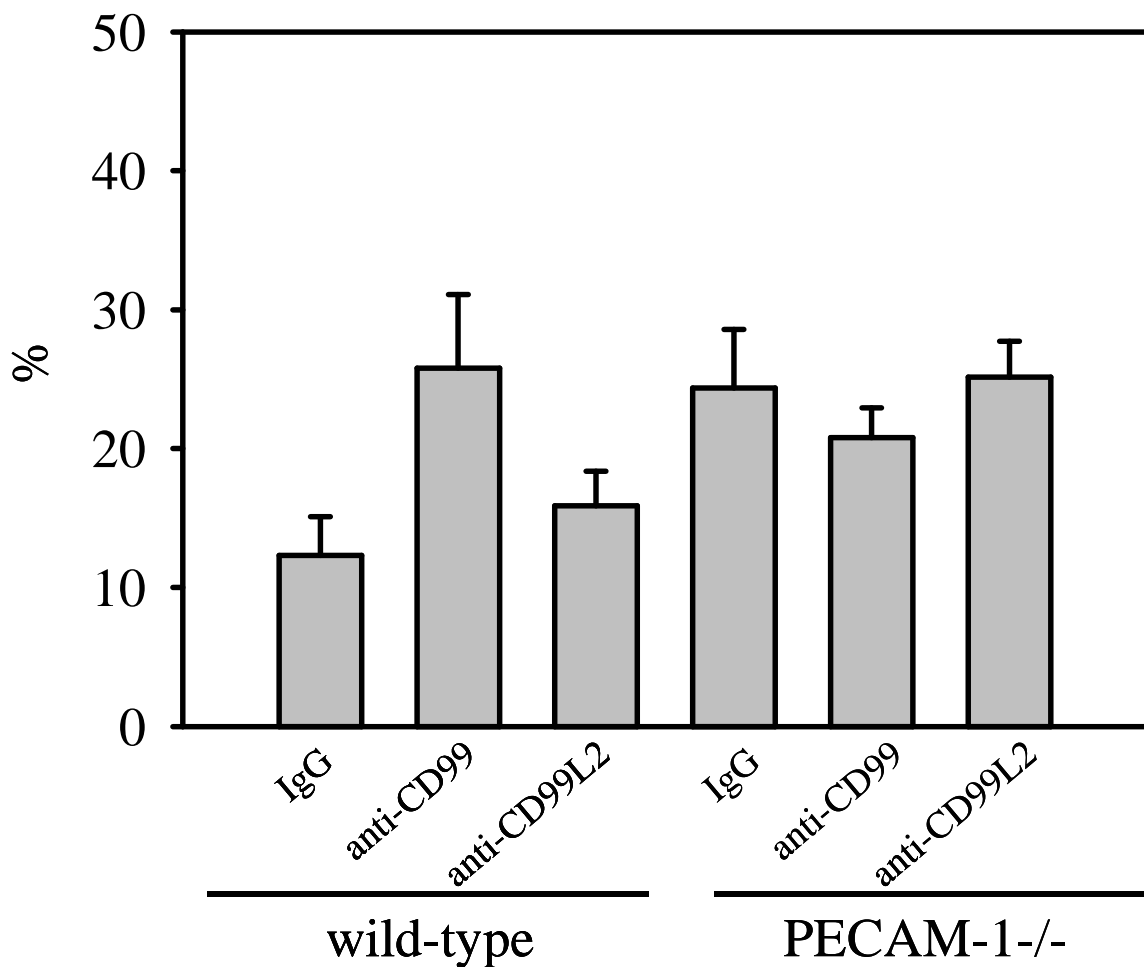


**Fig. 12.** Leukocyte rolling flux fraction in postcapillary venules of wild-type and PECAM-1 $^{-/-}$  mice 4h after i.s. injection of IL-1 $\beta$  and after i.v. application of either preimmune IgG, anti-CD99, or anti-CD99L2 antibodies; mean  $\pm$  SEM, \* $p$ <0.05;  $n$ =6.

As an additional control, leukocyte rolling flux fraction was measured in microvessels of wild-type mice and PECAM-1<sup>-/-</sup> mice treated with F(ab')<sub>2</sub>-fragments of IgG, CD99 or CD99L2 antibodies (Fig. 13). Similarly to the results obtained with intact antibodies, the F(ab')<sub>2</sub>-fragments did not affect IL-1 $\beta$ -induced leukocyte rolling.

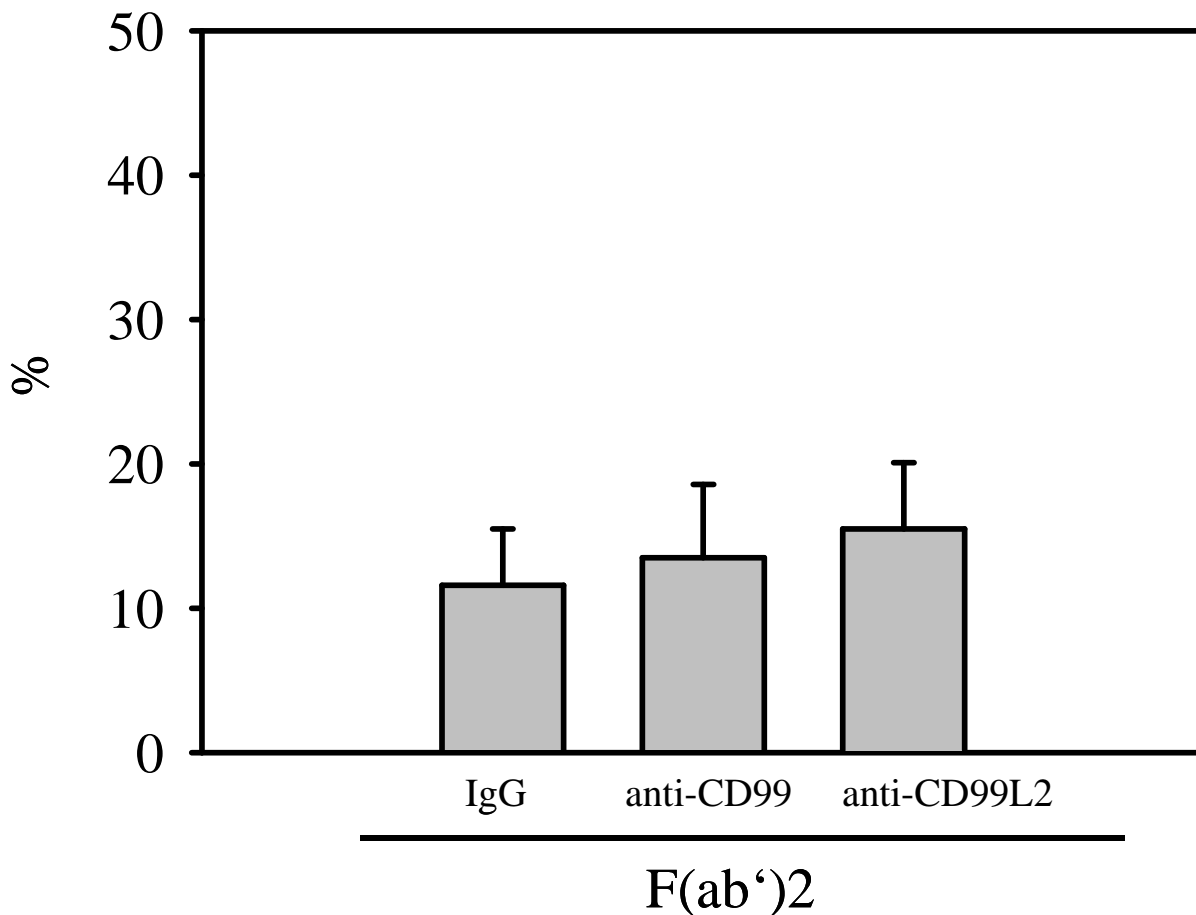


**Fig. 13.** Leukocyte rolling flux fraction in postcapillary venules of wild-type mice 4h after i.s. injection of IL-1 $\beta$ . The mice were treated with F(ab')<sub>2</sub>-fragments of either preimmune IgG, anti-CD99, or anti-CD99L2 antibodies; mean  $\pm$  SEM, \*  $p < 0.05$ ;  $n = 6$ .

#### 4.2.2.2 Leukocyte adhesion

In the group pretreated with control (preimmune) IgG,  $11.1 \pm 1.5$  n/10<sup>4</sup> $\mu$ m<sup>2</sup> adherent leukocytes were detected 4h after intrascrotal injection of IL-1 $\beta$  (Fig. 14). Upon pretreatment with anti-CD99 antibody or anti-CD99L2 antibody, the extent of IL-1 $\beta$ -induced leukocyte adhesion remained not significantly different ( $12.5 \pm 5.3$  n/10<sup>4</sup> $\mu$ m<sup>2</sup> and  $11.3 \pm 0.9$  n/10<sup>4</sup> $\mu$ m<sup>2</sup>, respectively) as compared to

the group pretreated with control IgG. In PECAM-1<sup>-/-</sup> mice, leukocyte adhesion remained on the same level as observed in wild-type mice and was not significantly affected by the antibodies applied (Fig. 14).

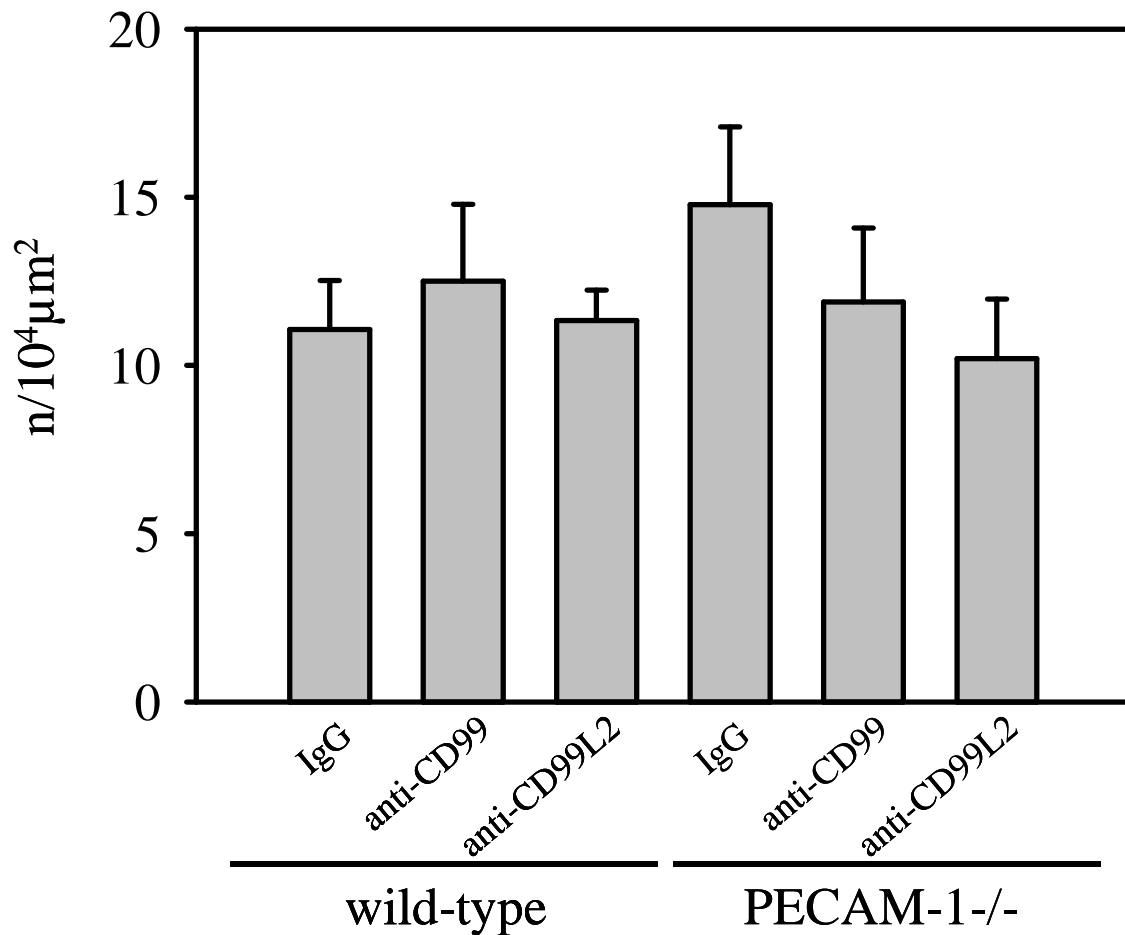


**Fig. 14.** Leukocyte adhesion in postcapillary venules of wild-type and PECAM-1<sup>-/-</sup> mice 4h after i.s. injection of IL-1 $\beta$  with i.v. application of either preimmune IgG, anti-CD99, or anti-CD99L2 antibodies; mean  $\pm$  SEM, \*  $p < 0.05$ ;  $n = 6$ .

In a separate set of experiments, leukocyte adhesion was assessed in wild-type mice treated with F(ab')<sub>2</sub>-fragments of IgG, anti-CD99, or anti-CD99L2 antibodies. As demonstrated in Fig. 15, no significant differences were detected between experimental groups.

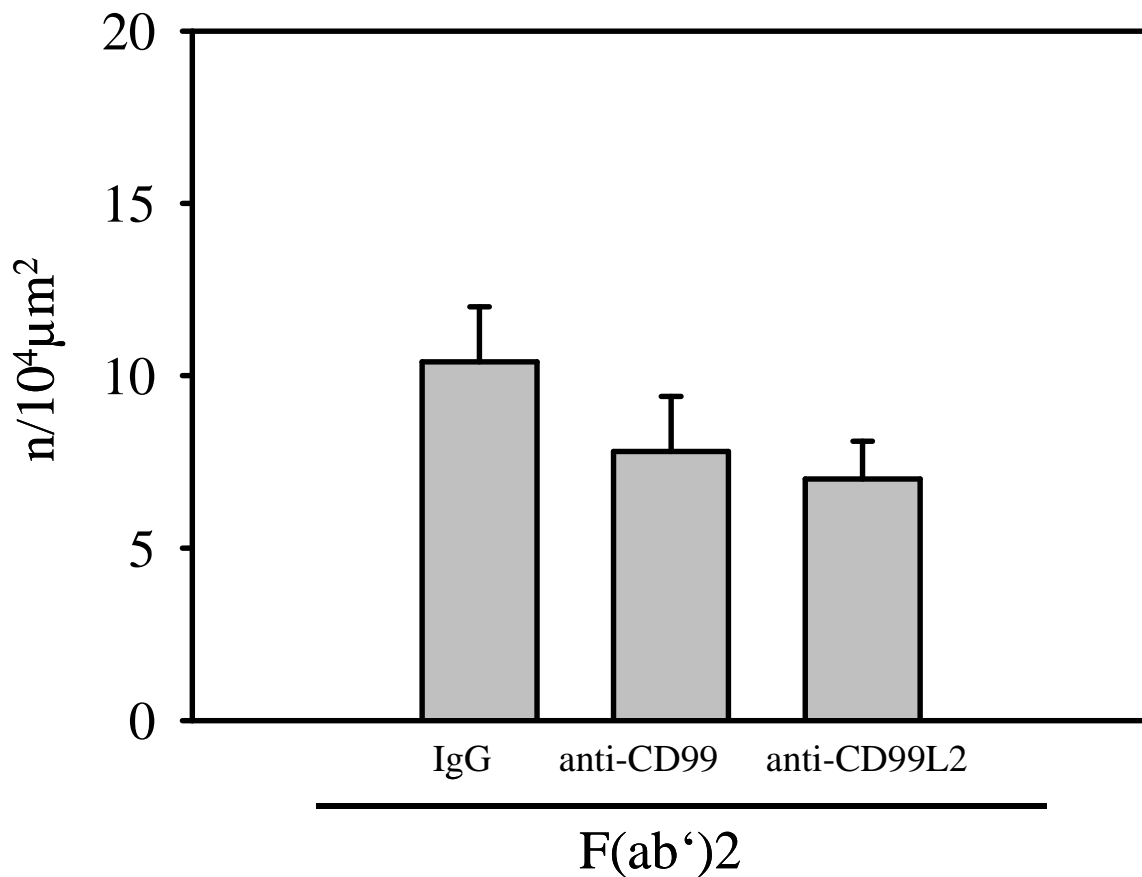


**Fig. 15.** Leukocyte adhesion in postcapillary venules of wild-type mice 4h after i.s. injection of IL-1 $\beta$  with i.v. application of F(ab')<sub>2</sub>-fragments of either preimmune IgG, anti-CD99, or anti-CD99L2 antibodies; mean  $\pm$  SEM, \*  $p < 0.05$ ;  $n = 6$ .

#### 4.2.2.3 Leukocyte transmigration

In wild-type mice pretreated with IgG, intrascrotal injection of IL-1 $\beta$  strongly induced transendothelial migration of leukocytes into the perivascular space ( $20.2 \pm 0.6$  n/10<sup>4</sup>μm<sup>2</sup>) (Fig. 16). In contrast, the number of emigrated leukocytes was significantly lower in mice received antibodies against CD99 and CD99L2 ( $9.8 \pm 0.4$  n/10<sup>4</sup>μm<sup>2</sup> and  $10.4 \pm 0.8$  n/10<sup>4</sup>μm<sup>2</sup>, respectively). In PECAM-1<sup>-/-</sup> mice pretreated with control IgG, leukocyte transmigration was significantly attenuated as compared to wild-type mice (Fig. 16). Moreover, leukocyte transmigration was reduced by about 50% in PECAM-1<sup>-/-</sup> mice received anti-CD99 or anti-CD99L2 antibodies as compared to PECAM-1<sup>-/-</sup> mice treated with IgG and by about 25% as compared to wild-type mice

treated with control IgG. The extent of leukocyte transmigration was comparable between wild-type mice and PECAM-1<sup>-/-</sup> mice which received anti-CD99 or anti-CD99L2 antibodies (Fig.16).

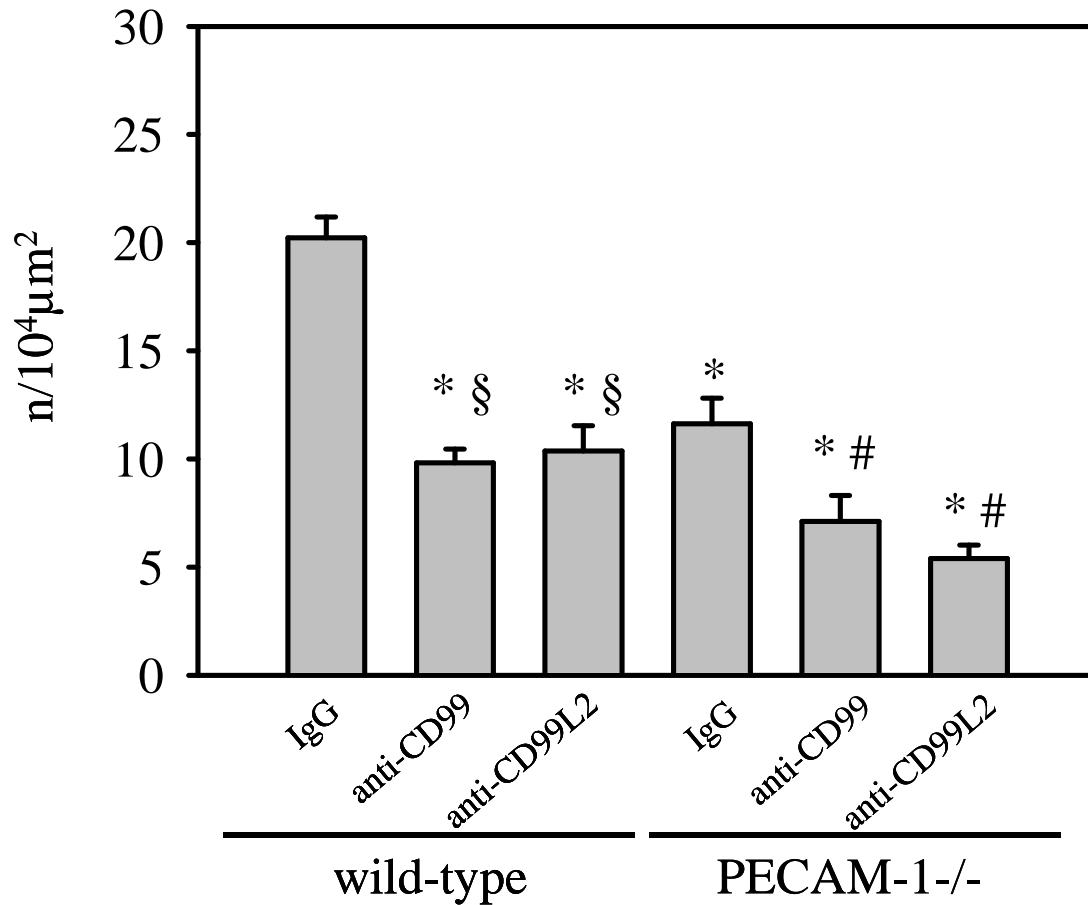


**Fig. 16.** Leukocyte transmigration in postcapillary venules of wild-type and PECAM-1<sup>-/-</sup> mice 4h after i.s. injection of IL-1 $\beta$  with i.v. application of either preimmune IgG, anti-CD99 or anti-CD99L2; mean  $\pm$  SEM, \*  $p < 0.05$  vs. preimmune IgG in C57BL/6 mice. #, §  $p < 0.05$  vs. preimmune IgG in PECAM-1<sup>-/-</sup> mice;  $n = 6$ .

Additional experiments using (Fab')<sub>2</sub>-fragments demonstrate that leukocyte transmigration in mice received anti-CD99-(Fab')<sub>2</sub> or anti-CD99L2-F(ab')<sub>2</sub> was significantly attenuated as compared to that in mice treated with IgG-(Fab')<sub>2</sub> fragments (Fig. 17). Noteworthy, the numbers of transmigrated leukocytes after administration of F(ab')<sub>2</sub>-fragments of antibodies were comparable with those after application of their intact forms (Fig. 16 and Fig. 17).

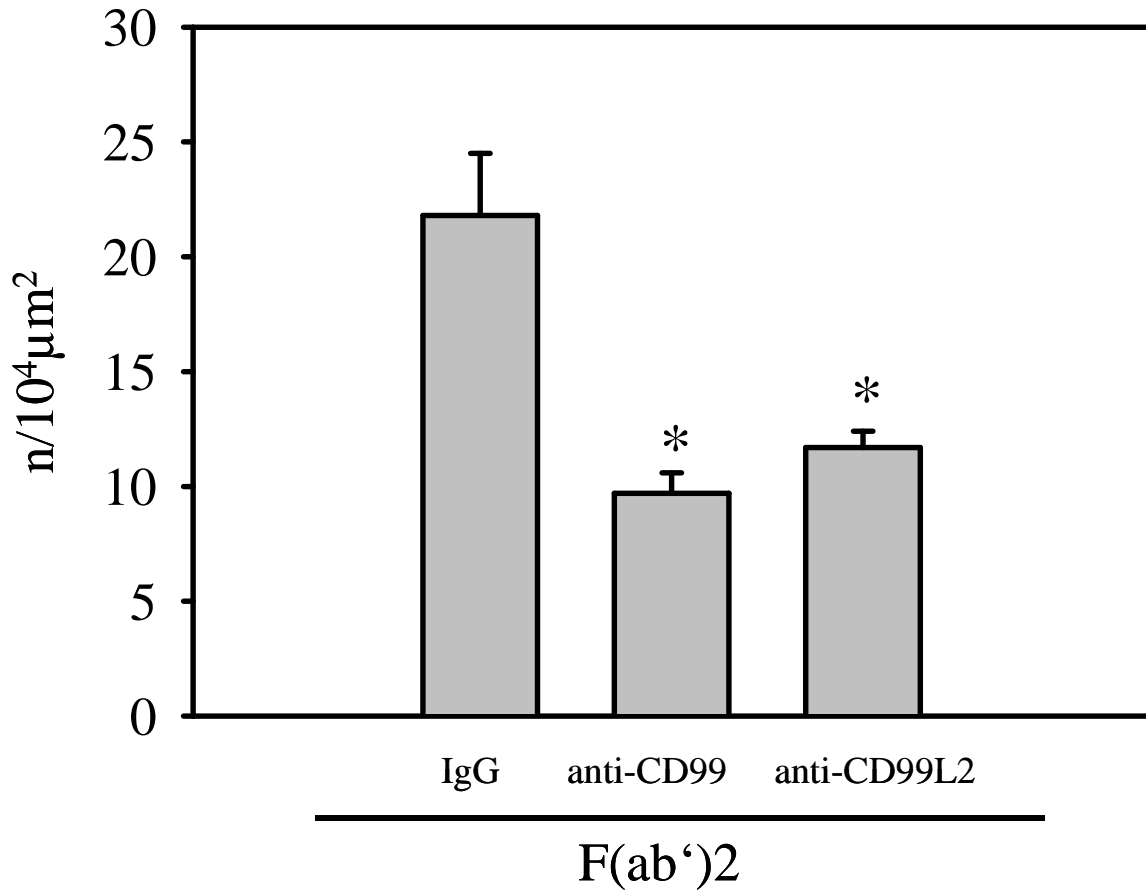


**Fig. 17.** Leukocyte transmigration in postcapillary venules of wild-type mice 4h after i.s. injection of IL-1 $\beta$  with i.v. application of F(ab')<sub>2</sub>-fragments of either preimmune IgG, CD99, or anti-CD99L2; mean  $\pm$  SEM, \*  $p < 0.05$  vs F(ab')<sub>2</sub>-fragments of preimmune IgG;  $n = 6$ .

### 4.3 Imaging and quantitative analysis of leukocyte directional interstitial migration *in vivo*

#### 4.3.1 Microhemodynamic parameters and systemic leukocyte counts

To assure intergroup comparability, diameters of analyzed microvessels, centerline blood flow velocity, wall shear rate, and systemic leukocyte counts were measured. No significant differences were detected among experimental groups (Tab. 8).

*Tab. 8. Microhemodynamic parameters.*

Parameter	Diameter ( $\mu\text{m}$ )	Centerline blood flow velocity (mm/s)	Newtonian shear rate ( $\text{s}^{-1}$ )	Interfacial shear rate ( $\text{s}^{-1}$ )	Systemic leukocyte counts ( $10^6$ cells/m)
saline	$30.4 \pm 1.6$	$1.95 \pm 0.1$	$318.5 \pm 33.1$	$1560.6 \pm 162.2$	$4.6 \pm 1.9$
MIP-1 $\alpha$	$29.9 \pm 5.9$	$1.76 \pm 0.2$	$302.0 \pm 57.5$	$1479.8 \pm 281.7$	$4.9 \pm 2.0$
PAF	$28.3 \pm 2.6$	$1.92 \pm 0.2$	$341.4 \pm 31.8$	$1670.9 \pm 155.8$	$4.6 \pm 1.5$
PAF intrascrotal	$29.4 \pm 2.0$	$1.79 \pm 0.8$	$320.4 \pm 20.1$	$1569.9 \pm 98.5$	$4.2 \pm 2.4$

*mean  $\pm$  SEM, \*  $p < 0.05$ ;  $n = 6$ .*

#### 4.3.2. Determination of the optimal distance for microinjection of chemoattractants

To find an optimal protocol for the perivenular microinjection of chemoattractants and to assess the extent of local inflammation in dependency on the distance of microinjection to the vessel, we first analyzed leukocyte adhesion and transmigration after microinjection of MIP-1 $\alpha$  performed at three different distances from a venule: 25-50  $\mu\text{m}$ , 75-100  $\mu\text{m}$ , and 175-200  $\mu\text{m}$  (Fig. 18A). Sixty minutes after microinjection of MIP-1 $\alpha$ , the number of adherent and transmigrated leukocytes was analyzed in regions of interests (ROIs; 100 x 75  $\mu\text{m}$ ). As a result, the highest number of adherent and transmigrated leukocytes was found when the microinjection was performed at a distance of 25-50  $\mu\text{m}$ , whereas the lowest numbers were found after microinjection at a distance of 175-200

$\mu\text{m}$  (Fig. 18). Therefore, these data show that *i*) the distance of 25-50  $\mu\text{m}$  from the postcapillary venule is optimal for microinjection of chemoattractants, since the inflammatory response is more stronger than after microinjections at the two longer distances analyzed. *ii*) microinjection of MIP-1 $\alpha$  induced an inflammatory response in an area of approximately 100  $\mu\text{m}$  in diameter. Consequently, microinjection was performed at a distance of 25-50  $\mu\text{m}$  from the postcapillary venule under investigation in all further experiments.

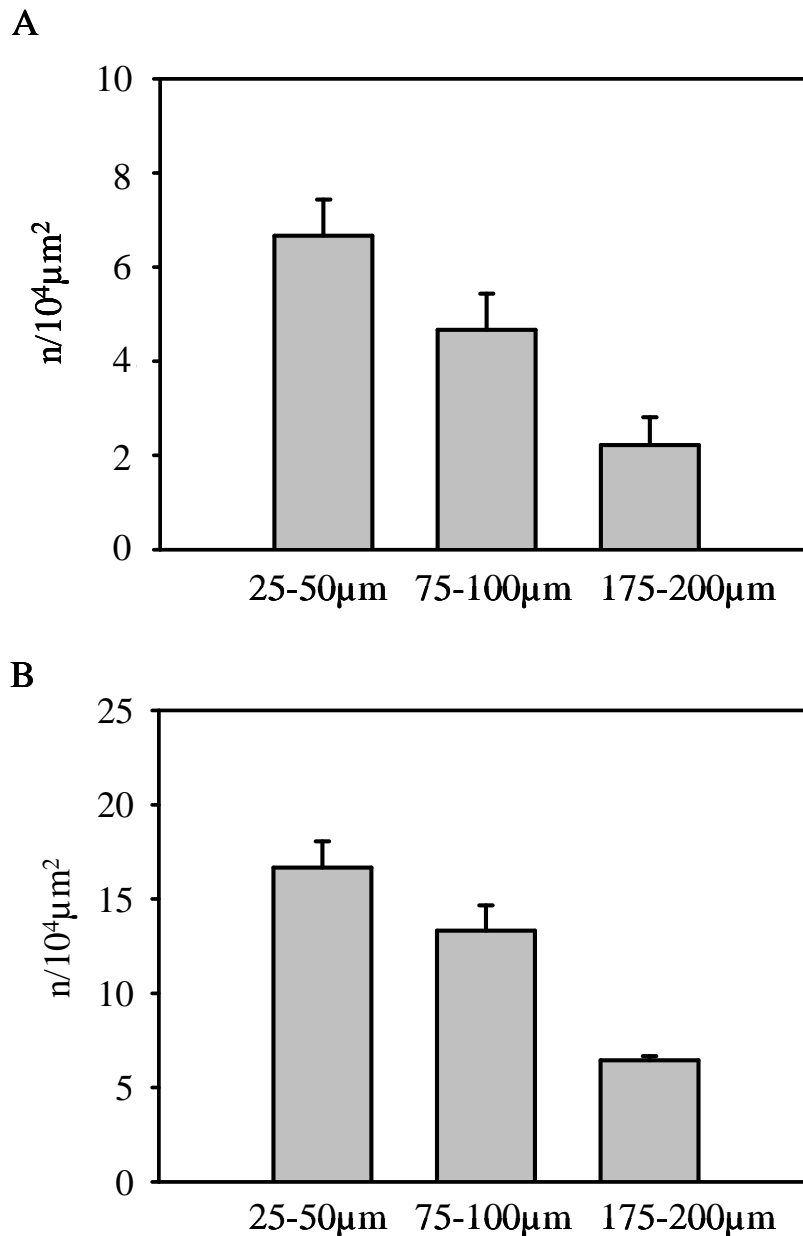


**Fig. 18.** Dependency of leukocyte adhesion and transmigration on the distance of microinjection of chemoattractants. Leukocyte adhesion (A) and transmigration (B) were analyzed 60 min after microinjection of MIP-1 $\alpha$  performed at the distances of 25-50, 75-100, and 175-200  $\mu\text{m}$  from the postcapillary venule. Both parameters were evaluated in the ROIs (100x50  $\mu\text{m}$ ) along the venule opposite the site of microinjection; mean  $\pm$  SEM;  $n=3$ .

### ***4.3.3 Tissue distribution of fluorescence dye rhodamine 6G applied via microinjection***

In a next step, we seek to evaluate how chemoattractant is distributed within the cremasteric tissue after microinjection. To answer this question, microinjection of the fluorescent dye rhodamine 6G was performed and its fluorescence intensity was measured within a time period of 60 min after microinjection. Fluorescence intensity was observed in three ROIs (100 x 75  $\mu\text{m}$ ): on the vessel side ipsilateral to microinjection, on the contralateral side, and 350  $\mu\text{m}$  from the venule (considered as background). At baseline conditions prior to microinjection of rhodamine 6G, mean gray values on both ipsi- and contralateral side did not differ from background levels (Fig. 19). Immediately after microinjection, fluorescence intensity was dramatically increased on the vessel side ipsilateral to the microinjection as compared to baseline levels, which remained comparable with the background intensity and with that on the contralateral vessel side. Despite a reduction by approximately one third already 10 min after microinjection, fluorescence intensity of rhodamine 6G on the ipsilateral side remained strongly increased as compared to background values as well as values detected on the contralateral side (Fig. 19D). Forty minutes after microinjection of rhodamine 6G, the fluorescent dye reached the contralateral vessel side as indicated by a slight elevation of mean gray values. (Fig. 19D).

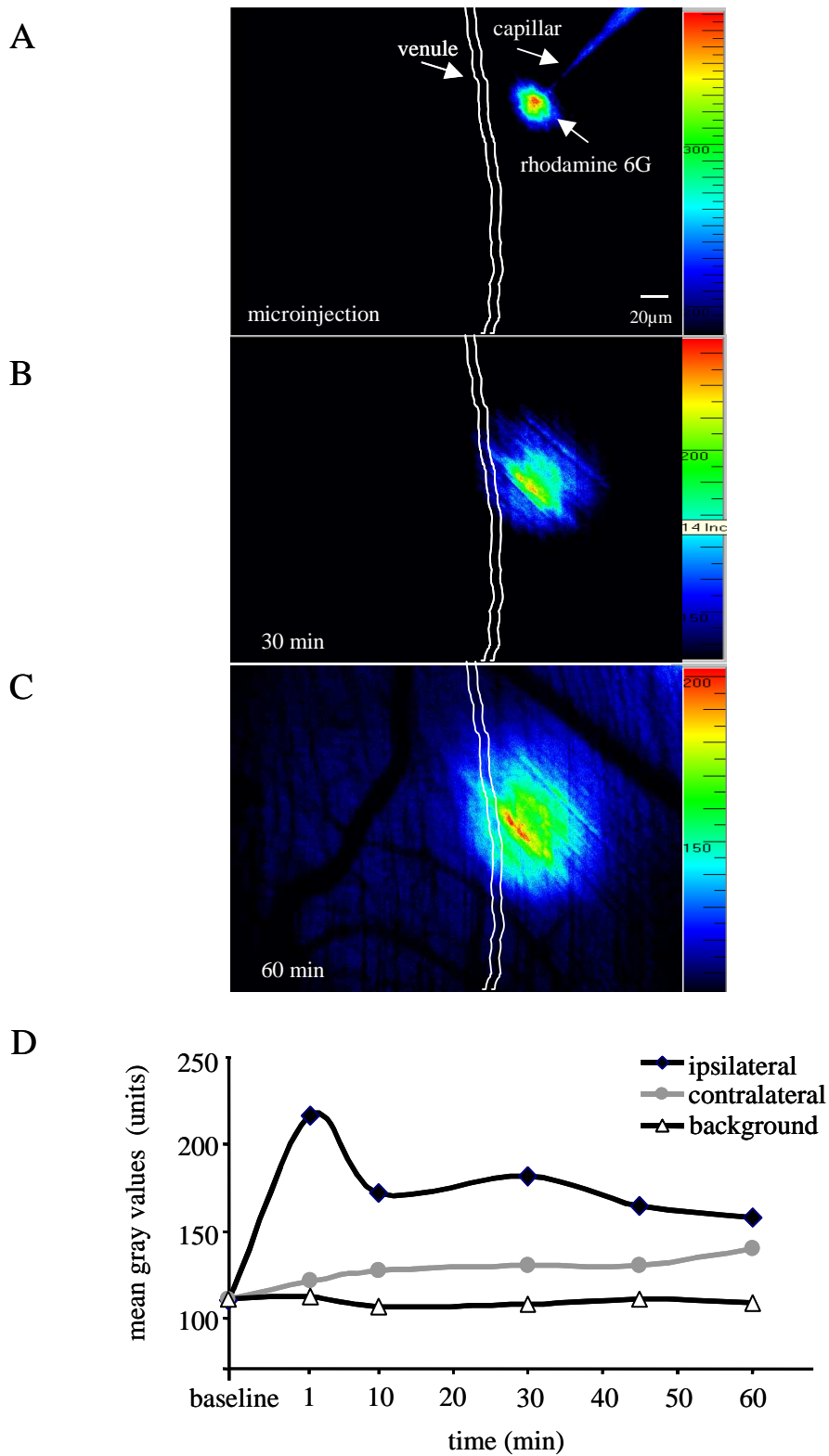


**Fig. 19.** A-C: Intravital microscopic images show tissue distribution of rhodamine 6G at 1st min (A), 30 min (B), and 60 min after microinjection (C). The fluorescence intensity was determined within 60 min; the results are presented in D. Three regions of interests  $100 \times 75 \mu\text{m}$  in cremasteric interstitial tissue were analyzed: on the side ipsilateral to microinjection, on the contralateral side, and in the interstitial tissue  $350 \mu\text{m}$  from the site of microinjection (considered as background);  $n=7$ .

#### 4.3.4 Leukocyte adhesion

In this part of the study, leukocyte adhesion was observed after microinjections of MIP-1 $\alpha$  or PAF. In order to compare the character of leukocyte adhesion after microinjection with that induced by the conventional route of stimulation, intrascrotal injection of PAF was performed in additional group. The numbers of adherent leukocytes were evaluated on both vessel sides (ipsi- and contralateral to the microinjection). Leukocyte adhesion was dramatically increased upon microinjection of MIP-1 $\alpha$  or PAF 60 min after microinjections as compared to microinjection of saline (Fig. 21). The extent of leukocyte adhesion did not significantly differ between the groups undergoing the microinjection of mediators (Fig. 21A). As a next step, we compared leukocyte adhesion on vessel side ipsilateral to the microinjection with that on the contralateral side (Fig. 21A). Upon microinjection of inflammatory mediators 65-70% of all adherent leukocytes, independent of the stimulus applied, were localized on the ipsilateral vessel side (Fig. 20, Fig. 21A and B). In contrast, intrascrotal microinjection of PAF was associated with a homogenous character of leukocyte adhesion without any preferential localization within the vessel lumen (Fig. 21A, C).

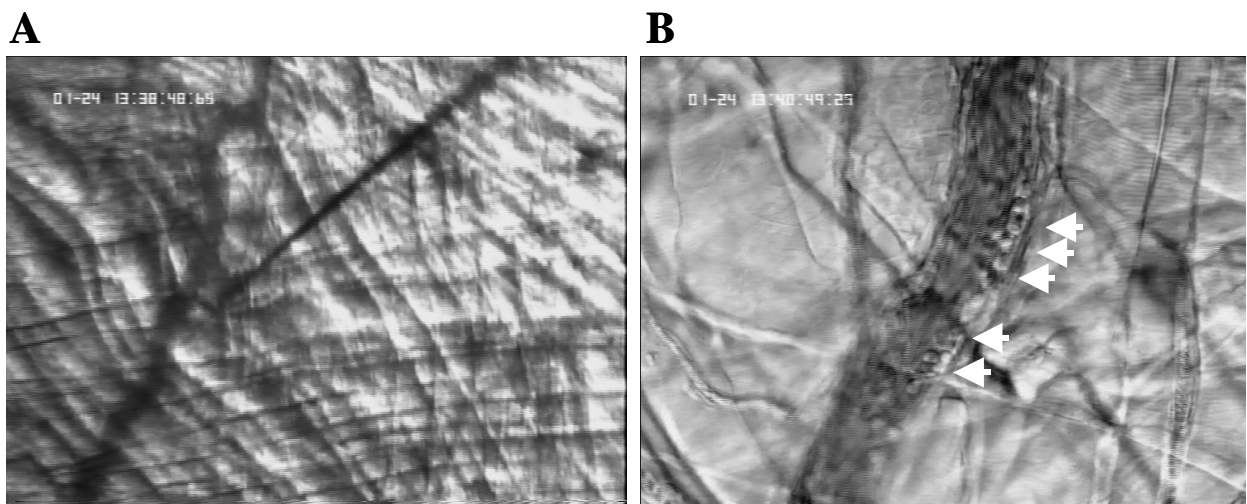


**Fig. 20.** *Intravital microscopic images of perivenular microinjection of chemoattractant at the moment of injection (magnification 4x) (A) and the same venule 2 min after microinjection with adherent leukocytes (shown by arrows) on the ipsilateral to microinjection side of the vessel (objective magnification 25x) (B).*

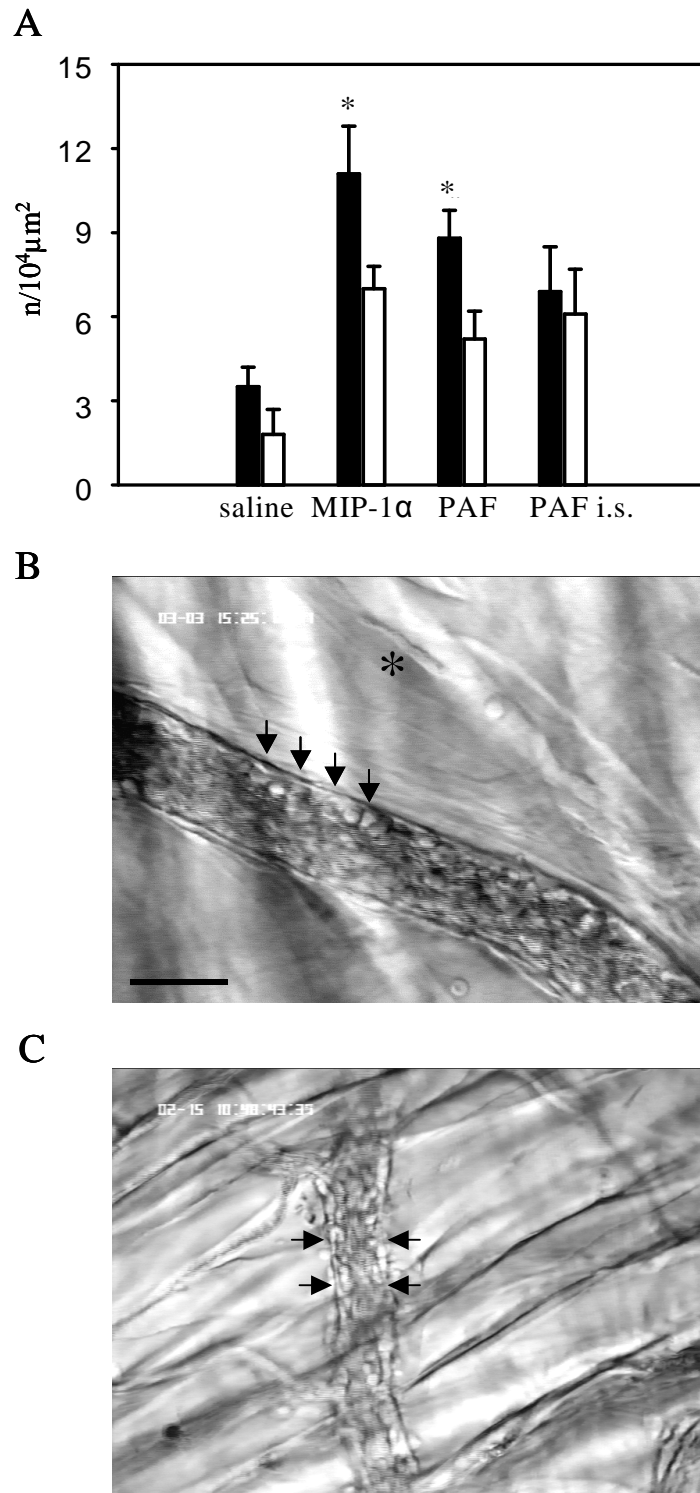


**Fig. 21.** Leukocyte adhesion. **A:** Numbers of adherent leukocytes 60 minutes after microinjection of saline, MIP-1 $\alpha$ , or PAF, and after intrascrotal injection of PAF (PAF i.s.) are presented on the vessel side ipsilateral to microinjection in black bars and on the contralateral side in white bars; mean  $\pm$  SEM; \* $<0.05$  vs. saline;  $n=6$ ; PAF i.s.  $n=3$ . **B-C:** Intravital microscopic images of the murine cremaster muscle demonstrate adherent leukocytes (arrows) after microinjection (**B**) and intrascrotal injection of PAF (**C**); asterisk shows the site of microinjection; objective magnification 20x; scale bar 25  $\mu$ m.

#### ***4.3.5 Leukocyte transmigration***

Emigrated leukocytes were counted in ROIs adjacent to the postcapillary venule on both vessel sides. As a result, microinjection of MIP-1 $\alpha$  or PAF led to progressive increase in the number of emigrated leukocytes, which was significantly increased 60 min after microinjection as compared to the microinjection of saline (Fig. 22). No significant differences were detected between all groups stimulated with the chemoattractants. Next, the extent of leukocyte transmigration was compared on the ipsilateral side with that on the contralateral side of each vessel analyzed (Fig. 22). As shown in Fig. 22A-B, the majority (more than 70%) of emigrated leukocytes were found on the ipsilateral vessel side after microinjection of MIP-1 $\alpha$  or PAF as compared to the contralateral side. In contrast, no difference was detected between the numbers of emigrated leukocytes on both perivascular areas in response to intrascrotal injection of PAF (Fig. 22A, C).

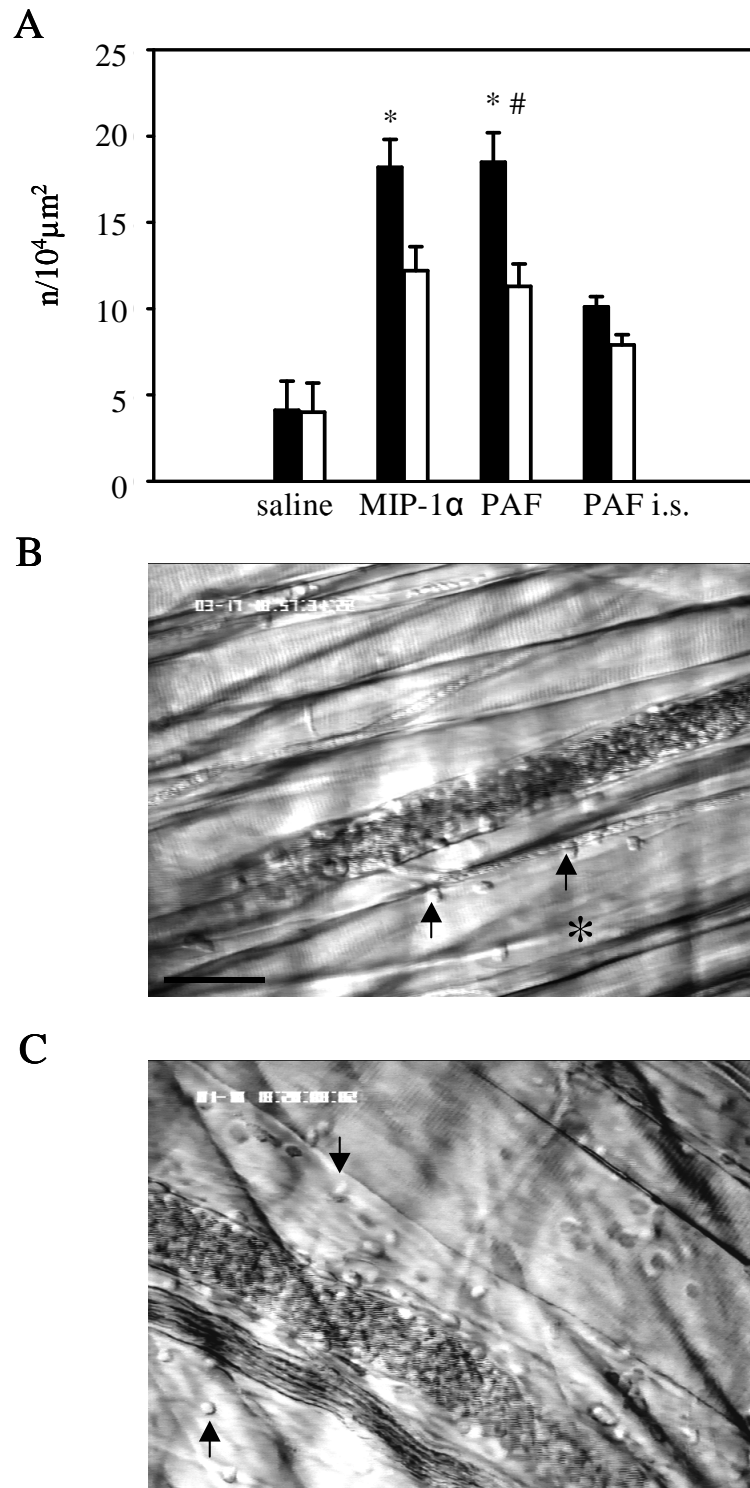


**Fig. 22.** Leukocyte transmigration. *A:* Numbers of transmigrated leukocytes 60 minutes after microinjection of saline, MIP-1 $\alpha$ , or PAF, and after intrascrotal injection of PAF (PAF i.s.) are presented on the vessel side ipsilateral to microinjection in black bars and on the contralateral side in white bars; mean  $\pm$  SEM; \* $<0.05$  vs. saline; #  $<0.05$  vs. contralateral side;  $n=6$ ; PAF i.s.  $n=3$ . *B-C:* Intravital microscopic images from the murine cremaster muscle demonstrate emigrated leukocytes (arrows) after microinjection (*B*) and intrascrotal injection of PAF (*C*); asterisk show the site of microinjection; objective magnification 20x; scale bar 25  $\mu\text{m}$ .

#### ***4.3.6 Motility of interstitially migrating leukocytes***

Tracking of emigrated single leukocytes was performed off-line in digitalized intravital microscopic time-lapse recordings using the imaging software SimplePCI. Emigrated leukocytes were captured in digital video sequences and the parameters of leukocyte interstitial migration, such as curve-line and straight-line migration velocity, curve-line and straight-line migration distances were determined 60 min upon microinjection of inflammatory mediators. As shown in Fig. 23A, B and Fig. 24A-D, microinjection of mediators induced interstitial migration of leukocytes. On the ipsilateral side, the interstitial migration was target-oriented toward the sites of local inflammation (Fig. 23A, B) and characterized by significantly increased curve-line and straight-line migration distances as well as curve-line and straight-line migration velocities as compared to emigrated leukocytes in the sham-operated group as well as to leukocytes migrating on the contralateral vessel side (Fig. 24A-D). Target-oriented character of interstitial leukocyte migration is underlined by the finding that the elevation of straight-line migration distance and velocity was several times higher than the increase in curve-line distance and velocity. It is worth to be noted that leukocyte motility did not significantly differ between the groups receiving MIP-1 $\alpha$  or PAF in almost all migration parameters, with exception of curve-line migration velocity and distance, which were significantly higher upon microinjection of MIP-1 $\alpha$ . On the contralateral vessel side, however, the differences in the migration parameters between the stimulated group and the control group were very weak. In contrary to the stimulation by microinjection of mediators, leukocyte migration was rather random during diffuse inflammation upon the PAF intrascrotal stimulation (Fig. 23C, D) as shown by significantly lower straight-line migration distance and velocity (Fig. 24C, D).

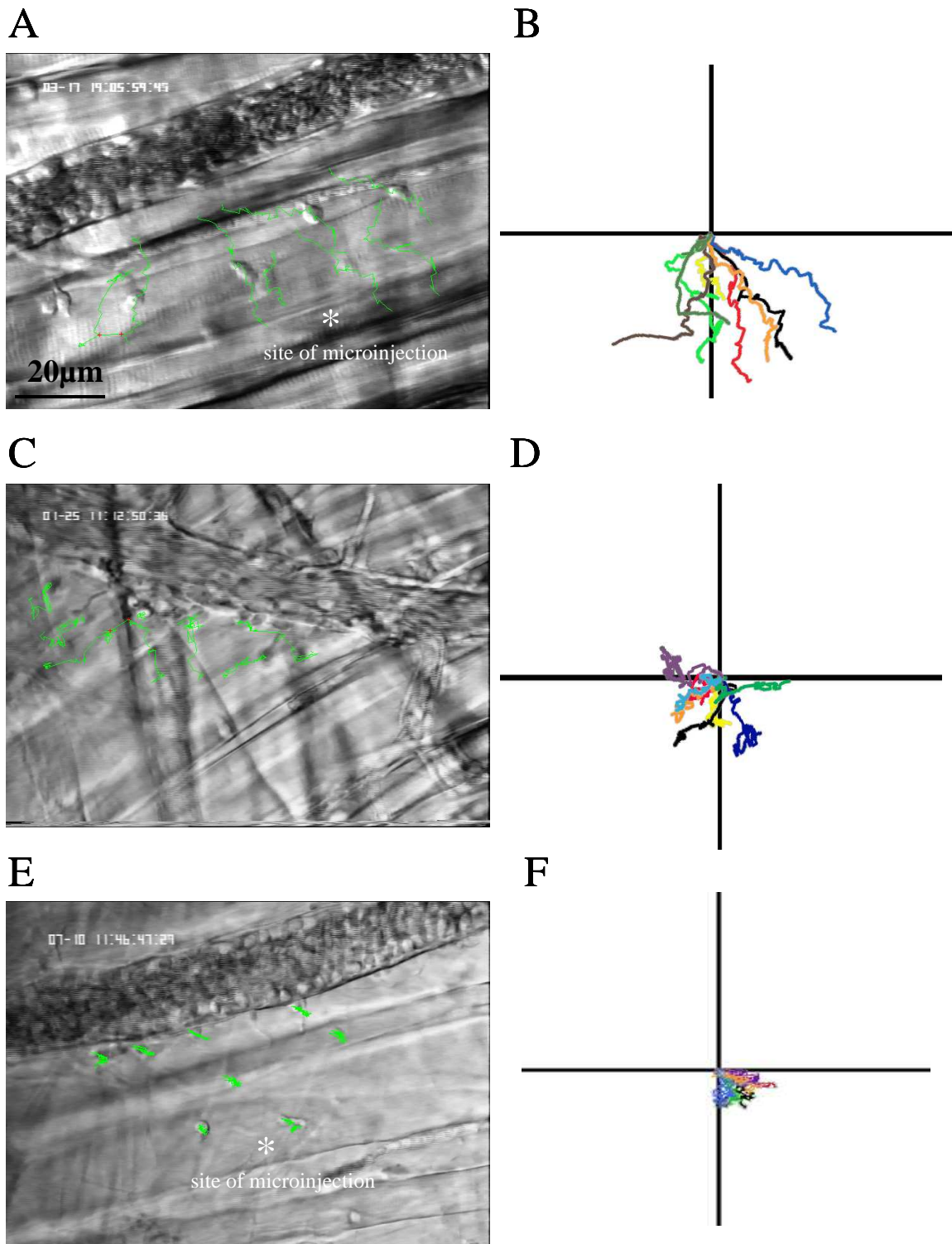


**Fig. 23.** Leukocyte interstitial migration. Interstitially migrating leukocytes were visualized using near-infrared RLOT IVM (objective magnification 20x) and tracked in digitalized video recordings using imaging software. Green lines on intravital microscopic images and colored lines on the panels show the migration tracks of single leukocytes after microinjection of MIP-1 $\alpha$  (A and B), intrascrotal injection of PAF (C and D), and after microinjection of MIP-1 $\alpha$  followed by superfusion with the Rho kinase inhibitor Y27632 (E and F); asterisks shows the site of microinjection.

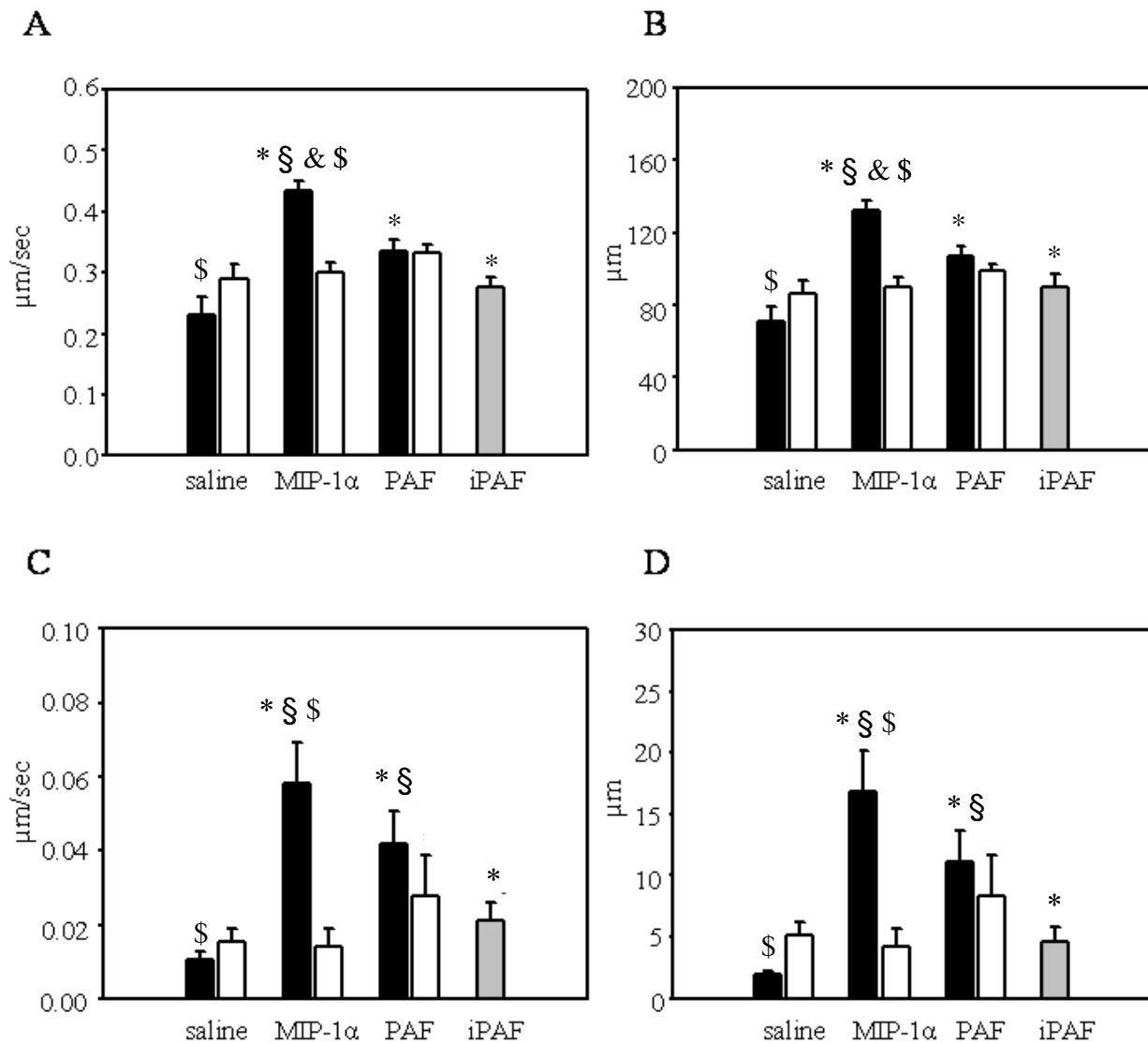


**Fig. 24.** Leukocyte motility. Parameters of leukocyte motility such as curve-line migration velocity (A) and distance (B), straight-line migration velocity (C) and distance (D) were determined in digitalized intravital microscopic video sequences 60 min after microinjection of mediators as well as upon intrascrotal application of PAF. Interstitially migrated leukocytes were analyzed during 5 min using SimplePCI software. Parameters of leukocyte motility on the ipsilateral vessel side are presented in black bars, on the contralateral vessel side – in white bars, and after of intrascrotal application of PAF – in gray bars; mean  $\pm$  SEM; \* $p$ <0.05 vs. saline, \$ $p$ <0.05 vs. PAF i.s., &  $p$ <0.05 vs. PAF, \$ $p$ <0.05 vs. contralateral side;  $n$ =15.

#### 4.3.7 Effect of the Rho kinase inhibitor Y27632 on leukocyte motility

To test our approach, we evaluated the role of Rho kinase for leukocyte interstitial migration *in vivo*. For this, an effect of a Rho kinase inhibitor Y27632 on leukocyte motility was analyzed at either 65 min or 90 min after microinjection of MIP-1 $\alpha$ . The results presented in Fig. 25 show that

5 min of superfusion of the cremaster muscle with Y-27632 reduced the motility of emigrated leukocytes by approximately 45% as compared to the control group. In contrast, leukocyte motility was almost completely blocked, if exposition of the tissue to the inhibitor was prolonged to 30 min (Fig. 23E, F; Fig. 25).

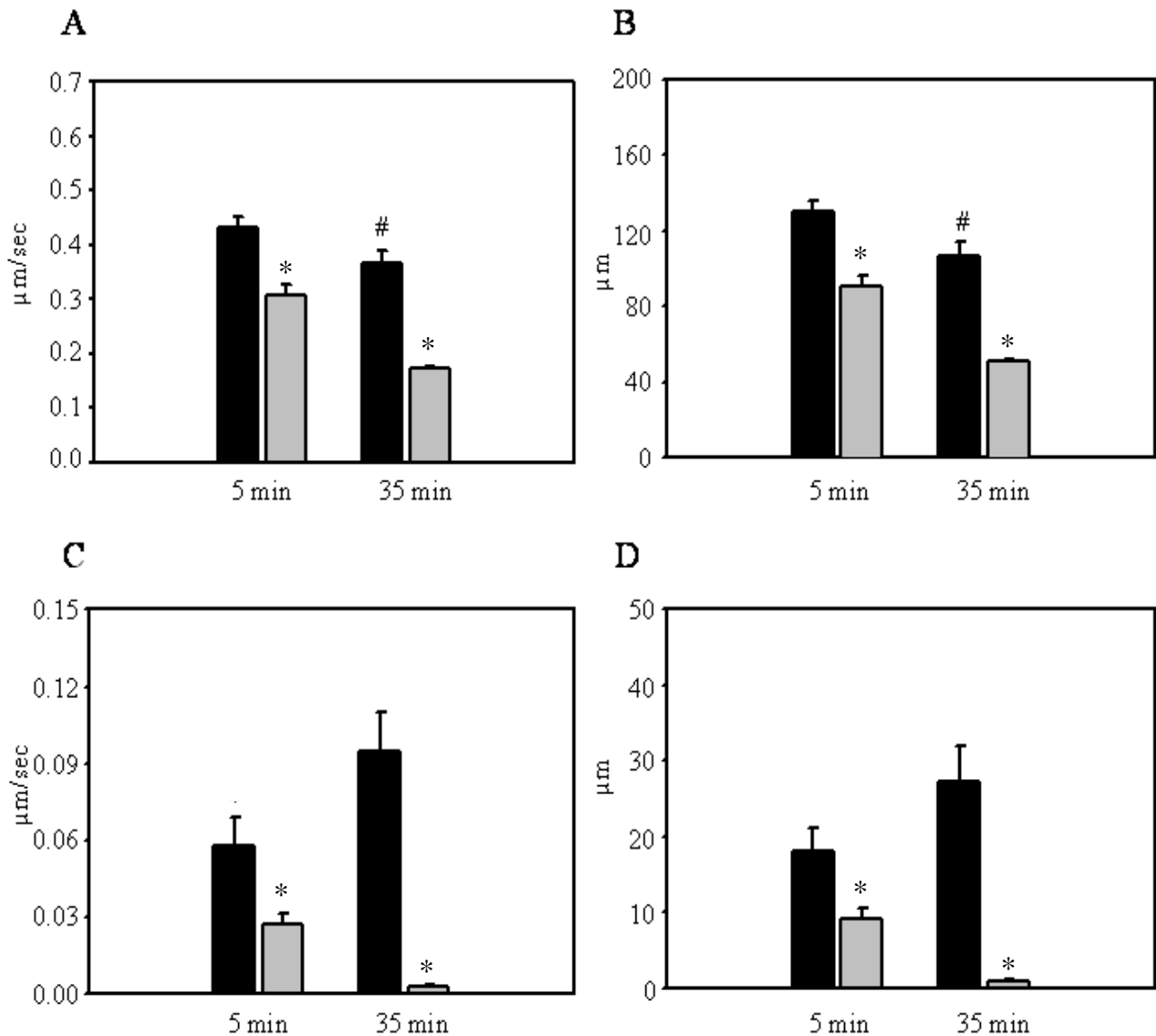


**Fig. 25.** Effect of Rho kinase inhibition on leukocyte motility. Leukocyte curve-line (A) and straight-line velocity (C), curve-line (B) and straight-line distance (D) were analyzed in cremaster muscle 60 min after microinjection of MIP-1 $\alpha$  (black bars) followed by the superfusion with the Rho kinase inhibitor Y27632 (gray bars) for either 5 min or 30 min. In control experiments, the cremaster muscle was superfused with saline alone upon microinjection of MIP-1 $\alpha$ ; mean  $\pm$  SEM; \* $p$ <0.05 vs. control; #  $p$ <0.05 vs. control at 60-65 min;  $n$ =15.

#### 4.3.8 Morphological changes and polarization of interstitially migrating leukocytes

Upon microinjection of PAF, leukocytes moved towards the applied chemoattractant and formed ruffles. Then, leukocytes adopted an elongated polarized shape change with a contracted tail and a broad front lamellipodia (Fig. 26A). Similar shape changes could be observed in interstitially migrating leukocytes moving randomly in animals receiving the chemoattractant via intrascrotal injection (Fig. 26B). After application of the Rho kinase inhibitor, interstitially migrating leukocytes lost their ability to locomote toward the applied source of chemoattractant (Fig. 26C). Thereby, leukocytes became less elongated and more spherical, non polar with single protrusions (Fig. 26C).

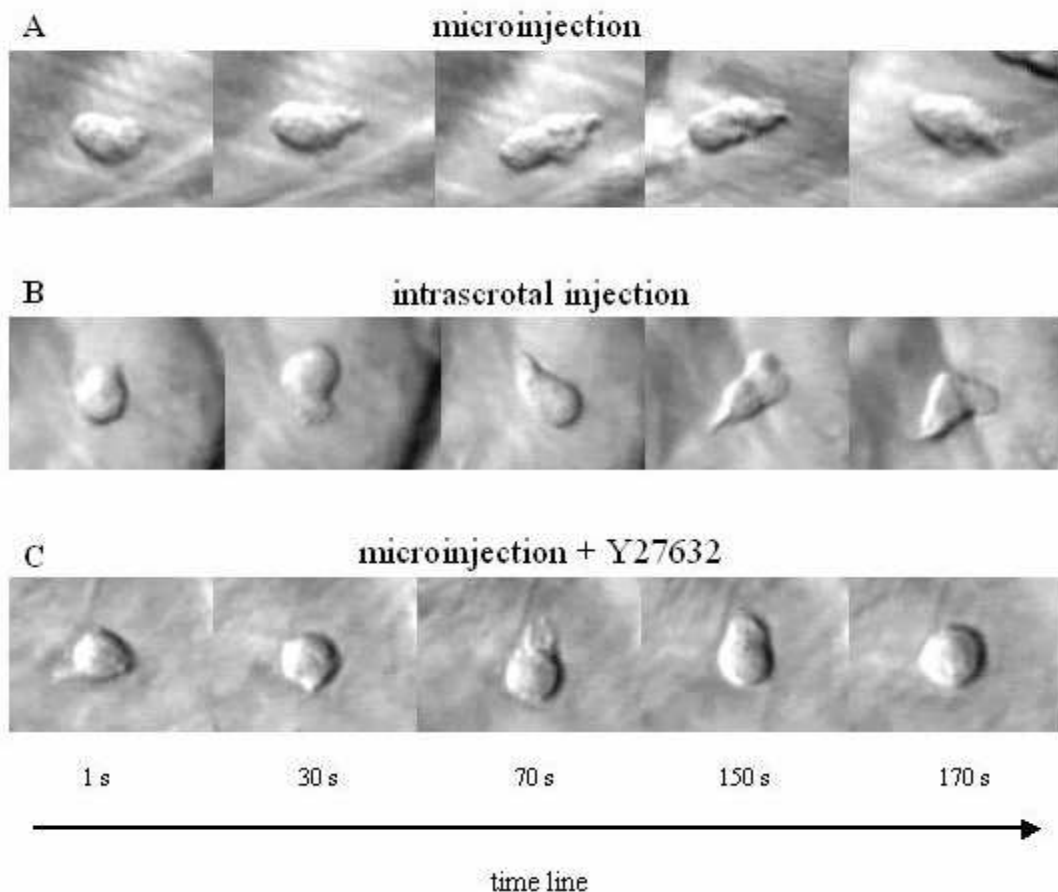


**Fig. 26.** Shape changes in single interstitially migrating leukocytes at different time-points of migration tracks. Still images from IVM video recordings obtained 60 min after microinjection of PAF (A), 60 min after intrascrotal injection of PAF (B), and 60 min after microinjection of PAF in combination with superfusion of Rho kinase inhibitor Y27632 for 30 min (C). A: Directional locomotion of leukocyte with protrusions of lamellipodia at the front and tailing uropod after microinjection of PAF. B: Polarized leukocyte during random interstitial migration after intrascrotal injection of PAF. C: Blocking effect of Rho kinase inhibitor Y27632 on leukocyte polarization induced by microinjection of PAF (objective magnification 40x).

After microinjection of PAF, leukocytes become strongly polarized with an eccentricity of about 1.8. (Fig. 27A, D). Although intrascrotal injection of PAF also induced leukocyte polarization, the values of cell eccentricity were here significantly less as compared with that after microinjection of PAF (Fig. 27B, D). Application of Y27632 abolished the PAF-induced leukocyte polarization and the ratio between cell long and short axis was less than 1.2 (Fig. 27C, D).

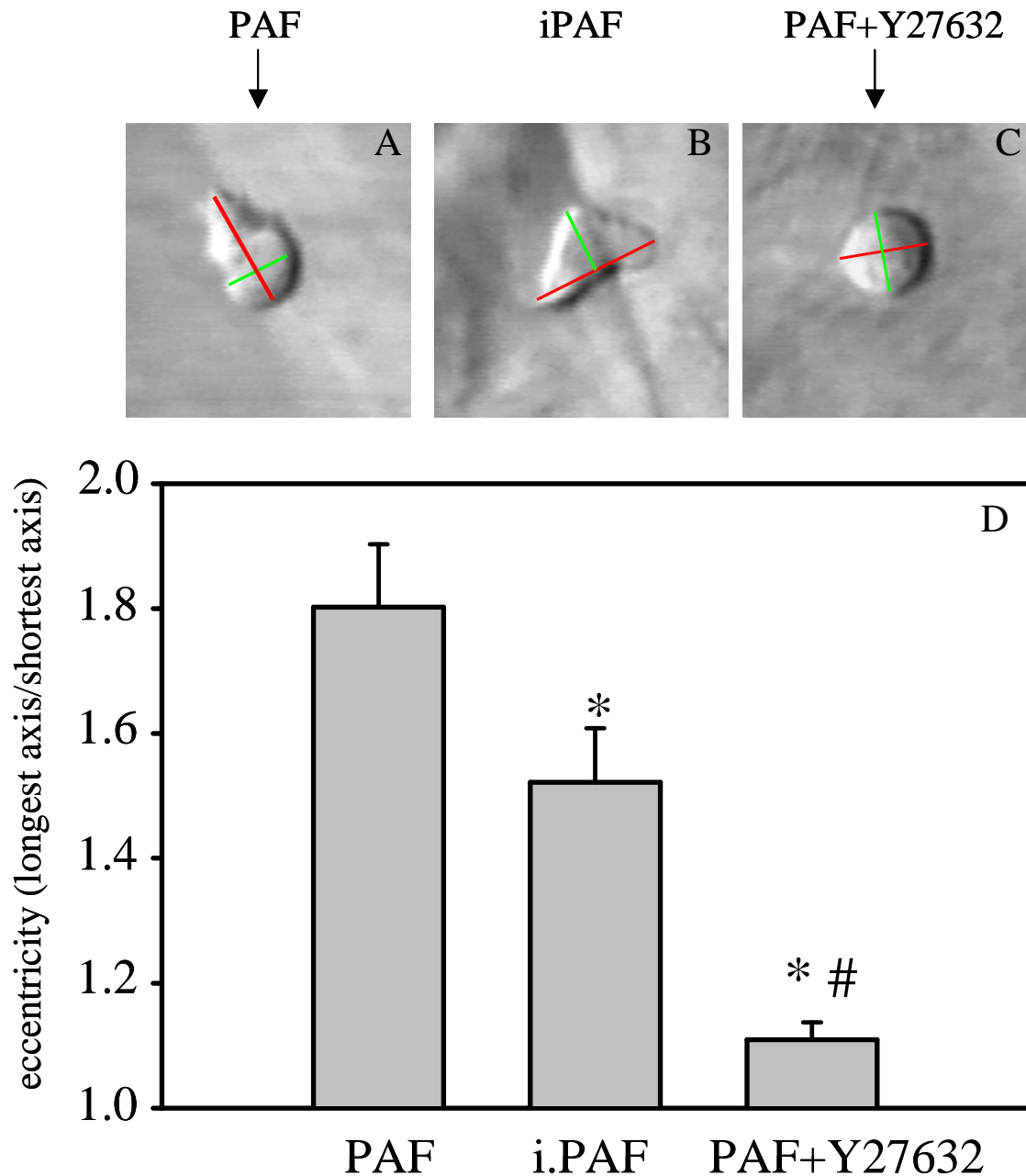


**Fig. 27.** Polarization of interstitially migrating leukocytes in vivo. Still images from intravital microscopic video recordings of interstitially migrating leukocytes obtained at 60 min after microinjection of PAF (A), intrascrotal injection of PAF (i.PAF) (B), and microinjection of PAF in combination with superfusion of Rho kinase inhibitor Y27632 for 30 min (C) (objective magnification 50x). Cell major and minor axes are presented in red and green, respectively. D: Quantitative data of the average leukocyte eccentricity after microinjection of PAF, intrascrotal injection of PAF, and microinjection of PAF with superfusion of Y27632; mean  $\pm$  SEM; \* $p$ <0.05 vs. microinjection of PAF, #  $p$ <0.05 vs. intrascrotal injection of PAF;  $n$ =15.

#### ***4.3.9 Colocalization of leukocyte migration to the site of microinjection of chemoattractant***

Next, we addressed the question of whether leukocyte really migrate toward the site of microinjection. Rhodamine 6G (50-65 PI; 0.05%) was mixed with MIP-1 $\alpha$  and applied via microinjection. Leukocyte migration was visualized within the time period from 60 to 80 min after microinjection. A switching of near-infrared-RLOT microscopy with fluorescent microscopy allowed a simultaneous visualization of migrating leukocytes and tissue distribution of the infused chemoattractant.

As shown in Fig. 28A-C, microinjection was performed in the perivenular regions within 25-50  $\mu$ m from the venule. A clear majority of attached and extravasated leukocytes was observed on the vessel side ipsilateral to the microinjection (Fig. 28D, F). Single cell tracking revealed that interstitially migrating leukocytes moved directly toward the site of application (Fig. 28E). Thus, microinjection of MIP-1 $\alpha$  induces target-oriented leukocyte adhesion, transendothelial, and interstitial migration towards the site of microinjection of chemoattractant.

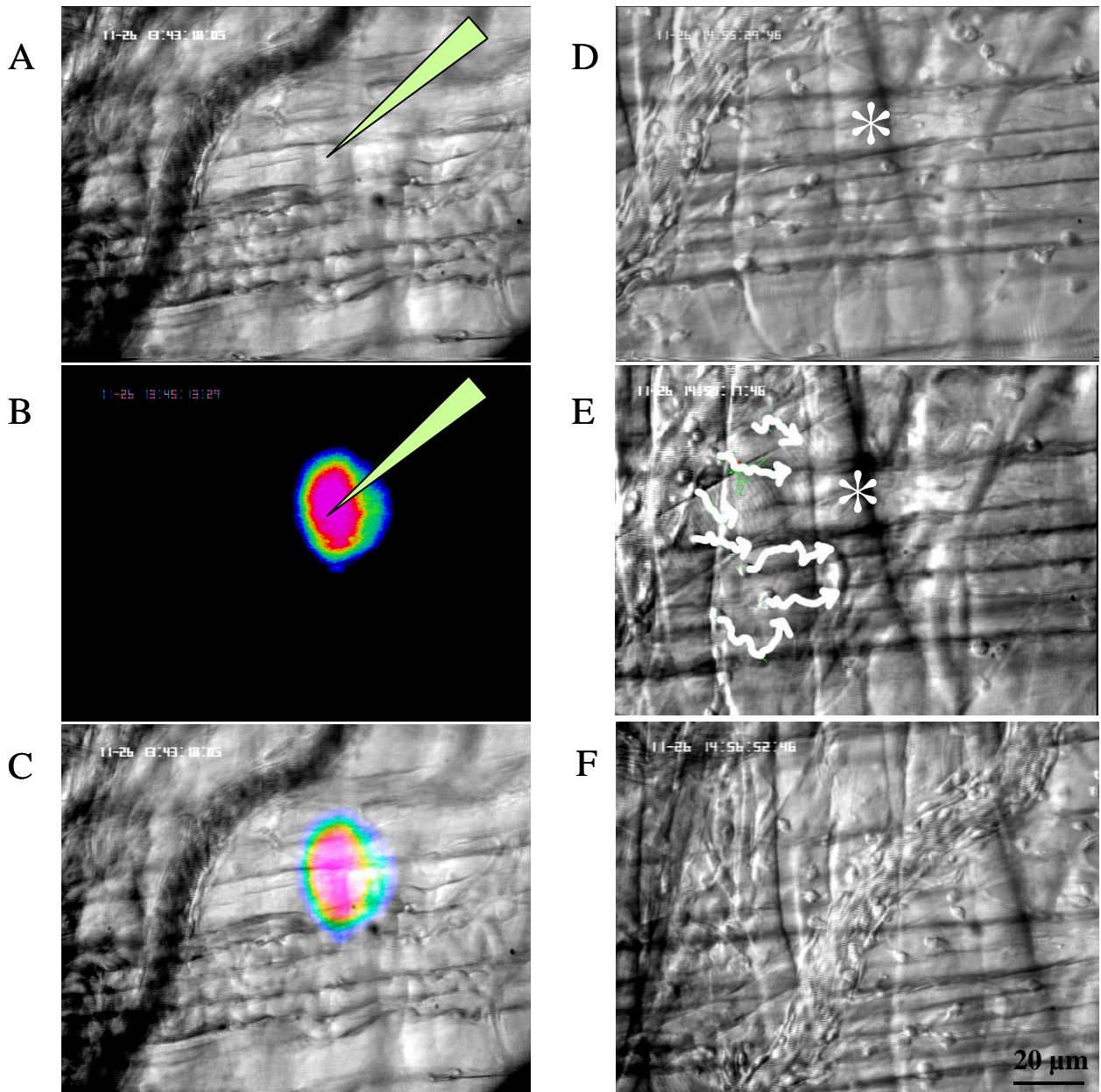


**Fig. 28.** A-C: Visualization of the application site of MIP-1 $\alpha$  with rhodamine 6G at the 1st min after microinjection using near-infrared RLOT (A) and fluorescence microscopy (B); C- Merged image (objective magnification 10x). D - Directional leukocyte adhesion and emigration visualized by RLOT microscopy (asterisk shows microinjection site). E - Interstitially migrating leukocytes towards the site of microinjection (shown by asterisk); tracking lines of single leukocytes are presented as white arrows (objective magnification 20x). F - Comparison of leukocyte emigration on ipsi- vs. contralateral vessel side with prevalence of leukocyte transmigration on the ipsilateral side (right side) as compared to the contralateral side (left side) (objective magnification 20x).

#### 4.3.10 Visualization of mitochondria redistribution in interstitially migrating leukocytes

In this part of the study, we combined RLOT and fluorescence microscopy and observed redistribution of mitochondria in single interstitially migrating leukocytes upon intrascrotal injection of PAF. For imaging of mitochondria, green-fluorescent mitochondrial stain MitoTracker® Green was applied systemically. Switching of RLOT and fluorescence microscopy allowed simultaneous visualization of mitochondria redistribution in interstitially migrating leukocyte accordingly to the changing of cell shape. As shown in the Fig. 29, mitochondria were mostly concentrated in the region of the cell corresponding to the uropod in polarizing and randomly migrating MitoTracker Green-positive leukocytes.

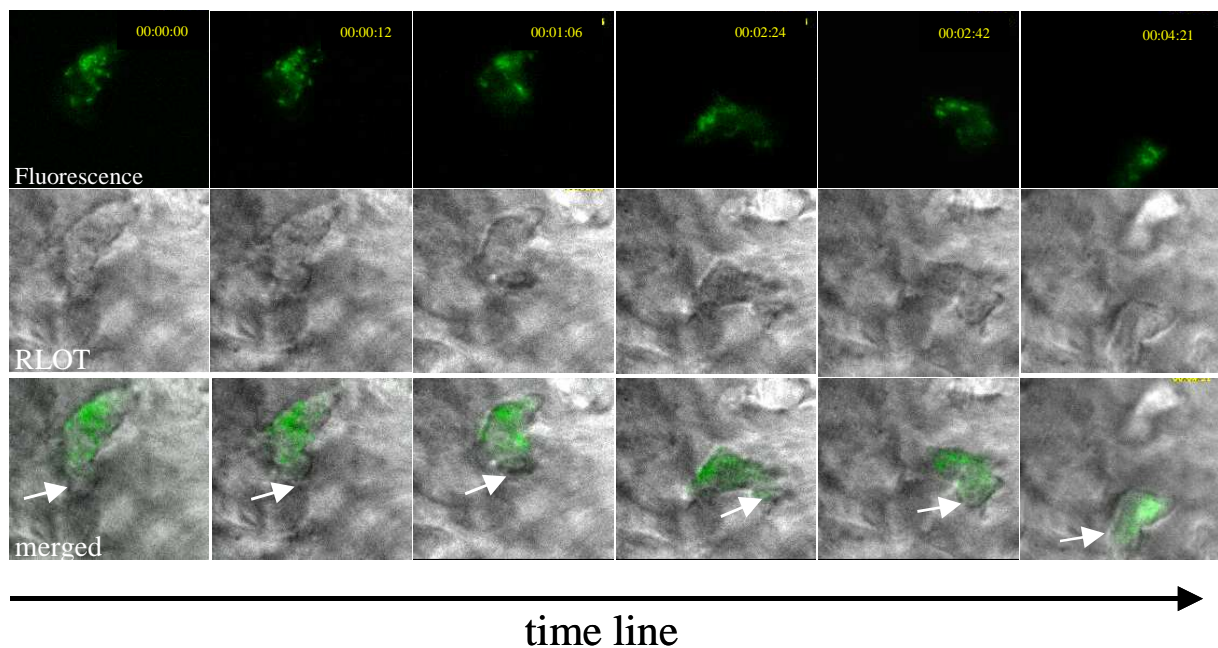


**Fig. 29.** Representative intravital microscopic images demonstrate redistribution of mitochondria in single interstitially migrating leukocyte during 5 min (objective magnification 63x). The analysis was performed 60 min after intrascrotal injection of PAF. Fluorescence microscopic images show mitochondria localization and dynamics during random migration of a leukocyte in the interstitial tissue; near-infrared RLOT images represent motility and dynamic shape changes of a leukocyte during the observed time period. Merged images show colocalization of mitochondria and lamellipodia (leading edge) as well as uropod (trailing edge) in the polarized, chaotically migrating leukocyte (arrows point to the leading edge).

#### ***4.3.11 Migration patterns of different leukocyte subsets***

In the final part of the study, we used a combination of RLOT with fluorescence microscopy in order to analyze transmigration and interstitial migration of monocytes. For this, microinjection of MCP-1 was performed in Cx3CR1<sup>gfp/gfp</sup> mice, in which blood monocytes express GFP (98). The second aim of this experimental set was to compare the migration behavior of GFP-positive monocytes with that of neutrophils. As well known, neutrophils comprise more than 85% of the leukocyte response to MCP-1 (99). Therefore, we assume that GFP-negative leukocytes extravasated after microinjection of MCP-1 in our experiments are neutrophils.

In our experiments, the number of transmigrated GFP-negative neutrophils and GFP-positive monocytes was significantly increased 60 min after microinjection of MCP-1 (Fig. 30) as compared to the baseline conditions (data not shown). Transmigration of leukocytes had a directional character as shown by the prevalence of the number of extravasated neutrophils and monocytes on the vessel side ipsilateral to the microinjection (Fig. 30A). The quantitative analysis of leukocyte interstitial migration demonstrated that perivenular microinjection of MCP-1 induces a target-oriented migration of neutrophils within the interstitial tissue as shown by increased straight-line migration velocity (Fig. 30B) and distance (Fig 30C) as compared to those after microinjection of saline (Fig. 24C, D). Straight-line migration velocity of neutrophils was comparable between three analyzed time periods (Fig. 30B, C). Monocytes, however, did not move toward MCP-1, at least at 60-65 min after microinjection, as indicated by lower levels of straight-line migration velocity and directionality (Fig. 30B, C). Interestingly, straight-line velocity and distance of monocytes were slightly increased after 70 min and 80 min after microinjection of MCP-1 as compared to those after 60 min. (Fig 30B, C). These results suggest a delayed chemotactic response of monocytes as compared to neutrophils. Although monocytes displayed a target-oriented character of interstitial migration 70 and 80 min after microinjection of MCP-1, they migrated slower than neutrophils as presented by lower straight-line migration parameters (Fig 7A-D).

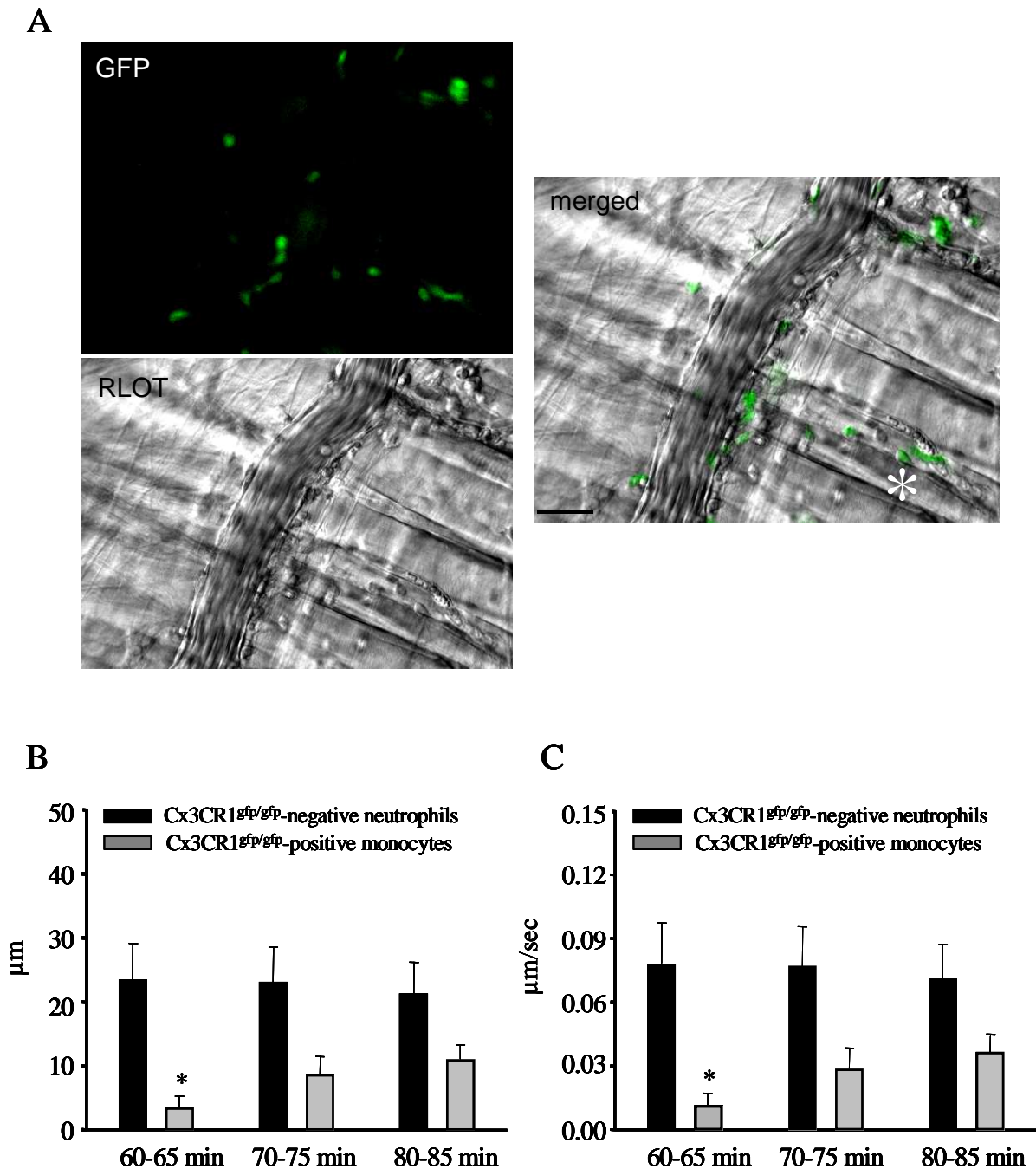


**Fig. 30.** A: Representative intravital microscopic images show monocyte and neutrophil transmigration 60 min after microinjection of MCP-1 in  $Cx3CR1^{gfp/gfp}$  mice (objective magnification 20x). Fluorescence intravital microscopic image demonstrates target-oriented transmigration of monocytes, RLOT image - target-oriented transmigration of neutrophils; merged image - colocalization of extravasated monocytes and leukocytes in the interstitial tissue (asterisk shows the site of microinjection; scale bar 20µm). Motility parameters such as straight-line migration distance (B) and velocity (C) of interstitially migrating neutrophils (black bars) and monocytes (gray bars) were analyzed 60, 70, and 80 min after microinjection of MCP-1 in  $Cx3CR1^{gfp/gfp}$  mice for 5 min, respectively; mean  $\pm$  SEM; \* $p < 0.05$  vs. straight-line migration velocity of neutrophils;  $n = 5$ .

## 5. DISCUSSION

### 5.1 Discussion of material and methods

#### 5.1.1 Animals

The experiments were performed in mice. The mouse is immunologically well characterized and a wide range of specific antibodies is commercially available. Important advantages are also the opportunity to use genetically modified animals, the rapid breeding, and low costs for animal care. In this study, we used ESAM- and PECAM-1-deficient mice. There are no phenotypic differences described for these mouse strains except that ESAM<sup>-/-</sup> mice have a 10% reduction in weight. Absolute and differential leukocyte counts (determined for leukocytes stained for CD4, CD8, CD19, Gr-1, and F4-80 antigen) were normal in ESAM<sup>-/-</sup> mice (51). PECAM-1<sup>-/-</sup> mice are viable, fertile, normal in size and do not display any gross physical or behavioral abnormalities (100). Additionally, PECAM-1<sup>-/-</sup> mice have a normal number of red blood cells, platelets, monocytes and lymphocytes but significantly fewer circulating neutrophils than their wild-type counterparts (100). Isolated skeletal muscle arterioles from homozygous PECAM-1<sup>-/-</sup> mice exhibit reduced vessel dilation and no significant change in wall shear stress responses when intraluminal flow is increased (101).

#### 5.1.2 Experimental model and surgical preparation

*Murine cremaster muscle.* Murine cremaster muscle model is widely used in investigations of the microcirculation *in vivo*. This muscle is recognized to be very eligible for studies on leukocyte recruitment because of some important specialties, such as the almost two-dimensional vessel structure, the “typical” pattern of the expression of endothelial adhesion molecules, and a high vessel density. In contrast to parenchymal organs, such as liver or spleen, there is a well-defined perivascular space in muscle tissue. This specialty is of particular importance and a prerequisite for the analysis of interstitial migration of leukocytes. In addition, there are different application routes possible for induction of inflammation in the cremaster muscle, such as a systemic application (e.g.

LPS in endotoxemia models), local application of mediators via intramuscular (intrascrotal) injection or local superfusion. The anatomically favorable localization of supplying vessels also allows the investigation of ischemia-reperfusion injury or even studies on transplantation (102), (103), (104).

*Surgical preparation.* The preparation of cremaster muscle for IVM was performed according to the technique described by *Baez* with several modifications (93). The preparation technique requires some basic microsurgical skills and is routinely unproblematic after a learning phase of 6-8 weeks. The quality of the surgical preparation was controlled using IVM (low number of adherent leukocytes and normal blood flow velocity in non-stimulated mice) and histology (no tissue damage in sham-groups). A well-known limitation of the model is the relatively high level of leukocyte rolling immediately after surgical preparation.

*Monitoring of experimental animals.* In all experiments, the microhemodynamics (centerline blood flow velocity), the body temperature, and the white blood cell counts were routinely controlled.

### **5.1.3 Induction of an inflammatory response**

*Inflammatory mediators.* In these studies, we used three different mediators: IL-1 $\beta$ , MIP-1 $\alpha$ , and PAF. IL-1 $\beta$  is produced by various cell types and involved in a variety of cellular activities, including cell proliferation, differentiation, and apoptosis. IL-1 $\beta$  acts through two IL-1-receptors: IL-1-receptor type 1 and 2. According to classical concept, the IL-1 $\beta$  pathway promotes nuclear transcription factor (NF- $\kappa$ B) activation with subsequent synthesis of various inflammatory mediators (105). Moreover, IL-1 $\beta$  can directly affect different cells causing the release of other proinflammatory mediators such as IL-4, IL-5, IL-8, tumor-necrosis factor (TNF- $\alpha$ ), or monocyte chemoattractant protein-1 (MCP-1) (106), (107), (108), (109).

The CC chemokine MIP-1 $\alpha$  and the potent phospholipid mediator PAF are both nonspecific inflammatory mediators which have been shown to initiate leukocyte recruitment and chemotaxis (89), (110), (111), (112), (113). MIP-1 $\alpha$  (CCL3) is produced by a variety of cells, including

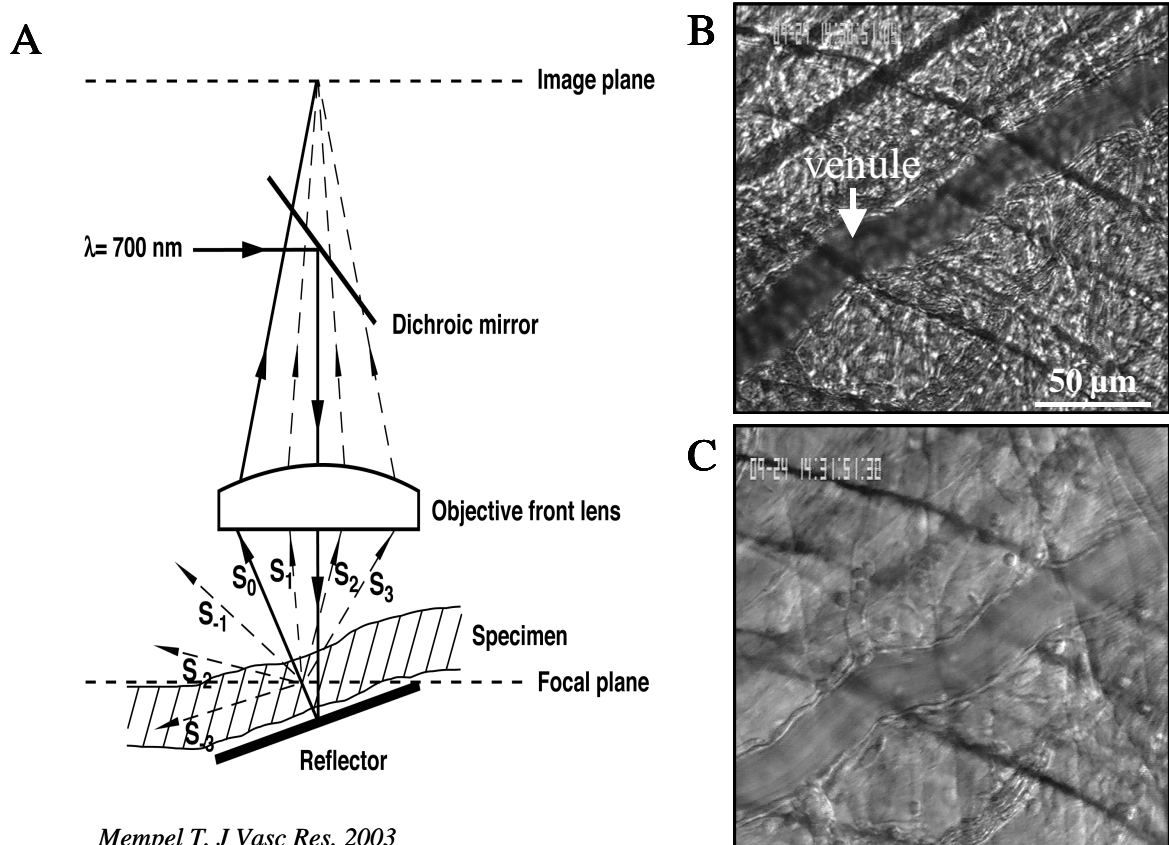
lymphocytes, monocytes/macrophages, mast cells, basophils, epithelial cells, and fibroblasts, and binds to CC chemokine receptors-1 and -5 (CCR1 and CCR5) with high affinity to exert its biological effects (112). MIP-1 $\alpha$  binds to GPCRs CCR1, CCR3, and CCR5, whereas PAF interacts with leukocytes via the PAF-receptor, which is also the member of the GPCR-superfamily. Activation of GPCRs on leukocytes can lead to the activation of “inside-out” signaling of  $\beta$ 2-integrins with consequent adhesiveness and aggregation (114), priming for enhanced inflammatory responses, polarization and directional migration, degranulation, and oxygen radical generation (115). Moreover, MIP-1 $\alpha$  and PAF can affect leukocyte migration indirectly by stimulating other interstitial cells (116), (117). For instance, PAF can activate MAPK and trigger cytokine production in fibroblasts (118) as well as stimulate TNF- $\alpha$  production in macrophages (119). Many signaling events and subsequent functional responses triggered by the PAF-receptor occur in seconds to minutes and do not require new gene expression.

*Application of the inflammatory stimuli.* Intrascrotal injection was performed 4 h prior to intravital microscopic analysis as described previously (51), (96), (120). For injection, a very fine needle was used in an attempt to avoid additional tissue damage. The time period of 4h between the injection and intravital microscopy was chosen on the basis of previous work from our laboratory (110) as well as from the literature (43), (121), which demonstrated a strong inflammatory response 4h after intrascrotal injection. In our own experiments presented in 4.1.2, we observed that the extent of leukocyte migration is rather low at 2h after stimulation, at least, if the intrascrotal route was chosen.

One of the major goals of this work was to establish a novel technique for the induction of a local inflammatory response as well as target-oriented leukocyte migration – application of micro-amounts of mediators *via* controlled microinjection in paravascular regions. The technique is discussed in detail in 5.2.3.

#### 5.1.4 Intravital microscopy

Intravital fluorescence microscopy represents the gold standard for the investigation of the microcirculation and is widely applied in various organs, such as brain (122), heart (123), lungs (124), mesenterium (125), liver (60), small intestine (126) and pancreas (127). Imaging of the behavior of already transmigrated leukocytes in the interstitial tissue is, however, limited because of difficulties to differentiate leukocytes in the interstitial tissue. The visualization of phase gradients within unstained specimens using phase contrast, differential interference contrast or Hoffman modulation contrast microscopy enables the study of dynamic cellular events *in vitro*. Recently, our laboratory established a novel method called near-infrared RLOT microscopy which combines previously described optical principles with IVM (89). Near-infrared RLOT IVM possesses several advantages in comparison to conventional fluorescence microscopy. First, the reduction of extinction of hemoglobin and myoglobin by near-infrared light enables high-contrast visualization of leukocytes in the interstitial tissue (Fig. 31). Second, low energy transfer on cremaster muscle tissue through the usage of the near-infrared light would minimize phototoxicity. Third, the division in different phase gradients provides a high tissue penetration of near-infrared light in combination with enhanced image quality. In addition, RLOT allows the dynamic visualization of leukocyte intravascular recruitment such as leukocyte rolling, adherence, transendothelial, and interstitial migration of single leukocytes without the usage of any fluorescent dye. However, the resolution of RLOT does not allow the differentiation of various leukocyte subpopulations. For phenotyping of transmigrated leukocytes, immunohistochemistry of cremasteric tissue samples was performed.



Mempel T, *J Vasc Res*, 2003

**Fig. 31.** A - Principle of near-infrared RLOT microscopy (description in text). B - Intravital microscopic image of cremasteric tissue made using conventional transillumination microscopy (objective magnification 20x). Identification of extravasated leukocytes in the interstitial tissue is limited because of muscle myoglobin. C- Reduction of myo- and hemoglobin extinction by near-infrared light during RLOT microscopy allows identifying transmigrated leukocytes as well as endothelial structures.

## 5.2 Discussion of the results

### 5.2.1 The role of ESAM for IL-1 $\beta$ -induced leukocyte migration *in vivo*

ESAM is specifically expressed at endothelial tight junctions and on platelets (54). However, the involvement of this adhesion molecule in the regulation of leukocyte migration has been not yet investigated. Recent studies demonstrated that ESAM-deficient mice have defects in tumor angiogenesis, although embryonic angiogenesis was unaffected (54). Because ESAM localizes at endothelial cell junctions and is related to the JAM family (60), which has been discovered as an essential regulator of leukocyte diapedesis, we decided to investigate the role of ESAM in leukocyte transmigration in the mouse cremaster muscle model using ESAM-disrupted gene mice. Local inflammation in the cremaster muscle was induced via intrascrotal injection of IL-1 $\beta$  at 4 h prior to intravital microscopic observation. Using near-infrared RLOT microscopy, we analyzed leukocyte rolling, adhesion, and transmigration in five randomly chosen postcapillary venules. Local application of IL-1 $\beta$  induced leukocyte rolling, adhesion, and transmigration at 4 h after application. Although we did not find any significant difference in the number of rolling and adherent cells between wild-type and ESAM<sup>-/-</sup> mice, the number of extravasated leukocytes was significantly reduced by almost 50% in ESAM<sup>-/-</sup> mice as compared to wild-type mice. To rule out that the difference in extravasation was caused by differences in leukocyte rolling or adhesion at an earlier time point during the 4 h-period of cytokine stimulation, we analyzed leukocyte migration at 2 hours after intrascrotal injection of IL-1 $\beta$ . As a result, only few transmigrated leukocytes were observed at this time point, whereas leukocyte rolling and adhesion were already well detectable and again did not differ between wild-type and ESAM<sup>-/-</sup> mice. Thus, we conclude that the absence of ESAM blocks leukocyte extravasation on the level of transendothelial migration. These data provide the first *in vivo* evidence that ESAM plays a crucial role in leukocyte transmigration and are supported by data in a peritonitis model (51) demonstrating that leukocyte extravasation is reduced by 70% in ESAM<sup>-/-</sup> mice.

How could ESAM mediate leukocyte transmigration? Can platelet-derived ESAM contribute to leukocyte migration? Interestingly, we did not observe platelet recruitment in the murine cremaster model upon ischemia-reperfusion in several pilot experiments (data not shown). However, we can not exclude that platelet ESAM might mediate leukocyte migration upon stimulation with IL-1 $\beta$  or in other organs. With or without platelet ESAM, the endothelial ESAM seems to be predominantly relevant in mediating leukocyte transmigration. It has been found that the expression of ESAM supports the activation of GTPase Rho (51) and therefore may be involved in signaling mechanisms that trigger the opening of endothelial cell contacts (51). In addition, ESAM is involved in neutrophil extravasation mechanisms independent of the type of stimulating cytokine (TNF- $\alpha$  or IL-1 $\beta$ ) (51). This is in contrast to PECAM-1 and ICAM-2 because the disruption of their genes in the C57BL/6 mouse strain affects neutrophil extravasation only if IL-1 $\beta$ , but not if TNF- $\alpha$  was used for stimulation (128), (129). Phenotyping of emigrated leukocytes after IL-1 $\beta$  application in the cremaster muscle and in the peritonitis assay showed that more than 80% of all extravasated leukocytes were neutrophils (30). This indicates that ESAM, similar to PECAM-1, is a molecule at endothelial cell contacts that selectively affects neutrophil, but not lymphocyte extravasation (51). In conclusion, our results suggest ESAM as a new membrane protein at endothelial cell junctions that is involved in neutrophil extravasation *in vivo*.

### 5.2.2 The role of CD99 and CD99L2 for IL-1 $\beta$ -induced leukocyte migration *in vivo*

CD99 and CD99L2 are recently identified surface proteins expressed on endothelial cells and hematopoietic cells (7), (59). Comparing the functions of CD99 with those of CD99L2 in more detail revealed important similarities and striking differences. It has been found that both proteins are structurally related with 32% amino acid identity between mouse CD99 and CD99L2 (59). They are both type 1 transmembrane proteins with extracellular domains, only slightly larger than 100 amino acids, rich in O-linked carbohydrates, with no resemblance to any known protein family (59). Recently, it has been shown *in vitro* that antibodies against CD99 blocked the transmigration of monocytes through HUVEC monolayers without any inhibitory effect on adhesion (55). However, the role of both CD99 and CD99L2 for leukocyte migration *in vivo* has not yet been studied. In this context, cloning of mouse CD99 and CD99L2 antibodies allowed the analysis of both proteins *in vivo* (7). Herein, we analyzed the relevance of CD99 or CD99L2 for IL-1 $\beta$ -induced leukocyte migration in the mouse cremaster muscle using IVM.

Our results show that both CD99 and CD99L2 participate in the diapedesis process and are not involved in rolling and docking of leukocytes to the vessel wall (130). While this was already anticipated for CD99 from *in vitro* transmigration assays (55), (56), (130) we demonstrate here for the first time *in vivo* that blocking of CD99 or CD99L2 results in a significant reduction of leukocyte transendothelial migration, whereas leukocyte rolling and adhesion remain unaffected.

Since blocking antibodies against CD99 or CD99L2 were applied by intravenous application, we were not able to differentiate whether it is the leukocyte CD99/CD99L2 or the endothelial CD99/CD99L2 that plays a critical role in mediating leukocyte diapedesis. This interesting aspect became an object of controversial discussion. On the one hand, it seems unlikely that endothelial CD99 and CD99L2 participate in diapedesis by homophilic binding to their respective counterpart on neutrophils since CD99L2 was almost undetectable on bone marrow neutrophils and CD99 was only weakly expressed (59). The *in vitro* data, showing that incubating neutrophils with antibodies against CD99 and CD99L2 did not reduce transmigration, support this hypothesis. Thus, it seems

likely that endothelial CD99 and CD99L2 mediate neutrophil transmigration independent of their respective counterparts on the neutrophils (59). On the other hand, however, it can not be excluded that CD99 or CD99L2 on peripheral neutrophils are involved in diapedesis, because both proteins are expressed at much higher levels on these cells than on bone marrow neutrophils. Moreover, it has been reported that binding of antibodies to either neutrophil CD99 or endothelial CD99 resulted in an equivalent quantitative block of transmigration, suggesting a homophilic interaction between CD99 on the endothelial cells or neutrophils (130).

Recent *in vitro* study provides evidence about an interdependence of CD99 with PECAM-1 in mediation of monocyte migration (55). So, CD99 homophilic interactions between EC and neutrophils have been shown to occur downstream of PECAM-1-PECAM-1 interactions (130). An analysis by Nomarski optics and confocal microscopic imaging showed that while PECAM-1 blocked arrest on the EC surface overlying the junctions, CD99 blocked neutrophils that are already lodged within the interendothelial junctional space (57). The mechanisms, by which CD99-blocked leukocytes become lodged downstream of those blocked by PECAM-1 remains to be elucidated. In our study, we analyzed whether CD99 or CD99L2 cooperate with PECAM-1 in mediating leukocyte migration *in vivo*. According to the data *in vitro*, blocking CD99 alone prevents >80% of PMN from transmigrating PMNs; blocking PECAM-1 generally prevents 70-75% of PMN from transmigrating neutrophils (131). In our experiments, blocking of CD99 and CD99L2 in IL-1 $\beta$ -induced local inflammation decreased leukocyte transmigration on 50%; the same levels of leukocyte transmigration were found in IL-1 $\beta$ -induced inflammation in cremaster muscle in PECAM-1-deficient mice, treated with preimmune IgG (59). We do not know why some PMN manage to transmigrate despite the presence of blocking antibodies. We hypothesize that PMNs in different stages of their lifespan or different states of activation have a different sensitivity to CD99 or PECAM-1. Interesting fact is that blocking both PECAM-1 and CD99 had an additive effect, blocking >90% of PMN *in vitro* (57). In our study, blocking of CD99 and CD99L2 with monoclonal antibodies in PECAM-1-deficient mice also showed an additive effect,

allowing only 37% of leukocytes to transmigrate through the endothelium. It is possible that some functional redundancy exists between PECAM-1 and CD99; however, our data are more suggestive of a sequential relationship with CD99 functioning downstream of PECAM-1. Temporal and spatial relationship between these molecules and their signaling will be an important area for research. Interestingly, a functional relationship between PECAM-1 with JAM-A have been investigated recently *in vivo* in the mouse cremaster model (36). The data from *Nourshargh's* group showed that dual blockade/deletion of these proteins did not lead to an inhibitory effect greater than that seen with blockade/deletion of either molecule alone (36).

Other molecules are also involved in diapedesis. The existence of PECAM-1 and CD99-independent pathways is supported by our data as well as by previous studies (59), (130) while even with or without blocking antibodies, a small proportion of neutrophils or monocytes are capable of transmigration (130).

In conclusion, our results establish CD99 and CD99L2 as novel endothelial surface proteins that participate in leukocyte transmigration into inflamed tissue.

### 5.2.3 Imaging and quantitative analysis of leukocyte directional interstitial migration *in vivo*

Leukocyte migration toward the site of inflammation is critical for tissue injury and regeneration. Although leukocyte interstitial migration was mostly studied *in vitro* using two-dimensional substrates, the mechanisms triggering interstitial migration of extravasated leukocytes *in vivo* remain poorly investigated. *In vitro* studies do not take into account leukocyte phenotypic and functional changes due to interactions of leukocytes with endothelial cells and basement membrane during adhesion and transendothelial migration, which include increased leukocyte polarization, phagocytosis, degranulation, release of mediators, and enhanced survival (19). In addition, the pro-emigratory action of chemokines on blood leukocytes *in vivo* is dramatically different from their capacity to induce chemotaxis *in vitro* (65). Although 2D substrates were preferentially used for *in vitro* studies on leukocyte chemotaxis, the mechanisms mediating this process seem to be rather different in 2D vs. 3D settings. In contrast to 2D migration, the 3D tissue network confines and mechanically anchors cells from all sides so they intercalate alongside and perpendicular to tissue structures (136). In this context, recent studies have shown that 2D but not 3D leukocyte migration seems to be integrin-dependent (136), (77).

In the present study, we have established a novel approach allowing the *in vivo* imaging and quantitative analysis of directional leukocyte migration and polarization in inflamed tissue. Our technique comprises the combination of near-infrared RLOT and multicolor fluorescence IVM in the murine cremaster muscle, a microinjection technique for induction of directional leukocyte migration, and an imaging program for quantitative analysis of cell motility. Microinjection *in vivo* was applied in several works during the last decade. Using a micromanipulator, a very fine tipped pipette can be inserted into a blood vessel or surrounding tissue to introduce a variety of substances, pharmaceuticals, peptides, oxygen sensing electrodes (138), (139) antibodies as well as cells. Several recent studies applied microinjection in the mouse cremaster muscle. So, *Constantinescu et al* used this technique for continuous injection of reagents intravenously (140). *Ley et al* used the microinjection of chemokine in the murine cremaster

muscle for local perivascular application of chemoattractants in studies on mechanisms mediating leukocyte rolling and adhesion *in vivo* (141). In this study, we used perivenular microinjection of relevant inflammatory mediators in order to initiate target-oriented leukocyte transendothelial and interstitial migration toward the applied stimulus.

For microinjection, the same concentrations of the mediators were used as applied previously by our group and by others to induce an inflammatory response in cremaster muscle via intrascrotal injection (89), (110). Although we applied only  $4.3 \times 10^{-8}$  % of the total dose needed for intrascrotal stimulation, this dose was strong enough to locally induce a strong leukocyte recruitment response comparable to that after intrascrotal injection. However, microinjection of chemotactic mediators did not induce inflammation in remote areas of the cremaster tissue, at least within the time period investigated. Inflammatory mediators were injected in tissue at a distance of 25-50  $\mu\text{m}$  from the unbranched postcapillary venule, since we observed in previous studies using this model that emigrated leukocytes are localized predominantly in tissue areas adjacent 0-25  $\mu\text{m}$  to the venular vessels (102). It is worth to be noted that microinjection alone neither induced local inflammation nor leukocyte recruitment due to mechanical tissue irritation, as it has been observed in additional control experiments (data not shown). Noteworthy, in our pilot experiments we tried to visualize migration of single interstitially migrating leukocytes during a longer time period (10-20 min). However, it was often difficult to follow a leukocyte for a long time, since it can also move in Z-axis and can simply disappear into the tissue from the focus unreachable by IVM.

At the beginning of the study, we answered the question, how far from the analyzed vessel microinjection should be performed. MIP-1 $\alpha$  was injected on different distances from the venule: 25-50  $\mu\text{m}$ , 75-100  $\mu\text{m}$ , and 175-200  $\mu\text{m}$ . As result, we found that a distance of 25-50  $\mu\text{m}$  was optimal for inducing chemotaxis, since microinjection on distances 75-100  $\mu\text{m}$  and 175-200  $\mu\text{m}$  initiated less leukocyte adhesion and transmigration. Moreover, we evaluated how target-oriented leukocyte migration colocalizes with the site of microinjection of chemoattractant. We found that

leukocytes adhered, transmigrated and moved in the interstitium predominantly towards the microinjection site.

Next, we evaluated how the applied mediator is distributed in the tissue after microinjection. To answer this question, the distribution of the fluorescent dye rhodamine 6G was analyzed after its microinjection. The results showed a prevalence of fluorescence intensity of rhodamine 6G on the ipsilateral side during the analyzed time period of 60 min. However, it is worth to be noted that the distribution of the fluorescent dye may be different from the tissue distribution of a chemoattractant. Taken together, these results allow us to suggest that, using this setup, we can generate a chemotactic gradient in the interstitial tissue with a directional character of leukocyte migration.

*Interstitial migration of leukocytes upon stimulation with different mediators.* Here, we compared the character of leukocyte migration after microinjection of MIP-1 $\alpha$  or PAF with that induced using a conventional route of stimulation such as intrascrotal injection of PAF. Our results showed that microinjection of MIP-1 $\alpha$  or PAF initiated a local inflammatory response, which was characterized by enhanced leukocyte adhesion, transendothelial migration, and motility of interstitially migrating leukocytes. In contrast to the diffuse inflammation upon intrascrotal injection of PAF, microinjection of chemoattractants led to leukocyte adhesion and transmigration preferentially on the vessel side ipsilateral to the analyzed vessel. This finding indicates that target-oriented leukocyte recruitment occurs already at the level of intravascular interactions of leukocytes with endothelial cells.

Local injection of the chemoattractants initiated leukocyte interstitial migration as shown by significantly increased curve-/straight-line migration distance and velocity as compared to the contralateral vessel side as well as to the control group. Whereas the curve-line velocity and distance were slightly increased upon mediator microinjection, the effect of local stimulation was stronger at the level of straight-line distance and velocity. Indeed, curve-line distance and velocity describe the real migration trajectory and characterize general cell motility rather than their

movement toward stimuli. Therefore, it is not surprising that the curve-line distance and velocity were elevated after intrascrotal injection of PAF, since also a random leukocyte migration would increase these parameters. Thus, the common locomotional ability of leukocytes – characterized by the curve-line parameters – does not seem to be dependent on the type and route of stimulation. In contrast, the elevation of straight-line migration distance that shows how far leukocytes move toward the stimuli within the time period analyzed was several times higher than curve-line migration parameters after microinjection of chemoattractants as compared to saline microinjection. Taken together, these findings demonstrate that local microinjection of relevant mediators induces directional leukocyte migration toward the chemotactic stimuli. Comparison of the parameters of leukocyte motility between the groups stimulated with MIP-1 $\alpha$  and PAF revealed, however, a similar response. These data support our previous observations that intrascrotal injection or superfusion of these mediators initiates comparable extent of leukocyte recruitment and transmigration (89), (110).

How could microinjection of chemoattractants induce directional leukocyte migration? On the one hand, chemoattractants administered via microinjection into a perivascular region of the interstitium could diffuse through extracellular matrix and directly activate endothelium on the ipsilateral vessel side via G-protein-coupled receptors (GPCRs) on endothelial cells. So called “interceptors” such as DARC (Duffy antigen receptor for chemokines) and D6 could transport PAF or MIP-1 $\alpha$  and present them on the apical side of endothelium (13), (19). Alternatively, the endothelium on the ipsilateral side might be stimulated via indirect mechanisms involving the release of mediators derived from cells in the interstitium (e.g. myocytes, fibroblasts, mast cells, smooth muscle cells). Interestingly, glycosaminoglycans have been shown to bind to chemokines and retain them locally in the interstitium, thus creating a chemotactic gradient and preventing rapid distribution of the chemokine in the tissue (21), (22).

Why does intrascrotal injection induce diffuse inflammation in the cremaster muscle? After intrascrotal injection, the chemoattractant is homogeneously distributed in the whole cremaster

muscle and induces an inflammatory response in all venules. This suggestion is supported by the fact that we found comparable levels of leukocyte migration in 5-7 vessels from different areas of the cremaster tissue after intrascrotal injection of IL-1 $\beta$  or PAF. Thus, absence of a chemotactic gradient and uniform presence of the mediator in the cremasteric tissue cause “chemotactic chaos” in the interstitium with diffuse character of leukocyte adhesion, transmigration, and random motility in the interstitium.

*Role of Rho kinase for polarization and motility of interstitially migrating leukocytes.* To prove our approach, we addressed the question of whether specific inhibition of Rho kinase would influence the motility and polarization of interstitially migrating leukocytes *in vivo*. Rho kinase, a small GTPase, is thought to be the molecular switch to mediate signals to various molecules and implicated in the formation of stress fibers and focal adhesions, cell morphology, and smooth muscle contraction. Rho kinase acts as the key mediator in cytoskeleton reorganization during leukocyte migration by regulating microtubuli disassembly (87), actin polymerization and contraction (142), activation and downregulation of  $\beta_2$ -integrins in leukocytes (143). *In vitro* studies have shown that Rho kinase is involved in the polarization of T cells (86), the retraction of the tail of migrating monocytes (85), neutrophil motility (144), as well as chemoattractant-mediated actin assembly during neutrophil chemotaxis (145). In our study, inhibition of Rho kinase not only attenuated the target-oriented movement and polarization of emigrated leukocytes upon microinjection of MIP-1 $\alpha$  as shown by significantly reduced straight-line migration parameters and eccentricity. In addition, Rho kinase inhibitor also almost completely blocked common ability of leukocytes to move in muscle tissue, as shown by marked reduction of curve-line velocity and distance. Therefore, our study provides *in vivo* evidence that Rho kinase plays a critical role for motility and polarization of emigrated leukocyte toward local chemokine stimulation and supports *in vitro* data from the literature. However, several studies demonstrate that Y27632 on monocytes elaborate lamellipodia protrusions, inhibits tail retractions and has no

effect on forward movement (85), (146). These controversial data can be explained by stimulus-, tissue- and leukocyte subtype-specificity of Rho kinase activity.

*Visualization of mitochondria redistribution in single interstitially migrating leukocytes.* In the past few years, the generation of transgenic mice expressing GFP or GFP-like molecules under cell-specific promoters of multiple fluorescent proteins (147) as well as an application of fluorescent antigen-specific antibodies have provided a simultaneous visualization of intravascularly recruited leukocyte subsets in living mice (148). Although the assays allowing an imaging of intravascular recruitment of different leukocyte subsets were already established *in vivo*, there is no such an approach allowing it regarding leukocyte interstitial migration. Since the advantages of RLOT microscopy give an opportunity to visualize dynamics of interstitially migrating leukocytes in high quality, we decided to combine RLOT with multicolor fluorescence microscopy. First, we visualized the redistribution of mitochondria in single interstitially migrating leukocytes during their movement upon intrascrotal injection of PAF. We showed that mitochondria were distributed predominantly at the trailing edge of migrating polarized leukocyte during a 5 min time period. Recent *in vitro* studies provide a strong evidence that chemoattractants induce the redistribution of mitochondria towards the uropod of polarized migrating leukocytes (149), (150). Thus, mitochondrial fission seems to regulate chemoattractant-dependent organelle redistribution (150). Mitochondria concentrated at the uropod could provide adenosine triphosphate to sustain actomyosin contraction here, thereby enabling retraction of the trailing edge and cell advance (150). Based on our pilot experiments, we present here preliminary results, which constitute, in the line with the data *in vitro*, an important advance in our understanding of how leukocytes move. However, further investigations are required in order to analyze this phenomenon in detail *in vivo*.

*Migration behavior of neutrophils vs. monocytes.* Next, we analyzed migratory patterns of neutrophils and monocytes during their directional interstitial migration. Cx3CR1<sup>gfp/gfp</sup> mice were selected as reporters because in the blood all monocytes express GFP (98). Since only few GFP-

positive cells in the interstitial tissue (which can be tissue macrophages, NK cells, and dendritic cells in Cx3CR1<sup>gfp/gfp</sup> mice (98)) were visualized in ROIs at the baseline, we assumed that almost all GFP-positive cells interstitially migrated toward applied MCP-1 were blood monocytes. We found that monocytes, despite the ability to locomote directionally toward applied chemoattractant, started their target-oriented interstitial migration later as neutrophils and moved rather slowly as neutrophils. Interestingly, monocytes have been reported to move slower as neutrophils upon stable chemotactic gradient *in vitro* (151), (152). It seems possible that this capability of neutrophils would enable them to accumulate more rapidly at the site of inflammation. Moreover, it has been shown that under certain inflammatory conditions, neutrophils produce chemotactic factors for monocytes (153), (154), (155). However, the mechanisms of these different locomotive patterns of monocytes and neutrophils during inflammatory response should be investigated in detail.

In conclusion, we have validated a novel approach for analysis of leukocyte interstitial migration *in vivo*. In contrast to recently used *in vivo* chemotaxis assays (91), (137), our technique allows not only quantitative analysis of cell motility, but also gives a possibility for *in vivo* investigation of shape changes/polarization and subcellular events in motile immune cells during their directional migration. In addition, our assay would enable simultaneous visualization and analysis of interstitial migration of different leukocyte subsets during their directed interstitial migration as well as their interactions with each other or with apoptotic/necrotic cells *in vivo*. Local administration of bacteria into the interstitium via microinjection technique would permit the evaluation of leukocyte chemotaxis towards bacteria as well as bacterial clearance *in vivo*. This approach opens new avenues for *in vivo* investigations on the mechanisms and spatiotemporal dynamics of target-oriented interstitial migration of single leukocytes.

## 6. SUMMARY

The emigration of leukocytes from the circulation is a critical step during immune surveillance and inflammatory reactions that is governed by a coordinated interplay involving a spectrum of adhesion and signal molecules. While a great deal has been learned about the early steps of leukocyte recruitment, i.e. rolling and adhesion, little is known about the subsequent steps, transendothelial and interstitial migration when leukocytes migrate across the endothelial layer lining the blood vessel and move to the sites of inflammation. In particular, it is not fully understood which endothelial receptors are responsible for extravasation of leukocytes into the perivascular space. Moreover, the mechanisms of interstitial migration of leukocytes during inflammation remain to be clarified *in vivo*.

In the first part of the study, we analyzed the role of ESAM for leukocyte migration *in vivo*. ESAM is a novel adhesion receptor which is specifically expressed at endothelial tight junctions and on platelets. Using RLOT intravital microscopy of the murine cremaster muscle, we have shown that IL-1 $\beta$ -induced leukocyte transmigration was reduced by about 50% in ESAM-deficient mice without affecting leukocyte rolling and adhesion. Our data are supported by findings in the model of chemically-induced peritonitis in which the migration of neutrophils was inhibited to a similar extent. In summary, ESAM at endothelial tight junctions participates in the migration of neutrophils through the vessel wall.

In the second part of the study, we investigated the role of two other recently discovered receptors, CD99 and CDL2, for leukocyte migration. Similar to ESAM, these receptors are expressed at endothelial cell contacts but did not belong to any of the known protein families. We demonstrate that CD99L2 and CD99 mediate transendothelial migration of neutrophils *in vivo* without any effect on leukocyte rolling and adhesion. Similar findings were also reported in the model of chemically-induced peritonitis (59). Finally, we show that the inhibitory effect of anti-CD99 and CD99L2 antibodies on cytokine-induced leukocyte transmigration in cremasteric venules is amplified in PECAM-1 $^{-/-}$  mice. This fact suggests that a functional relationship between PECAM-

1 and CD99/ CD99L2 might exist in mediating leukocyte transmigration. Taken together, our study provides the first evidence for a role of CD99 and CD99L2 in the process of leukocyte transendothelial migration *in vivo*.

In the third part of the study, we established a novel approach allowing the visualization and analysis of directional leukocyte interstitial migration *in vivo*. Our technique combines RLOT and multicolor fluorescence microscopy with microinjection for local application of chemoattractants.

In the mouse cremaster muscle, we show that microinjection of chemoattractants (MIP-1 $\alpha$  and PAF) induced directional leukocyte polarization and migration. Combination of RLOT microscopy with fluorescence microscopy allowed simultaneous visualization and analysis of migratory behavior of different leukocyte subsets upon chemotactic stimulation. Moreover, this approach enabled an imaging of subcellular events such as mitochondria redistribution in single polarized interstitially migrating leukocytes *in vivo*. This technique opens new avenues for investigations of the mechanisms of interstitial migration of leukocytes as well as the observation of morphological changes and subcellular events in different leukocyte subsets during their interstitial migration *in vivo*.

## 7. ZUSAMMENFASSUNG

Die durch ein koordiniertes Zusammenspiel zwischen Adhäsions- und Signalmolekülen regulierte Migration von Leukozyten aus den mikrovaskulären Stromgebieten in interstitielle Kompartimente stellt einen entscheidenden Schritt in der Pathophysiologie der Immunantwort und entzündlicher Reaktionen dar. Während die Mechanismen der initialen, intravaskulären Interaktion der Leukozyten mit den Endothelzellen, wie z. B. *Rolling* und Adhäsion in den letzten Jahren weitgehend aufgeklärt wurden, sind die der transendothelialen und interstitiellen Migration der Leukozyten zugrundeliegenden Mechanismen noch nicht genügend verstanden. Im Besonderen ist nicht vollständig geklärt, welche endothelialen Adhäsionsmoleküle für die Extravasation der Leukozyten in den perivaskulären Raum verantwortlich sind. Auch die Mechanismen der interstitiellen Migration der Leukozyten werden äußerst kontrovers diskutiert.

Im ersten Teil dieser Studie wurde die Rolle von *endothelial cell selective adhesion molecule* (ESAM) für die Leukozytenmigration *in vivo* untersucht. ESAM ist ein erst vor kurzem entdecktes Mitglied der Immunglobulin-Superfamilie, welches sowohl in Endothelzellkontakten, sog. *tight-junctions*, als auch auf Thrombozyten exprimiert wird. Mittels *Reflected Light Oblique Transillumination* (RLOT)-Mikroskopie am *M. cremaster* der Maus konnten wir zeigen, dass die IL-1 $\beta$ -induzierte Leukozytentransmigration in ESAM-defizienten Mäusen um ca. 50 % reduziert war, während Leukozytenrollen und -adhärenz mit den Wildtyp-Tieren vergleichbar waren. Diese Ergebnisse legen nahe, dass ESAM den Prozess der Leukozytenauswanderung durch die Endothelbarriere vermittelt.

Im zweiten Teil der Arbeit wurde die Rolle von CD99 und CD99L2, zwei ebenfalls erst seit einigen Jahren bekannten Adhäsionsrezeptoren, analysiert. Ähnlich wie ESAM werden diese Rezeptoren in endothelialen Zellkontakten exprimiert. Unsere Ergebnisse zeigen, dass sowohl CD99 als auch CD99L2 die transendotheliale Migration von neutrophilen Granulozyten *in vivo*

mediieren, jedoch keinen Einfluss auf *Rolling* und Adhäsion haben. Interessanterweise war der die Leukozytenmigration hemmende Effekt von gegen CD99 bzw. CD99L2 gerichteten Antikörpern bei PECAM-1-defizienten Mäusen deutlich verstärkt, was auf eine kooperative Funktion von PECAM-1 und CD99/CD99L2 bei der Regulation der Leukozytentransmigration hinweist. Zusammengefasst liefert diese Studie erste deutliche Hinweise auf eine funktionelle Bedeutung von CD99 und CD99L2 bei der transendothelialen Migration der Leukozyten *in vivo*.

Der dritte Abschnitt der Arbeit beschäftigt sich mit dem *In-Vivo-Imaging* und den Mechanismen der interstitiellen Leukozytenmigration in entzündetem Gewebe. Im Rahmen dieser Studie ist es gelungen, eine neue Technik zu etablieren, welche sowohl die intravitale Visualisierung als auch die quantitative Analyse der directionalen interstitiellen Leukozytenmigration *in vivo* ermöglicht. Die Technik basiert auf der Kombination von lokaler Applikation chemotaktischer Substanzen mittels kontrollierter Mikroinjektion in das Gewebe mit RLOT- bzw. Fluoreszenz-Intravitalmikroskopie. Am *M. cremaster* an der Maus konnte gezeigt werden, dass die Applikation des Chemokins MIP-1 $\alpha$  (CCL3) sowie des Phospholipids PAF in das interstitielle Gewebe eine zielgerichtete Polarisierung und Migration der Leukozyten induziert. Darüber hinaus ermöglichte dieses Verfahren das *In-vivo-Imaging* von subzellulären Ereignissen, wie z.B. der Umverteilung von Mitochondrien in polarisierten, interstitiell migrierenden Leukozyten. Zusammengefasst erlaubt diese Technik Untersuchungen zu den Mechanismen der interstitiellen Leukozytenmigration *in vivo* sowie die Beobachtung morphologischer Veränderungen und subzellulärer Prozesse in interstitiell migrierenden Leukozyten.

## 8. REFERENCES

1. Mechnikov II. Immunity in infective diseases. By Il'ia Il'ich Mechnikov, 1905. *Rev Infect Dis* 1988; 10(1):223-227.
2. Jutila MA, Berg EL, Kishimoto TK, Picker LJ, Bargatze RF, Bishop DK et al. Inflammation-induced endothelial cell adhesion to lymphocytes, neutrophils, and monocytes. Role of homing receptors and other adhesion molecules. *Transplantation* 1989; 48(5):727-731.
3. Springer TA. Traffic signals for lymphocyte recirculation and leukocyte emigration: the multistep paradigm. *Cell* 1994; 76(2):301-314.
4. Luster AD, Alon R, von Andrian UH. Immune cell migration in inflammation: present and future therapeutic targets. *Nat Immunol* 2005; 6(12):1182-1190.
5. Patel KD, Cuvelier SL, Wiehler S. Selectins: critical mediators of leukocyte recruitment. *Semin Immunol* 2002; 14(2):73-81.
6. Kinashi T, Katagiri K. Regulation of immune cell adhesion and migration by regulator of adhesion and cell polarization enriched in lymphoid tissues. *Immunology* 2005; 116(2):164-171.
7. Vestweber D. Adhesion and signaling molecules controlling the transmigration of leukocytes through endothelium. *Immunol Rev* 2007; 218:178-96.:178-196.
8. Ley K, Laudanna C, Cybulsky MI, Nourshargh S. Getting to the site of inflammation: the leukocyte adhesion cascade updated. *Nat Rev Immunol* 2007; 7(9):678-689.
9. Kansas GS. Selectins and their ligands: current concepts and controversies. *Blood* 1996; 88(9):3259-3287.
10. Vestweber D, Blanks JE. Mechanisms that regulate the function of the selectins and their ligands. *Physiol Rev* 1999; 79(1):181-213.
11. Barreiro O, Vicente-Manzanares M, Urzainqui A, Yanez-Mo M, Sanchez-Madrid F. Interactive protrusive structures during leukocyte adhesion and transendothelial migration. *Front Biosci* 2004; 9:1849-63.:1849-1863.

12. Salas A, Shimaoka M, Kogan AN, Harwood C, von Andrian UH, Springer TA. Rolling adhesion through an extended conformation of integrin alphaLbeta2 and relation to alpha I and beta I-like domain interaction. *Immunity* 2004; 20(4):393-406.
13. Chesnutt BC, Smith DF, Raffler NA, Smith ML, White EJ, Ley K. Induction of LFA-1-dependent neutrophil rolling on ICAM-1 by engagement of E-selectin. *Microcirculation* 2006; 13(2):99-109.
14. Weber C. Novel mechanistic concepts for the control of leukocyte transmigration: specialization of integrins, chemokines, and junctional molecules. *J Mol Med* 2003; 81(1):4-19.
15. Giagulli C, Ottoboni L, Cavegion E, Rossi B, Lowell C, Constantin G et al. The Src family kinases Hck and Fgr are dispensable for inside-out, chemoattractant-induced signaling regulating beta 2 integrin affinity and valency in neutrophils, but are required for beta 2 integrin-mediated outside-in signaling involved in sustained adhesion. *J Immunol* 2006; 177(1):604-611.
16. Shattil SJ. Integrins and Src: dynamic duo of adhesion signaling. *Trends Cell Biol* 2005; 15(8):399-403.
17. Liu S, Kiosses WB, Rose DM, Slepak M, Salgia R, Griffin JD et al. A fragment of paxillin binds the alpha 4 integrin cytoplasmic domain (tail) and selectively inhibits alpha 4-mediated cell migration. *J Biol Chem* 2002; 277(23):20887-20894.
18. Phillipson M, Heit B, Colarusso P, Liu L, Ballantyne CM, Kubes P. Intraluminal crawling of neutrophils to emigration sites: a molecularly distinct process from adhesion in the recruitment cascade. *J Exp Med* 2006; 203(12):2569-2575.
19. Nourshargh S, Marelli-Berg FM. Transmigration through venular walls: a key regulator of leukocyte phenotype and function. *Trends Immunol* 2005; 26(3):157-165.
20. Muller WA. Leukocyte-endothelial-cell interactions in leukocyte transmigration and the inflammatory response. *Trends Immunol* 2003; 24(6):327-334.
21. Bazzoni G. Endothelial tight junctions: permeable barriers of the vessel wall. *Thromb Haemost* 2006; 95(1):36-42.
22. Dejana E. The transcellular railway: insights into leukocyte diapedesis. *Nat Cell Biol* 2006; 8(2):105-107.

23. Kvietys PR, Sandig M. Neutrophil diapedesis: paracellular or transcellular? *News Physiol Sci* 2001; 16:15-9.:15-19.
24. Engelhardt B, Wolburg H. Mini-review: Transendothelial migration of leukocytes: through the front door or around the side of the house? *Eur J Immunol* 2004; 34(11):2955-2963.
25. Carman CV, Sage PT, Sciuto TE, de la Fuente MA, Geha RS, Ochs HD et al. Transcellular diapedesis is initiated by invasive podosomes. *Immunity* 2007; 26(6):784-797.
26. Varon D, Jackson DE, Shenkman B, Dardik R, Tamarin I, Savion N et al. Platelet/endothelial cell adhesion molecule-1 serves as a costimulatory agonist receptor that modulates integrin-dependent adhesion and aggregation of human platelets. *Blood* 1998; 91(2):500-507.
27. Chosay JG, Fisher MA, Farhood A, Ready KA, Dunn CJ, Jaeschke H. Role of PECAM-1 (CD31) in neutrophil transmigration in murine models of liver and peritoneal inflammation. *Am J Physiol* 1998; 274(4 Pt 1):G776-G782.
28. Johnson-Leger C, Aurrand-Lions M, Imhof BA. The parting of the endothelium: miracle, or simply a junctional affair? *J Cell Sci* 2000; 113(Pt 6):921-933.
29. Nakada MT, Amin K, Christofidou-Solomidou M, O'Brien CD, Sun J, Gurubhagavatula I et al. Antibodies against the first Ig-like domain of human platelet endothelial cell adhesion molecule-1 (PECAM-1) that inhibit PECAM-1-dependent homophilic adhesion block in vivo neutrophil recruitment. *J Immunol* 2000; 164(1):452-462.
30. Dangerfield J, Larbi KY, Huang MT, Dewar A, Nourshargh S. PECAM-1 (CD31) homophilic interaction up-regulates alpha6beta1 on transmigrated neutrophils in vivo and plays a functional role in the ability of alpha6 integrins to mediate leukocyte migration through the perivascular basement membrane. *J Exp Med* 2002; 196(9):1201-1211.
31. Wang S, Dangerfield JP, Young RE, Nourshargh S. PECAM-1, alpha6 integrins and neutrophil elastase cooperate in mediating neutrophil transmigration. *J Cell Sci* 2005; 118(Pt 9):2067-2076.
32. Ebnet K, Suzuki A, Ohno S, Vestweber D. Junctional adhesion molecules (JAMs): more molecules with dual functions? *J Cell Sci* 2004; 117(Pt 1):19-29.

33. Mandell KJ, Parkos CA. The JAM family of proteins. *Adv Drug Deliv Rev* 2005; 57(6):857-867.
34. Bazzoni G. The JAM family of junctional adhesion molecules. *Curr Opin Cell Biol* 2003; 15(5):525-530.
35. Nourshargh S, Krombach F, Dejana E. The role of JAM-A and PECAM-1 in modulating leukocyte infiltration in inflamed and ischemic tissues. *J Leukoc Biol* 2006; 80(4):714-718.
36. Woodfin A, Reichel CA, Khandoga A, Corada M, Voisin MB, Scheiermann C et al. JAM-A mediates neutrophil transmigration in a stimulus-specific manner in vivo: evidence for sequential roles for JAM-A and PECAM-1 in neutrophil transmigration. *Blood* 2007; 110(6):1848-1856.
37. Bazzoni G, Tonetti P, Manzi L, Cera MR, Balconi G, Dejana E. Expression of junctional adhesion molecule-A prevents spontaneous and random motility. *J Cell Sci* 2005; 118(Pt 3):623-632.
38. Bradfield PF, Nourshargh S, Aurrand-Lions M, Imhof BA. JAM family and related proteins in leukocyte migration (Vestweber series). *Arterioscler Thromb Vasc Biol* 2007; 27(10):2104-2112.
39. Iyer S, Ferreri DM, DeCocco NC, Minnear FL, Vincent PA. VE-cadherin-p120 interaction is required for maintenance of endothelial barrier function. *Am J Physiol Lung Cell Mol Physiol* 2004; 286(6):L1143-L1153.
40. Vestweber D. Regulation of endothelial cell contacts during leukocyte extravasation. *Curr Opin Cell Biol* 2002; 14(5):587-593.
41. Lampugnani MG, Corada M, Caveda L, Breviario F, Ayalon O, Geiger B et al. The molecular organization of endothelial cell to cell junctions: differential association of plakoglobin, beta-catenin, and alpha-catenin with vascular endothelial cadherin (VE-cadherin). *J Cell Biol* 1995; 129(1):203-217.
42. Su WH, Chen HI, Jen CJ. Differential movements of VE-cadherin and PECAM-1 during transmigration of polymorphonuclear leukocytes through human umbilical vein endothelium. *Blood* 2002; 100(10):3597-3603.

43. Huang MT, Larbi KY, Scheiermann C, Woodfin A, Gerwin N, Haskard DO et al. ICAM-2 mediates neutrophil transmigration in vivo: evidence for stimulus specificity and a role in PECAM-1-independent transmigration. *Blood* 2006; 107(12):4721-4727.
44. Lehmann JC, Jablonski-Westrich D, Haubold U, Gutierrez-Ramos JC, Springer T, Hamann A. Overlapping and selective roles of endothelial intercellular adhesion molecule-1 (ICAM-1) and ICAM-2 in lymphocyte trafficking. *J Immunol* 2003; 171(5):2588-2593.
45. Reiss Y, Engelhardt B. T cell interaction with ICAM-1-deficient endothelium in vitro: transendothelial migration of different T cell populations is mediated by endothelial ICAM-1 and ICAM-2. *Int Immunol* 1999; 11(9):1527-1539.
46. Schenkel AR, Mamdouh Z, Muller WA. Locomotion of monocytes on endothelium is a critical step during extravasation. *Nat Immunol* 2004; 5(4):393-400.
47. Becker MD, Garman K, Whitcup SM, Planck SR, Rosenbaum JT. Inhibition of leukocyte sticking and infiltration, but not rolling, by antibodies to ICAM-1 and LFA-1 in murine endotoxin-induced uveitis. *Invest Ophthalmol Vis Sci* 2001; 42(11):2563-2566.
48. McLaughlin F, Hayes BP, Horgan CM, Beesley JE, Campbell CJ, Randi AM. Tumor necrosis factor (TNF)-alpha and interleukin (IL)-1beta down-regulate intercellular adhesion molecule (ICAM)-2 expression on the endothelium. *Cell Adhes Commun* 1998; 6(5):381-400.
49. Osborn L, Hession C, Tizard R, Vassallo C, Luhowskyj S, Chi-Rosso G et al. Direct expression cloning of vascular cell adhesion molecule 1, a cytokine-induced endothelial protein that binds to lymphocytes. *Cell* 1989; 59(6):1203-1211.
50. Berlin-Rufenach C, Otto F, Mathies M, Westermann J, Owen MJ, Hamann A et al. Lymphocyte migration in lymphocyte function-associated antigen (LFA)-1-deficient mice. *J Exp Med* 1999; 189(9):1467-1478.
51. Wegmann F, Petri B, Khandoga AG, Moser C, Khandoga A, Volkery S et al. ESAM supports neutrophil extravasation, activation of Rho and VEGF-induced vascular permeability. *J.Exp.Med.*2006; 203(7):1671-7.
52. Ebnet K, Aurrand-Lions M, Kuhn A, Kiefer F, Butz S, Zander K et al. The junctional adhesion molecule (JAM) family members JAM-2 and JAM-3 associate with the cell

- polarity protein PAR-3: a possible role for JAMs in endothelial cell polarity. *J Cell Sci* 2003; 116:3879-3891.
53. Nasdala I, Wolburg-Buchholz K, Wolburg H, Kuhn A, Ebnet K, Brachtendorf G et al. A transmembrane tight junction protein selectively expressed on endothelial cells and platelets. *J Biol Chem* 2002; 277(18):16294-16303.
54. Ishida T, Kundu RK, Yang E, Hirata K, Ho YD, Quertermous T. Targeted disruption of endothelial cell-selective adhesion molecule inhibits angiogenic processes in vitro and in vivo. *J Biol Chem* 2003; 278(36):34598-34604.
55. Schenkel AR, Mamdouh Z, Chen X, Liebman RM, Muller WA. CD99 plays a major role in the migration of monocytes through endothelial junctions. *Nat Immunol* 2002; 3(2):143-150.
56. Bixel G, Kloep S, Butz S, Petri B, Engelhardt B, Vestweber D. Mouse CD99 participates in T-cell recruitment into inflamed skin. *Blood* 2004; 104(10):3205-3213.
57. Lou O, Alcaide P, Luscinskas FW, Muller WA. CD99 is a key mediator of the transendothelial migration of neutrophils. *J Immunol* 2007; 178(2):1136-1143.
58. Suh YH, Shin YK, Kook MC, Oh KI, Park WS, Kim SH et al. Cloning, genomic organization, alternative transcripts and expression analysis of CD99L2, a novel paralog of human CD99, and identification of evolutionary conserved motifs. *Gene* 2003; 307:63-76.:63-76.
59. Bixel MG, Petri B, Khandoga AG, Khandoga A, Wolburg-Buchholz K, Wolburg H et al. A CD99-related antigen on endothelial cells mediates neutrophil but not lymphocyte extravasation in vivo. *Blood* 2007; 109(12):5327-5336.
60. Khandoga A, Kessler JS, Meissner H, Hanschen M, Corada M, Motoike T et al. Junctional adhesion molecule-A deficiency increases hepatic ischemia-reperfusion injury despite reduction of neutrophil transendothelial migration. *Blood* 2005; 106(2):725-733.
61. Anders HJ, Frink M, Linde Y, Banas B, Wornle M, Cohen CD et al. CC chemokine ligand 5/RANTES chemokine antagonists aggravate glomerulonephritis despite reduction of glomerular leukocyte infiltration. *J Immunol* 2003; 170(11):5658-5666.
62. Ley K. Healing without inflammation? *Am J Physiol Regul Integr Comp Physiol* 2003; 285(4):R718-R719.

63. Snyderman R, Goetzl EJ. Molecular and cellular mechanisms of leukocyte chemotaxis. *Science* 1981; 213(4510):830-837.
64. Sixt M, Bauer M, Lammermann T, Fassler R. Beta1 integrins: zip codes and signaling relay for blood cells. *Curr Opin Cell Biol* 2006; 18(5):482-490.
65. Colditz IG, Schneider MA, Pruenster M, Rot A. Chemokines at large: in-vivo mechanisms of their transport, presentation and clearance. *Thromb Haemost* 2007; 97(5):688-693.
66. Moser B, Wolf M, Walz A, Loetscher P. Chemokines: multiple levels of leukocyte migration control. *Trends Immunol* 2004; 25(2):75-84.
67. Middleton J, Patterson AM, Gardner L, Schmutz C, Ashton BA. Leukocyte extravasation: chemokine transport and presentation by the endothelium. *Blood* 2002; 100(12):3853-3860.
68. Heit B, Liu L, Colarusso P, Puri KD, Kubes P. PI3K accelerates, but is not required for, neutrophil chemotaxis to fMLP. *J Cell Sci* 2008; 121(Pt 2):205-214.
69. Franca-Koh J, Devreotes PN. Moving forward: mechanisms of chemoattractant gradient sensing. *Physiology (Bethesda)* 2004; 19:300-8.:300-308.
70. Vicente-Manzanares M, Sanchez-Madrid F. Cell polarization: a comparative cell biology and immunological view. *Dev Immunol* 2000; 7(2-4):51-65.
71. Patel DD, Koopmann W, Imai T, Whichard LP, Yoshie O, Krangel MS. Chemokines have diverse abilities to form solid phase gradients. *Clin Immunol* 2001; 99(1):43-52.
72. Linhardt RJ, Toida T. Role of glycosaminoglycans in cellular communication. *Acc Chem Res* 2004; 37(7):431-438.
73. Ridley AJ. Rho GTPases and cell migration. *J Cell Sci* 2001; 114(Pt 15):2713-2722.
74. Friedl P, Borgmann S, Brocker EB. Amoeboid leukocyte crawling through extracellular matrix: lessons from the Dictyostelium paradigm of cell movement. *J Leukoc Biol* 2001; 70(4):491-509.
75. Lishko VK, Yakubenko VP, Ugarova TP. The interplay between integrins alphaMbeta2 and alpha5beta1 during cell migration to fibronectin. *Exp Cell Res* 2003; 283(1):116-126.

76. Willeke T, Schymeinsky J, Prange P, Zahler S, Walzog B. A role for Syk-kinase in the control of the binding cycle of the beta2 integrins (CD11/CD18) in human polymorphonuclear neutrophils. *J Leukoc Biol* 2003; 74(2):260-269.
77. Lammermann T, Bader BL, Monkley SJ, Worbs T, Wedlich-Soldner R, Hirsch K et al. Rapid leukocyte migration by integrin-independent flowing and squeezing. *Nature* 2008; 453(7191):51-55.
78. Lindner JR, Kahn ML, Coughlin SR, Sambrano GR, Schauble E, Bernstein D et al. Delayed onset of inflammation in protease-activated receptor-2-deficient mice. *J Immunol* 2000; 165(11):6504-6510.
79. Khandoga A, Kessler JS, Hanschen M, Khandoga AG, Burggraf D, Reichel C et al. Matrix metalloproteinase-9 promotes neutrophil and T cell recruitment and migration in the postischemic liver. *J Leukoc Biol* 2006; 106(2):725-33.
80. Charest PG, Firtel RA. Feedback signaling controls leading-edge formation during chemotaxis. *Curr Opin Genet Dev* 2006; 16(4):339-347.
81. Lokuta MA, Nuzzi PA, Huttenlocher A. Calpain regulates neutrophil chemotaxis. *Proc Natl Acad Sci U S A* 2003; 100(7):4006-4011.
82. Heit B, Colarusso P, Kubes P. Fundamentally different roles for LFA-1, Mac-1 and alpha4-integrin in neutrophil chemotaxis. *J Cell Sci* 2005; 118(Pt 22):5205-5220.
83. Schymeinsky J, Then C, Walzog B. The non-receptor tyrosine kinase Syk regulates lamellipodium formation and site-directed migration of human leukocytes. *J Cell Physiol* 2005; 204(2):614-622.
84. Zen K, Liu Y. Role of different protein tyrosine kinases in fMLP-induced neutrophil transmigration. *Immunobiology* 2008; 213(1):13-23.
85. Worthylake RA, Lemoine S, Watson JM, Burridge K. RhoA is required for monocyte tail retraction during transendothelial migration. *J Cell Biol* 2001; 154(1):147-160.
86. Bardi G, Niggli V, Loetscher P. Rho kinase is required for CCR7-mediated polarization and chemotaxis of T lymphocytes. *FEBS Lett* 2003; 542(1-3):79-83.
87. Niggli V. Microtubule-disruption-induced and chemotactic-peptide-induced migration of human neutrophils: implications for differential sets of signalling pathways. *J Cell Sci* 2003; 116(Pt 5):813-822.

88. Sumen C, Mempel TR, Mazo IB, von Andrian UH. Intravital microscopy: visualizing immunity in context. *Immunity* 2004; 21(3):315-329.
89. Mempel TR, Moser C, Hutter J, Kuebler WM, Krombach F. Visualization of leukocyte transendothelial and interstitial migration using reflected light oblique transillumination in intravital video microscopy. *J Vasc Res* 2003; 40(5):435-441.
90. Wegmann F, Petri B, Khandoga AG, Moser C, Khandoga A, Volkery S et al. ESAM supports neutrophil extravasation, activation of Rho, and VEGF-induced vascular permeability. *J Exp Med* 2006; 203(7):1671-1677.
91. Tharp WG, Yadav R, Irimia D, Upadhyaya A, Samadani A, Hurtado O et al. Neutrophil chemorepulsion in defined interleukin-8 gradients in vitro and in vivo. *J Leukoc Biol* 2006; 79(3):539-554.
92. Nasdala I, Wolburg-Buchholz K, Wolburg H, Kuhn A, Ebnet K, Brachtendorf G et al. A transmembrane tight junction protein selectively expressed on endothelial cells and platelets. *J Biol Chem* 2002; 277(18):16294-16303.
93. Baez S. An open cremaster muscle preparation for the study of blood vessels by in vivo microscopy. *Microvasc Res* 1973; 5(3):384-394.
94. Cahalan MD, Parker I, Wei SH, Miller MJ. Two-photon tissue imaging: seeing the immune system in a fresh light. *Nat Rev Immunol* 2002; 2(11):872-880.
95. Schuschke DA, Saari JT, Ackermann DM, Miller FN. Microvascular responses in copper-deficient rats. *Am J Physiol* 1989; 257(5 Pt 2):H1607-H1612.
96. Thompson RD, Noble KE, Larbi KY, Dewar A, Duncan GS, Mak TW et al. Platelet-endothelial cell adhesion molecule-1 (PECAM-1)-deficient mice demonstrate a transient and cytokine-specific role for PECAM-1 in leukocyte migration through the perivascular basement membrane. *Blood* 2001; 97(6):1854-1860.
97. Redd MJ, Kelly G, Dunn G, Way M, Martin P. Imaging macrophage chemotaxis in vivo: Studies of microtubule function in zebrafish wound inflammation. *Cell Motil Cytoskeleton* 2006; .
98. Auffray C, Fogg D, Garfa M, Elain G, Join-Lambert O, Kayal S et al. Monitoring of blood vessels and tissues by a population of monocytes with patrolling behavior. *Science* 2007; 317(5838):666-670.

99. Wan MX, Wang Y, Liu Q, Schramm R, Thorlacius H. CC chemokines induce P-selectin-dependent neutrophil rolling and recruitment in vivo: intermediary role of mast cells. *Br J Pharmacol* 2003; 138(4):698-706.
100. Duncan GS, Andrew DP, Takimoto H, Kaufman SA, Yoshida H, Spellberg J et al. Genetic evidence for functional redundancy of Platelet/Endothelial cell adhesion molecule-1 (PECAM-1): CD31-deficient mice reveal PECAM-1-dependent and PECAM-1-independent functions. *J Immunol* 1999; 162(5):3022-3030.
101. Bagi Z, Frangos JA, Yeh JC, White CR, Kaley G, Koller A. PECAM-1 mediates NO-dependent dilation of arterioles to high temporal gradients of shear stress. *Arterioscler Thromb Vasc Biol* 2005; 25(8):1590-1595.
102. Reichel CA, Khandoga A, Anders HJ, Schlondorff D, Luckow B, Krombach F. Chemokine receptors Ccr1, Ccr2, and Ccr5 mediate neutrophil migration to postischemic tissue. *J Leukoc Biol* 2006; 79(1):114-122.
103. Bastiaanse J, Nanhekhan LV, Slaaf DW, Boeckx WD, oude Egbrink MG. Preservation of rat cremaster muscle microcirculation after prolonged cold storage and transplantation. *J Surg Res* 2006; 131(1):41-48.
104. Ozer K, Zielinski M, Unsal M, Siemionow M. Development of mouse cremaster transplantation model for intravital microscopic evaluation. *Microcirculation* 2002; 9(6):487-495.
105. Auron PE. The interleukin 1 receptor: ligand interactions and signal transduction. *Cytokine Growth Factor Rev* 1998; 9(3-4):221-237.
106. Koh Y, Hybertson BM, Jepson EK, Cho OJ, Repine JE. Cytokine-induced neutrophil chemoattractant is necessary for interleukin-1-induced lung leak in rats. *J Appl Physiol* 1995; 79(2):472-478.
107. Shimoya K, Moriyama A, Matsuzaki N, Ogata I, Koyama M, Azuma C et al. Human placental cells show enhanced production of interleukin (IL)-8 in response to lipopolysaccharide (LPS), IL-1 and tumour necrosis factor (TNF)-alpha, but not to IL-6. *Mol Hum Reprod* 1999; 5(9):885.
108. Rovin BH, Tan LC. Role of protein kinase pathways in IL-1-induced chemoattractant expression by human mesangial cells. *Kidney Int* 1994; 46(4):1059-1068.

109. Nourshargh S, Larkin SW, Das A, Williams TJ. Interleukin-1-induced leukocyte extravasation across rat mesenteric microvessels is mediated by platelet-activating factor. *Blood* 1995; 85(9):2553-2558.
110. Ninichuk V, Gross O, Reichel C, Khandoga A, Pawar RD, Ciubar R et al. Delayed chemokine receptor 1 blockade prolongs survival in collagen 4A3-deficient mice with Alport disease. *J Am Soc Nephrol* 2005; 16(4):977-985.
111. Gaudreault E, Stankova J, Rola-Pleszczynski M. Involvement of leukotriene B4 receptor 1 signaling in platelet-activating factor-mediated neutrophil degranulation and chemotaxis. *Prostaglandins Other Lipid Mediat* 2005; 75(1-4):25-34.
112. Ramos CD, Canetti C, Souto JT, Silva JS, Hogaboam CM, Ferreira SH et al. MIP-1alpha[CCL3] acting on the CCR1 receptor mediates neutrophil migration in immune inflammation via sequential release of TNF-alpha and LTB4. *J Leukoc Biol* 2005; 78(1):167-177.
113. Jan MS, Huang YH, Shieh B, Teng RH, Yan YP, Lee YT et al. CC chemokines induce neutrophils to chemotaxis, degranulation, and alpha-defensin release. *J Acquir Immune Defic Syndr* 2006; 41(1):6-16.
114. Kato M, Kimura H, Motegi Y, Tachibana A, Minakami H, Morikawa A et al. Platelet-activating factor activates two distinct effector pathways in human eosinophils. *J Immunol* 2002; 169(9):5252-5259.
115. Zimmerman GA, McIntyre TM, Prescott SM, Stafforini DM. The platelet-activating factor signaling system and its regulators in syndromes of inflammation and thrombosis. *Crit Care Med* 2002; 30(5 Suppl):S294-S301.
116. Oliveira SH, Lukacs NW. Stem cell factor and IgE-stimulated murine mast cells produce chemokines (CCL2, CCL17, CCL22) and express chemokine receptors. *Inflamm Res* 2001; 50(3):168-174.
117. Gaboury JP, Johnston B, Niu XF, Kubes P. Mechanisms underlying acute mast cell-induced leukocyte rolling and adhesion in vivo. *J Immunol* 1995; 154(2):804-813.
118. Sugano T, Narahara H, Nasu K, Arima K, Fujisawa K, Miyakawa I. Effects of platelet-activating factor on cytokine production by human uterine cervical fibroblasts. *Mol Hum Reprod* 2001; 7(5):475-481.

119. Aliberti JC, Machado FS, Gazzinelli RT, Teixeira MM, Silva JS. Platelet-activating factor induces nitric oxide synthesis in Trypanosoma cruzi-infected macrophages and mediates resistance to parasite infection in mice. *Infect Immun* 1999; 67(6):2810-2814.
120. Reichel CA, Rehberg M, Bihari P, Moser CM, Linder S, Khandoga A et al. Gelatinases mediate neutrophil recruitment in vivo: evidence for stimulus specificity and a critical role in collagen IV remodeling. *J Leukoc Biol* 2008; 83(4): 864-74.
121. Dangerfield JP, Wang S, Nourshargh S. Blockade of alpha6 integrin inhibits IL-1beta- but not TNF-alpha-induced neutrophil transmigration in vivo. *J Leukoc Biol* 2005; 77(2):159-165.
122. Kataoka H, Kim SW, Plesnila N. Leukocyte-endothelium interactions during permanent focal cerebral ischemia in mice. *J Cereb Blood Flow Metab* 2004; 24(6):668-676.
123. Schramm R, Menger MD, Kirsch S, Langer F, Harder Y, Hamacher J et al. The subepicardial microcirculation in heterotopically transplanted mouse hearts: an intravital multicolor fluorescence microscopy study. *J Thorac Cardiovasc Surg* 2007; 134(1):210-7, 217.
124. Tabuchi A, Mertens M, Kuppe H, Pries AR, Kuebler WM. Intravital microscopy of the murine pulmonary microcirculation. *J Appl Physiol* 2007;104(2):338-46.
125. Nakagawa NK, Jukemura J, Aikawa P, Nogueira RA, Poli-de-Figueiredo LF, Sannomiya P. In vivo observation of mesenteric leukocyte-endothelial interactions after cecal ligation/puncture and surgical sepsis source control. *Clinics* 2007; 62(3):321-326.
126. Massberg S, Enders G, Matos FC, Tomic LI, Leiderer R, Eisenmenger S et al. Fibrinogen deposition at the postischemic vessel wall promotes platelet adhesion during ischemia-reperfusion in vivo. *Blood* 1999; 94(11):3829-3838.
127. Oehmann C, Benz S, Drogitz O, Pisarski P, Hopt UT, Obermaier R. Remote preconditioning reduces microcirculatory disorders in pancreatic ischemia/reperfusion injury. *Pancreas* 2007; 35(4):e45-e50.
128. Huang MT, Larbi KY, Scheiermann C, Woodfin A, Gerwin N, Haskard DO et al. ICAM-2 mediates neutrophil transmigration in vivo: evidence for stimulus specificity and a role in PECAM-1-independent transmigration. *Blood* 2006; 107(12):4721-4727.
129. Wakelin MW, Sanz MJ, Dewar A, Albelda SM, Larkin SW, Boughton-Smith N et al. An anti-platelet-endothelial cell adhesion molecule-1 antibody inhibits leukocyte

- extravasation from mesenteric microvessels in vivo by blocking the passage through the basement membrane. *J Exp Med* 1996; 184(1):229-239.
130. Lou O, Alcaide P, Luscinskas FW, Muller WA. CD99 is a key mediator of the transendothelial migration of neutrophils. *J Immunol* 2007; 178(2):1136-1143.
131. Hirata K, Ishida T, Penta K, Rezaee M, Yang E, Wohlgenuth J et al. Cloning of an immunoglobulin family adhesion molecule selectively expressed by endothelial cells. *J Biol Chem* 2001; 276(19):16223-16231.
132. Shaw SK, Ma S, Kim MB, Rao RM, Hartman CU, Froio RM et al. Coordinated redistribution of leukocyte LFA-1 and endothelial cell ICAM-1 accompany neutrophil transmigration. *J Exp Med* 2004; 200(12):1571-1580.
133. Ludwig RJ, Zollner TM, Santoso S, Hardt K, Gille J, Baatz H et al. Junctional adhesion molecules (JAM)-B and -C contribute to leukocyte extravasation to the skin and mediate cutaneous inflammation. *J Invest Dermatol* 2005; 125(5):969-976.
134. Chavakis T, Keiper T, Matz-Westphal R, Hersemeyer K, Sachs UJ, Nawroth PP et al. The junctional adhesion molecule-C promotes neutrophil transendothelial migration in vitro and in vivo. *J Biol Chem* 2004; 279(53):55602-55608.
135. Johnson-Leger CA, Aurrand-Lions M, Beltraminelli N, Fasel N, Imhof BA. Junctional adhesion molecule-2 (JAM-2) promotes lymphocyte transendothelial migration. *Blood* 2002; 100(7):2479-2486.
136. Friedl P, Weigelin B. Interstitial leukocyte migration and immune function. *Nat Immunol* 2008; 9(9):960-969.
137. Hickey MJ, Forster M, Mitchell D, Kaur J, De Caigny C, Kubes P. L-selectin facilitates emigration and extravascular locomotion of leukocytes during acute inflammatory responses in vivo. *J Immunol* 2000; 165(12):7164-7170.
138. Khanna S, Roy S, Slivka A, Craft TK, Chaki S, Rink C et al. Neuroprotective properties of the natural vitamin E alpha-tocotrienol. *Stroke* 2005; 36(10):2258-2264.
139. Allamargot C, Pouplard-Barthelaix A, Fressinaud C. A single intracerebral microinjection of platelet-derived growth factor (PDGF) accelerates the rate of remyelination in vivo. *Brain Res* 2001; 918(1-2):28-39.

140. Constantinescu AA, Vink H, Spaan JA. Endothelial cell glycocalyx modulates immobilization of leukocytes at the endothelial surface. *Arterioscler Thromb Vasc Biol* 2003; 23(9):1541-1547.
141. Ley K, Allietta M, Bullard DC, Morgan S. Importance of E-selectin for firm leukocyte adhesion in vivo. *Circ Res* 1998; 83(3):287-294.
142. Vicente-Manzanares M, Sanchez-Madrid F. Role of the cytoskeleton during leukocyte responses. *Nat Rev Immunol* 2004; 4(2):110-122.
143. Anderson SI, Hotchin NA, Nash GB. Role of the cytoskeleton in rapid activation of CD11b/CD18 function and its subsequent downregulation in neutrophils. *J Cell Sci* 2000; 113(Pt 15):2737-2745.
144. Carstanjen D, Yamauchi A, Koornneef A, Zang H, Filippi MD, Harris C et al. Rac2 regulates neutrophil chemotaxis, superoxide production, and myeloid colony formation through multiple distinct effector pathways. *J Immunol* 2005; 174(8):4613-4620.
145. Sun CX, Downey GP, Zhu F, Koh AL, Thang H, Glogauer M. Rac1 is the small GTPase responsible for regulating the neutrophil chemotaxis compass. *Blood* 2004; 104(12):3758-3765.
146. Redd MJ, Kelly G, Dunn G, Way M, Martin P. Imaging macrophage chemotaxis in vivo: studies of microtubule function in zebrafish wound inflammation. *Cell Motil Cytoskeleton* 2006; 63(7):415-422.
147. Verkhusha VV, Lukyanov KA. The molecular properties and applications of Anthozoa fluorescent proteins and chromoproteins. *Nat Biotechnol* 2004; 22(3):289-296.
148. Chiang EY, Hidalgo A, Chang J, Frenette PS. Imaging receptor microdomains on leukocyte subsets in live mice. *Nat Methods* 2007; 4(3):219-222.
149. Campello S, Lacalle RA, Bettella M, Manes S, Scorrano L, Viola A. Orchestration of lymphocyte chemotaxis by mitochondrial dynamics. *J Exp Med* 2006; 203(13):2879-2886.
150. Sanchez-Madrid F, Serrador JM. Mitochondrial redistribution: adding new players to the chemotaxis game. *Trends Immunol* 2007; 28(5):193-196.
151. Migliorisi G, Folkes E, Cramer EB. Differences in the ability of neutrophils and monocytes to traverse epithelial occluding junctions. *J Leukoc Biol* 1988; 44(6):485-492.

152. Bae S.Y., Jung Y.J, Woo S.Y, Park M.H., Seoh J.Y, Ryu K.H. Distinct locomotive patterns of granulocytes, monocytes and lymphocytes in a stable concentration gradient of chemokines. *Int Jof Lab Hem(OnlineEarly Articles)*. In press.
153. Soehnlein O, Zernecke A, Eriksson EE, Rothfuchs AG, Pham CT, Herwald H et al. Neutrophil secretion products pave the way for inflammatory monocytes. *Blood* 2008; 112(4):1461-1471.
154. Miyazaki S., Matsukawa A., Ohkawara S., Takagi K., Yoshinaga M. Neutrophil infiltration as a crucial step for monocyte chemoattractant protein (MCP)-1 to attract monocytes in lipopolysaccharide-induced arthritis in rabbits. *Inflam Res* 2000; 49(12):673-678.
155. Pereira HA, Shafer WM, Pohl J, Martin LE, Spitznagel JK. CAP37, a human neutrophil-derived chemotactic factor with monocyte specific activity. *J Clin Invest* 1990; 85(5):1468-1476.

## 9. ACKNOWLEDGEMENTS

It is my privilege to express my sincere gratitude to Prof. Dr. med. Fritz Krombach for his expert and excellent supervision, mentorship and constant encouragement, which developed a sense of self confidence and independent thinking in computing the entire course of present work.

I would like to thank Prof. Dr. med. Alexander Baethmann, former Director of the Institute for Surgical Research, University of Munich, for accepting me to work in this institute.

I am very thankful to Dr. med Andrej Khandoga (Department of Surgery, Klinikum der Universität München-Großhadern, Munich) for his strong intellectual and other supports throughout this work, expert suggestions during the preparation of this dissertation.

I am also thankful to Prof. Dr. Dietmar Vestweber (Max-Planck Institute, Münster) for providing the ESAM-knockout mice as well as anti-CD99 and anti-CD99L2 antibodies.

Moreover, I would like to acknowledge the skilful assistance of Dr. rer. nat. Markus Rehberg during the experiments with combination of RLOT and multicolor fluorescence microscopy.

I am also thankful to Dr. med. Christoph Reichel, Peter Bihari, Marc Hanschen, Alke Schropp and Silvia Münzing for their mutual and technical support and all the help whenever I needed in public relation.

I am deeply indebted to all my colleagues at the Institute for Surgical Research and the friends from Munich for all their help and homely environment, which gave me a moral support and strength to work.

I am deeply grateful to my wife and my parents for their blessings, affections, moral support and constant encouragement.

## 10. PUBLICATION LIST

Original works:

1. Patole P.S., Schubert S., Hildinger K., **Khandoga S.**, Khandoga A., Segerer S., Henger A., Kretzler M., Werner M., Krombach F., Schlondorff D., and Anders H.J. 2005. Toll-like receptor-4: renal cells and bone marrow cells signal for neutrophil recruitment during pyelonephritis. *Kidney Int.* 68:2582-2587.
2. Khandoga A., Kessler J.S., Hanschen M., **Khandoga A.G.**, Burggraf D., Reichel C., Hamann G.F., Enders G., and Krombach F. 2006. Matrix metalloproteinase-9 promotes neutrophil and T cell recruitment and migration in the postischemic liver. *J.Leukoc.Biol.* 79: 1295-305.
3. Wegmann F., Petri B., **Khandoga A.G.**, Moser C., Khandoga A., Volkery S., Li H., Nasdala I., Brandau O., Fassler R., Butz S., Krombach F., and Vestweber D. 2006. ESAM supports neutrophil extravasation, activation of Rho, and VEGF-induced vascular permeability. *J.Exp.Med.* 203:1671-1677.
4. Bixel M.G., Petri B., **Khandoga A.G.**, Khandoga A., Wolburg-Buchholz K., Wolburg H., Marz S., Krombach F., and Vestweber D. 2007. A CD99-related antigen on endothelial cells mediates neutrophil but not lymphocyte extravasation *in vivo*. *Blood.* 109:5327-5336.
5. Ninichuk V., **Khandoga A.G.**, Segerer S., Loetscher P., Schlapbach A., Revesz L., Feifel R., Khandoga A., Krombach F., Nelson P.J., Schlondorff D., and Anders H.J. 2007. The role of interstitial macrophages in nephropathy of type 2 diabetic db/db mice. *Am.J.Pathol.* 170:1267-1276.
6. Furst R, Bubik M.F., Bihari P, Mayer B.A., **Khandoga A.G.**, Hoffmann F., Rehberg M., Krombach F., Zahler S., Vollmar A.M. 2008. Atrial natriuretic peptide protects against histamine-induced endothelial barrier dysfunction *in vivo* *Mol. Pharmacol.* 74 (1):1-8

7. **Khandoga A.G.**, Khandoga A., Anders H.J., Krombach F. 2008. Postischemic vascular permeability requires TLR-2 and TLR-4 but only TLR-2 mediates the transendothelial migration of leukocytes. *Shock (Epub ahead of print)*.

8. **Khandoga A.G.**, Khandoga A., Reichel C.A., Bihari P., Rehberg M., Krombach F. 2009. *In vivo* imaging and quantitative analysis of leukocyte directional migration and polarization in inflamed tissue. *PLoS ONE* 4(3): e4693.

Abstracts:

1. **Khandoga A.G.**, Khandoga A., Reichel C.A., Anders H.J., Schlöndorff D., Krombach F. 2006. Role of TLR4 For CXCL2-Induced Leukocyte Migration. *J. Vasc. Res.* 43: 43.

2. Butz S., Wegmann F., Petri B., **Khandoga A.G.**, Moser C., Khandoga A., Volkery S., Li H., Nasdala I., Brandau O., Fässler R., Krombach F., Vestweber D. 2006. ESAM supports neutrophil extravasation, activation of Rho and VEGF-induced vascular permeability. *J. Vasc. Res.*; 43: 536.

3. **Khandoga A.G.**, Khandoga A., Reichel C.A., Krombach F. 2006. Single cell tracking of interstitially migrating leukocytes upon chemoattractant microinjection in vivo. *J. Vasc. Res.* 43 S1: 68.

4. **Khandoga A.G.**, Khandoga A., Reichel C.A., Krombach F. 2007. Single cell tracking of interstitially migrating leukocytes upon chemoattractant microinjection in vivo. *Inflamm. Res.* 56, S2: 161.

5. **Khandoga A.G.**, Khandoga A., Rehberg M., Bihari P., Anders H.J., Krombach F. 2008. TLR2 and TLR4 differentially mediate postischemic leukocyte transmigration and vascular permeability. *J. Vasc. Res.* 45: S2: 144.

## 11. CURRICULUM VITAE

**Name:** Alexander Georg Khandoga

**Date of birth:** 23.02.1980

**Birthplace:** Mosty/Belarus

**Nationality:** belarussian

**Family status:** married with Anna Khandoga (Makarenko)

**Parents:** Georg Khandoga, medical doctor  
Maria Khandoga (Samara), biologist

### **Education:**

#### **School:**

Mosty/Belarus

1997 School diploma with honors

#### **University:**

09/1997 - 07/2003 Human medicine, State Medical University, Grodno, Belarus

07 - 09/2001 Clinical elective, Department of Surgery, Frankenwald Klinik, Kronach, Germany

#### **Professional career:**

8/2003 - 7/2004 First year resident, Department of Cardiology, 1st Clinic of the State Medical University Grodno, Belarus

22/06/2004 Internist examination (note 1.0)

07/2004 – 11/2008 PhD Student, Institute for Surgical Research, Ludwig-Maximilians-Universität München, Munich, Germany

Since 11/2008 Postdoc, Institute of Experimental Cardiology, Deutsches Herzzentrum München, Technical University of Munich, Germany